CHANGING SOIL CHARACTERISTICS AND BIOGEOMORPHIC SUCCESSION IN TUOLUMNE MEADOWS: IMPLICATIONS FOR RESTORATION

by

Kyle John Ankenbauer

A thesis submitted in partial fulfillment of
the requirements for the degree of

Master of Science
(Civil and Environmental Engineering)

at the

UNIVERSITY OF WISCONSIN-MADISON

2014

Acknowledgements

Prof. Steve Loheide is one of the best teachers, listener/observers, and mentors I have ever had in my whole life. He is a brilliant thinker and problem solver, and an incredible motivator. I know that I would have been unable to accomplish the success I had in graduate school without his unwavering belief that I was capable of it. I can fill at least four more pages about how meaningful Steve's efforts are to me and to the university, but I will spare the reader and just continue to regularly send the pages to the university as award nominations because everyone at this institution should be more like Steve and they all need to know it.

Prof. Chin Wu has the unique ability to be friendly and enthusiastic while being almost frighteningly demanding. I loved his coastal engineering class and I found it a joy to talk about waves or hurricanes or whatever with him, and he would always turn it right around on me and show me how much more work I had to do to really understand *the feeling*. I developed tremendously through this sort of motivation, maybe in a way similar to how the mountain climber's motivation increases as they approach the top despite the ever increasing difficulties of precipitous slopes and a thin atmosphere. Chin Wu has no mercy for precipitous slopes and thin atmospheres because he knows how great it is to reach the top, and he knows that you can make it there.

Prof. Sam Kung opened my eyes to a world of soil physics that I never knew existed. If a stamp is a clay particle, then silt is a baseball and sand is anything from a basketball to boulders that can crush you. No physical parameter varies over more orders of magnitude than hydraulic conductivity. Because of him, I am adamant about truly understanding the scope and range of possibilities in the universe, especially in places that are too small or too big for me to see (like between soil particles).

Figure 1: *Yosemite is an incredibly beautiful and interesting place.*

Over the last three years, I have enjoyed a life that I think very few people ever experience: I lived and worked in a National Park. I thrived in Yosemite with the responsibility to progress the understanding of hydroecological functions that keep meadows healthy, and this experience was enriched by my collaboration with ecologists Evan Wolf and Prof. David Cooper, as well as park hydrologist Jim Roche and the other NPS staff. I spent days, weeks, and months surveying the meadows with the sole purpose of observing ecosystems as closely as possible; wondering why water mattered so much to such an incredibly beautiful place (Figure 1). I don't think John Muir could have had a better experience than I did. For example, Muir wrote that he wondered about the life of a raindrop. He questioned how plants could survive here, clinging to what appeared to be bare rock. *Man*, I wish I could tell him about how plants depend on soil water retained by organic matter or groundwater delivered through moraines and granite fractures, or that his intuitive understanding of unit hydrographs was spot on. I wish Muir was still around so that I could tell him of all the things fellow badgers Prof. Loheide and I, as well as various non-badger researchers referenced in this thesis, figured out about what happens to raindrops in Yosemite. I will probably spend the rest of my life seeking the comfort and purpose I felt while I lived there.

Although this thesis could not have happened without the people and experiences described in the previous four paragraphs, the main reason I wrote it is for my family. My dad wrote a master's thesis and so I knew that I could do it. So did my brother. But it was my sister who demonstrated that an engineering education was possible, and my mom never let me give up.

THESIS ABSTRACT

Tuolumne Meadow is an impacted groundwater dependent ecosystem that is threatened by increased drying in meadow soil and increased channel widening of the Tuolumne River channel. We investigated two mechanisms which can reduce the availability of water to meadow vegetation and further degrade the meadow or maintain it in a degraded condition: (1) decreased soil water retention as a result of soil organic matter loss in dryer soils, and (2) the reduced trapping of sediment in places with limited willow establishment. The motivation for this study was to provide a process based understanding of the interactions between meadow vegetation condition and soil maintenance and formation so that processes that inhibit and encourage meadow recovery can be identified. While the findings presented in this manuscript are based on observations in Tuolumne Meadows, they are meaningful to meadows throughout the Sierra Nevada because they all experience a similar climate and were formed by similar geologic processes.

We measured soil organic content and soil water retention at distributed sites across Tuolumne Meadows and found that soil water retention is strongly influenced by soil organic content. With the use of a field-validated 1-D variably saturated groundwater flow numerical model, we demonstrated the impact of soil organic matter loss by simulating seasonal transpiration under a range of soil organic contents. We showed that the difference in cumulative seasonal transpiration between soils with 0% organic content and 20% organic content is 8.8 cm. Additionally, the simulations show this difference occurs over the latter half of the growing season, which is a critical time for root growth and seed development in plants.

To characterize the role of willows in sedimentation processes along the Tuolumne River channel, we measured sedimentation deposition on top of inert clay pads placed around willow plants. To understand the role of four different biogeomorphic factors, we chose to compare (1) willows inside and outside of deer proof fencing and (2) willows on gravel bars and on banks. Additionally, we compared sedimentation deposition (3) in areas upstream, downstream, and adjacent to willows and (4) around willows close to the river and those farther away. Low peak flows over the duration of this portion of the study (2012 to 2013) limited our ability to observe sedimentation, but we were able to show the robustness of the methodology with the limited data we collected. The results show that the occurrence of deposition is significantly different for organic duff debris than for mineral sediments on gravel bars as opposed to river banks and around willows close to the river as opposed to those farther away.

Table of Contents

Chapter 2: The Linked Effects of Soil Hydraulic Properties and Soil Organic Matter on Root Water Uptake in a Subalpine Meadow

Chapter 3: The Implementation of the Clay Pad Method for Characterization of Biogeomorphic Succession along Riparian Areas in the Tuolumne River

Chapter 1

Thesis Introduction

Subalpine wet meadows exist in riparian areas where surface water and groundwater and serve as a link between the aquatic and terrestrial environments. The area occupied by mountain meadows is small, relative to forested areas and bare rock, but the value of the ecosystem functions they perform is disproportionately large. For example, riparian areas constitute less 0.4% of the land area in the Inyo National Forest, but are essential for at least one phase of life for about 75% of local wildlife species (Kondolf et al., 1987). In fact, 21% of the 401 Sierran species of mammals, birds, reptiles and amphibians depend regularly on riparian areas for water and shelter (Graber, 1996). Therefore, riparian meadows serve multiple functions for habitat preservation and chemical and nutrient cycling, as well as flood attenuation, and the purification and filtration of water (Loheide & Gorelick, 2007). These functions are driven by a strong hydrologic connection between the meadow streams and meadow aquifers (Loheide & Gorelick, 2006). Because subalpine wet meadows are groundwater dependent ecosystems (Allen-Diaz, 1991), they become degraded under impacts that cause hydrologic change. Wet meadows are considered to be the most degraded of Sierra Nevadan environments (SNEP, 1996), so there is a great need to understand the hydrologic processes that support healthy meadows to accurately predict the meadow response to impacts so scientists and National Park Service staff can manage these valuable places appropriately. While this research was conducted in Tuolumne Meadows, the conclusions can be applied elsewhere in other groundwater dependent ecosystems in Mediterranean climates.

In groundwater dependent ecosystems, vegetation relies on the availability of groundwater retained from snowmelt to survive long dry summers (Allen-Diaz, 1991), so groundwater availability is a key driver of vegetation condition and distribution (Lowry, Loheide, Moore, & Lundquist, 2011a). If available, vegetation can also make use of the vadose zone soil moisture (Lowry & Loheide, 2010). The amount of water retained in soil has been shown to be dependent on the amount of organic matter in the soil (Saxton & Rawls, 2006; Rawls et al., 2003), and many of the impacts recorded in the Sierras promote aridification which can cause losses of soil organic matter from 50% (Norton et al., 2011) to 97% of original content (Sigua et al., 2009). Although it is uncertain how water availability for vegetation will change under continued degradation, literature suggests that losses of organic matter and soil water retention are likely, which may decrease water availability.

The morphology of a river channel affects groundwater levels throughout a groundwater dependent meadow (Loheide & Booth, 2011; Loheide & Gorelick, 2006), so alterations to river stage can lead to losses of native wet meadow vegetation (Loheide et al., 2009).

Riparian vegetation such as willows can interact with water and sediment flows to induce sedimentation and resist erosion (Corenblit et al., 2009), which can in turn contribute to the formation of new landforms through a process called biogeomorphic succession (Corenblit et al., 2010; Gurnell et al., 2012). Riparian vegetation has been disturbed throughout the Sierra Nevada (SNEP, 1996), which has increased erosion in riparian areas (Behnke and Raleigh, 1979; Platts, 1991; Dudley and Dietrich, 1995) and in meadows in particular (Odion et al, 1990). Although a reduction in grazing pressure on riparian vegetation does not directly result in restored riparian areas (Marshall, Hobbs, & Cooper, 2013), an apparent abundance of herbivory in Tuolumne Meadows has raised concerns for the future of riparian willow populations. Therefore, it is unclear exactly how grazing and willows interact to maintain the health of the meadow.

The motivation of this research is to provide a process based understanding of the interactions between meadow vegetation and soil maintenance and formation so that processes that inhibit and encourage meadow recovery can be identified. We act on this motivation through two main goals: (1) to evaluate the dependency of soil water retention on soil organic matter and determine the impact to plants under changes of soil organic matter and (2) to examine the role of willows in trapping sediment along the riparian areas of the Tuolumne River. Developing an understanding of these two processes helps paint a more complete picture of the hydrologic dependency of wet meadows and how meadows are likely to respond to continued degradation or climate change. Additionally, these conclusions can be used to guide ecosystem management plans by identifying strategies that promote the maintenance and formation of organic matter and encourage willow establishment in riparian areas.

The main contribution of this work (Chapter 2) is the experimental discovery of a very strong correlation between soil organic content and soil hydraulic properties in meadow soils. The influence of soil organic content on soil hydraulic properties has been a source of controversy between studies that show it increases retention (Rawls et al., 2003); (Saxton & Rawls, 2006) and those that show it has a limited effect (Teepe et al., 2003). We produced a set of 19 complete soil water retention curves (not just moisture-pressure values at critical points) over an unprecedented wide range of organic content in soils with similar mineral content. This allows for a clear view into the effect of soil organic content on soil water retention without the confounding effects of large variability in texture or clay content, which can obfuscate the organic signal (Ebrahimi et al., 2014; Kern, 1995).

We demonstrate the influence of the soil organic content on plant water use with the use of a 1-D variably saturated groundwater flow numerical model built in COMSOL. Water availability is a key driver of vegetation condition and distribution in groundwater dependent ecosystems (Lowry et al., 2011a), and we add to this body of knowledge by showing the impact of changes in soil water retention on root water uptake. The correlation of soil water retention to soil organic matter provides a focal point for management strategists to address the water availability requirements of a healthy meadow.

The second contribution of this work (Chapter 3) is a thorough documentation of a successful implementation of the clay pad method to characterize biogeomorphic succession in the Tuolumne River. We measured the deposition of sediment on the surface of inert clay pads around willows that vary in proximity to the river to determine the role willows play in sedimentation processes. Additionally, we investigate the effect of grazing by deer by measuring sedimentation around willows inside and outside of deer-proof fences. The two years over which this portion of the study took place were unusually dry, so our ability to observe active sedimentation processes was limited by low peak discharges. Nevertheless, the method was able to show an increased likelihood of duff deposition on river banks and around willows farther from the river and an increased likelihood of mineral deposition on gravel bars and around willows closer to the river. A continuation of this study through years with higher peak discharges could produce enough data to show statistically significant relationships between willows and sedimentation based on depth, which would help to direct management strategies even more.

In the following chapters, we describe in detail the methods used to observe and measure the hydrologic processes related to these two contributions. We discuss the implications of the results to the water availability of meadow vegetation, and for overall meadow health. Finally, we propose how our findings help contribute to the development of sound management strategies, and offer suggestions for worthy future research efforts.

REFERENCES

Allen-Diaz, B. (1991). Water-Table and Plant-Species Relationships in Sierra-Nevada Meadows. *American Midland Naturalist*, *126*(1), 30–43. doi:10.2307/2426147

Behnke, R.J., and R.F. Raleigh. 1979. Grazing and the riparian zone: Impact and management perspectives. General Technical Report WO-12. Washington, DC: U.S. Forest Service.

Corenblit, D., Steiger, J., Gurnell, A. M., Tabacchi, E., & Roques, L. (2009). Control of \ sediment dynamics by vegetation as a key function driving biogeomorphic succession within fluvial corridors. *Earth Surface Processes and Landforms*, *34*(13), 1790–1810. doi:10.1002/esp.1876

Corenblit, D., Steiger, J., & Tabacchi, E. (2010). Biogeomorphologic succession dynamics in a Mediterranean river system. *Ecography*, *33*(6), 1136–1148. doi:10.1111/j.1600-0587.2010.05894.x

Dudley, T.L., and W.E. Dietrich. 1995. Effects of cattle grazing exclosures on the recovery of riparian ecosystems in the southern Sierra Nevada. Technical Completion Report UCAL-WRC-W-831. Davis: University of California, Water Resources Center.

Ebrahimi, E., Bayat, H., Neyshaburi, M. R., & Abyaneh, H. Z. (2014). Prediction capability of different soil water retention curve models using artificial neural networks. *Archives of Agronomy and Soil Science*, *60*(6), 859–879. doi:10.1080/03650340.2013.837219

Gurnell, A. M., Bertoldi, W., & Corenblit, D. (2012). Changing river channels: The roles of hydrological processes, plants and pioneer fluvial landforms in humid temperate, mixed load, gravel bed rivers. *Earth-Science Reviews*, *111*(1-2), 129–141. doi:10.1016/j.earscirev.2011.11.005

Kern, J. (1995). Evaluation of Soil-Water Retention Models Based on Basic Soil Physical-Properties. *Soil Science Society of America Journal*, *59*(4), 1134–1141.

Kondolf, G., Webb, J., Sale, M., & Felando, T. (1987). Basic Hydrologic Studies for Assessing Impacts of Flow Diversions on Riparian Vegetation - Examples from Streams of the Eastern Sierra-Nevada, California, Usa. *Environmental Management*, *11*(6), 757–769. doi:10.1007/BF01867243

Loheide, S. P., & Booth, E. G. (2011). Effects of changing channel morphology on vegetation, groundwater, and soil moisture regimes in groundwater-dependent ecosystems. *Geomorphology*, *126*(3-4), 364–376. doi:10.1016/j.geomorph.2010.04.016

Loheide, S. P., Deitchman, R. S., Cooper, D. J., Wolf, E. C., Hammersmark, C. T., & Lundquist, J. D. (2009). A framework for understanding the hydroecology of impacted wet meadows in the Sierra Nevada and Cascade Ranges, California, USA. *Hydrogeology Journal*, *17*(1), 229–246. doi:10.1007/s10040-008-0380-4

Loheide, S. P., & Gorelick, S. M. (2006). Quantifying stream-aquifer interactions through the analysis of remotely sensed thermographic profiles and in situ temperature histories. *Environmental Science & Technology*, *40*(10), 3336–3341. doi:10.1021/es0522074

Loheide, S. P., & Gorelick, S. M. (2007). Riparian hydroecology: A coupled model of the observed interactions between groundwater flow and meadow vegetation patterning. *Water Resources Research*, *43*(7), W07414. doi:10.1029/2006WR005233

Lowry, C. S., & Loheide, S. P. (2010). Groundwater-dependent vegetation: Quantifying the groundwater subsidy. *Water Resources Research*, *46*(6), n/a–n/a. doi:10.1029/2009WR008874

Lowry, C. S., Loheide, S. P., Moore, C. E., & Lundquist, J. D. (2011). Groundwater controls on vegetation composition and patterning in mountain meadows. *Water Resources Research*, *47*(10), n/a–n/a. doi:10.1029/2010WR010086

Marshall, K. N., Hobbs, N. T., & Cooper, D. J. (2013). Stream hydrology limits recovery of riparian ecosystems after wolf reintroduction. *Proceedings of the Royal Society B-Biological Sciences*, *280*(1756), 20122977. doi:10.1098/rspb.2012.2977

Norton, J. B., Jungst, L. J., Norton, U., Olsen, H. R., Tate, K. W., & Horwath, W. R. (2011). Soil Carbon and Nitrogen Storage in Upper Montane Riparian Meadows. *Ecosystems, 14*(8), 1217–1231. doi:10.1007/s10021-011-9477-z

Rawls, W. J., Pachepsky, Y. A., Ritchie, J. C., Sobecki, T. M., & Bloodworth, H. (2003). Effect of soil organic carbon on soil water retention. *Geoderma*, *116*(1-2), 61–76. doi:10.1016/S0016-7061(03)00094-6

Odion, D.C., T.L. Dudly, and C.M. D'Antonio. 1990. Cattle grazing in southeastern Sierra meadows: Ecosystem change and prospects for recovery. In Plant biology of eastern California, edited by C.A. Hall and V. Doyle-Jones, 277-92. Los Angles: University of California, White Mountain Research Station.

Platts, W.S. 1991. Livestock grazing. In Influences of forest and rangeland management on salmonoid fishes and their habitats, edited by W.R. Meehan, 389-423. Special Publication 19. Bethesda, MD: American Fisheries Society.

Saxton, K. E., & Rawls, W. J. (2006). Soil water characteristic estimates by texture and organic matter for hydrologic solutions. *Soil Science Society of America Journal*, *70*(5), 1569–1578. doi:10.2136/sssaj2005.0117

Sigua, G. C., Coleman, S. W., & Albano, J. (2009). Beef cattle pasture to wetland reconversion: Impact on soil organic carbon and phosphorus dynamics. *Ecological Engineering*, *35*(8), 1231–1236. doi:10.1016/j.ecoleng.2009.05.004

Teepe, R., Dilling, H., & Beese, F. (2003). Estimating water retention curves of forest soils from soil texture and bulk density. *Journal of Plant Nutrition and Soil Science*, *166*(1), 111–119. doi:10.1002/jpln.200390001

Chapter 2

The Linked Effects of Soil Organic Matter and Soil Water Retention on Root Water Uptake in a Subalpine Meadow

ABSTRACT

Tuolumne Meadows is a groundwater dependent ecosystem that is threatened by hydrologic impacts that may lead to a substantial loss of organic matter in the soil. In order to provide a scientific basis for management of this type of ecosystem, this paper quantifies the changes in soil water retention and water use by plants under different levels of soil organic content. First, we show a substantial dependence of soil water retention on soil organic content by correlating Van Genuchten soil water retention parameters with soil organic content. Then, we demonstrate the impact of organic content on plants by simulating the degree to which RWU is affected by soil water retention with the use of a physically-based hydrological numerical model. Our results demonstrate that the increased water retention by soil organic matter contributes as much as 8.8 cm to transpiration during the dry second half of summer when plants experience increased water stress.

INTRODUCTION

Tuolumne Meadows is a wet meadow ecosystem located high in the Sierra Nevada Mountains of California. Mediterranean climates, like that of the Sierra Nevada, are characterized by wet winters and dry summers, which cause riparian ecosystems to depend on the availability of groundwater retained from snowmelt to survive (Allen-Diaz, 1991). Wet meadows are classified as groundwater dependent ecosystems because the composition, distribution, and function of vegetation is controlled or strongly influenced by groundwater processes (Booth & Loheide, 2012b; Hammersmark et al., 2009). Unfortunately, riparian meadow ecosystems are some of the most degraded ecosystems in the Sierra Nevada Mountain Range (SNEP, 1996). SNEP also noted that the degradation of these areas is the result of gold and gravel mining, cattle grazing, removal of riparian vegetation, hydroelectric development, land clearance and drainage, and water diversions for irrigation, some of which result in channel erosion. While the causes of degradation are numerous, channel widening and stream incision are known to contribute to the declining water table elevation in meadows and associated drying of soils (Loheide & Booth, 2011; Loheide & Gorelick, 2007; Hammersmark et al., 2010; Choate, 1972).

Degradation can result in the destabilization and loss of soil organic matter (Sollins et al., 1996). The amount of organic carbon in the soil is a balance between the supply of organic material by plants (the input) and the loss of organic matter due to soil respiration (the output) (Six et al., 2002). The supply of carbon based plant material is derived from above and below ground biomass (leaves, stems, and roots) (Six, Feller, et al., 2002), which is altered by changes in plant productivity (Luo et al., 2002). Because the productivity of plants changes when water availability changes, the input of organic material is a function soil-water dynamics. The output of organic carbon from soil respiration is higher in conditions that are less persistently saturated (Moyano et al., 2013; Davidson et al., 2012). Therefore, it has been shown that both the input and output of organic material to soil can be a function of soil-water dynamics, which helps to explain why aridification in riparian environments can result in losses of soil organic carbon from 50% (Norton et al., 2011) to 97% of original content (Sigua et al., 2009).

For many years, research has produced contradicting claims about effect of organic content on soil water retention (Olness & Archer, 2005). Buckingham (1907) showed that organic carbon retained more water than mineral soils for equivalent gravitational heads. More recently, organic content in soil has been shown to have a significant influence on soil water retention (Rawls et al., 2003; Saxton & Rawls, 2006). Other studies, however, have found that organic matter is not necessary to accurately estimate soil water retention properties (Nemes & Rawls, 2006; Arya & Paris, 1981; Kern, 1995; Kozak & Ahuja, 2005), implying that organic content plays a small, and perhaps negligible role in controlling as soils water retention characteristics. In general, soil texture is considered to be the main driver of the soil water retention properties of soil (Zhuang et al., 2001) and for that reason fractions of sand, silt, and clay are typically included as an input to soil water retention property predictor algorithms such as pedotransfer functions (Schaap et al., 2001; Vereecken et al., 1989; Gupta & Larson, 1979; Carsel & Parrish, 1988). In studies of large datasets with wide ranges of sand, silt, and clay fractions, texture is the strongest driver of soil water retention (Rawls, 2003; Olness, 2005; Saxton & Rawls, 2006). Jamison (1953) showed that in sandy soils with little or no clay, the influence of organic matter is pronounced. This suggests that clay content and organic matter have similar effects on soil water retention (Ebrahimi et al., 2014; Kern, 1995), which helps to explain why organic content typically has less of an impact on soil water retention in pedotransfer functions derived from large datasets. However, in systems like Tuolumne Meadows where the soils are predominately similar in texture organic content likely plays a significant role in retention. Therefore, continued hydrologic degradation to the meadow threatens to alter the existing levels of soil organic content and soil water retention, and it is unknown how this will impact water availability for plants.

Informed decision making and management of meadow ecosystems requires a deeper understanding the role that changing organic matter in the soil may play in altering plant water availability and use in this ecosystem. This paper quantifies the changes in soil water retention and water use by plants caused by changes in soil organic matter. We frame the research around the question *how much does soil water retention depend on soil organic content, and what is the impact to plants if soil organic content changes*. First, we quantify the extent to which soil water retention depends on organic content by correlating measured soil water retention parameters and organic content. We compare the dependence of the retention parameters on organic matter to the dependence on soil texture. Then, we determine how plants respond to reduced organic content by simulating the degree to which RWU is affected by soil water retention with the use of a physically-based hydrological numerical model. Finally, we discuss potential implications for plant communities of altered soil hydraulic properties, which is a relatively undocumented hydrologic effect on plants in impacted riparian ecosystems.

SITE DESCRIPTION

Tuolumne Meadows is located in the Sierra Nevada mountain range within Yosemite National Park at an elevation of 8600 m. With an area of 1.6 km^2, Tuolumne Meadows is one of the largest sub-alpine meadows in the Sierra Nevada. A 234 km^2 upstream watershed supplies the meadow with surface water via the Tuolumne River and groundwater through fractured granite bedrock and hillslope moraines. More than 80% of the 1,000 mm average annual precipitation falls as snow during the winter (California Department of Water Resources station ID TUM), so annual hydrology is largely defined by the peak snow melt in the late spring. Soils in Sierra Nevada basins are generally thin, rocky, and have limited water storage capacity, but a thick top layer of organic rich mineral soil can exist in basins with sufficient moisture.

Observations of sediment in Tuolumne meadows reveal the composition consists of sands and gravels overlain by a layer of highly organic mineral soil. The sand and gravel aquifer drains rapidly after the spring melt, which is observable as a sharp decline in the water table. Residual meltwater is stored in the meadow as groundwater in the shallow aquifer or as soil moisture in the meadow sediments. Records of measured soil moisture (Figure 1b, solid lines) illustrate how soil moisture is stored disproportionately across the dual domain architecture of meadow stratigraphy. Saturated spring melt conditions decrease rapidly in the gravel layer with groundwater decline, while soil moisture is retained in the fine grained upper layer late into the growing season (Lowry and Loheide, 2010).

Vegetation communities range from sagebrush (*Artemisia tridentate*) in the driest regions to sedges (*E.G. Carex vesicaria*) and willows (*Salix eastwoodiae*) in the wettest regions (Cooper et al., 2006). The health and productivity of meadow vegetation is largely dependent on access to shallow groundwater (Lowry et. al. 2011), so the arrangement of vegetation is strongly correlated to groundwater availability (Loheide and Gorelick, 2007; Hammersmark et al., 2008; Loheide et al., 2009). The motivation of this study is to investigate the effects of organic matter on soil water retention and its role in supplying water for transpiration.

METHODS

A three pronged approach was used to further develop the linkages among soil organic matter, soil water retention and water availability in Tuolumne Meadows. First we observed soil moisture dynamics in the meadow through depth and over time. Then we measured the soil water retention of soil samples that vary in soil organic content and defined trends to describe how soil water retention and soil organic matter relate to each other. Finally, we incorporated the measured trends into a validated numerical model to replicate the observed soil moisture dynamics and demonstrate the sensitivity of plants to changes of soil organic matter.

Monitoring Soil Moisture Dynamics

To observe the soil moisture dynamics in Tuolumne Meadows, we recorded soil moisture data with MLX2 Theta Probes (Delta-T Devices Ltd.) at depths of 15 cm, 30 cm, 50 cm, 75 cm, and 100 cm (Figure 1a) in the summer of 2011. The three shallowest probes are in the fine-grained highly organic soil, while the bottom two are in the sands and gravel. A pressure transducer housed in a monitoring well within a 2 m distance measured the depth of

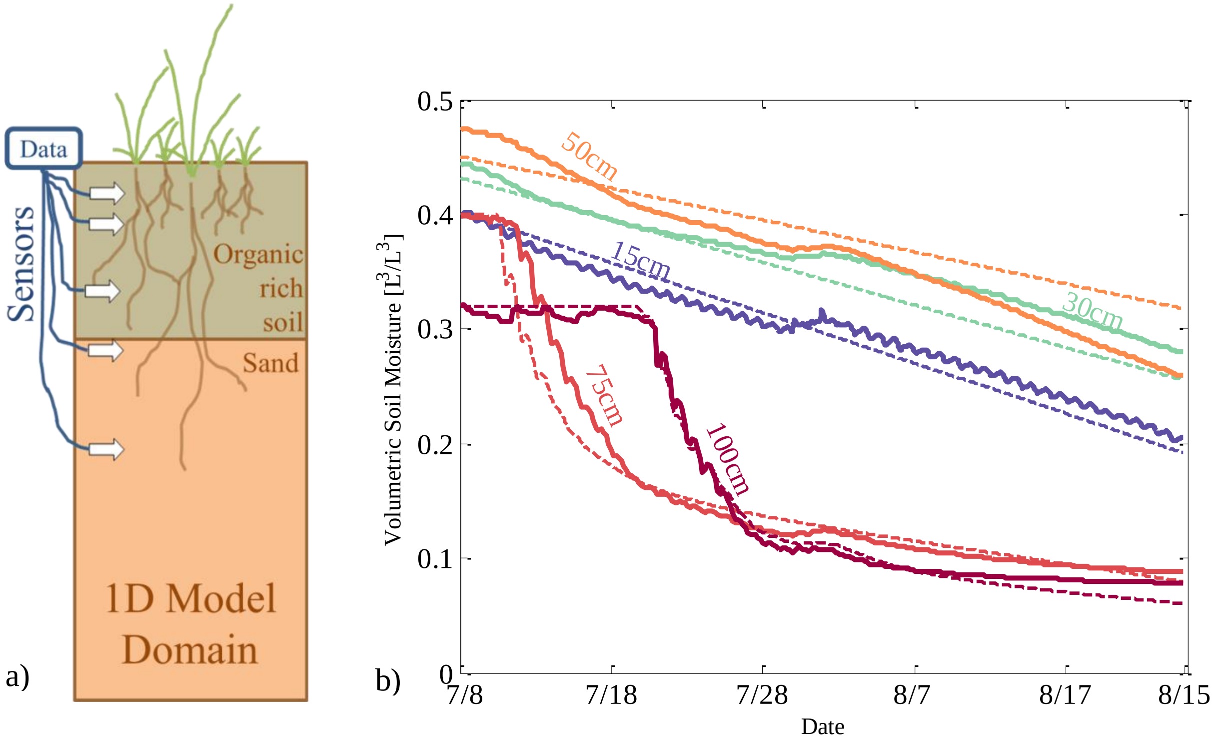

Figure 1: *(a) Typical subalpine meadow stratigraphy consists of sands and gravels overlaid by a layer of fine grained organic rich soil. Soil moisture measurements (b, solid lines) were recorded in the summer of 2011 and compared to the model simulations (b, dotted lines). The measurements show that water drains rapidly from the deep sandy gravel layer (75 cm and 100 cm probes) but is retained in the organic rich meadow topsoil (15 cm, 30 cm, and 50 cm probes).*

groundwater. The data recorded by the pressure transducer were corrected for barometric effects according to barometric readings measured in the meadow for the same time period.

Characterization of soil organic matter and water retention

We measured organic matter and soil water retention at nineteen sites distributed across the meadow. Using vegetation as a guide, we sampled locations that appeared to represent the range of conditions found within the meadow. Undisturbed soil samples were taken from a depth of 10 cm with a 5.1 cm diameter soil core sampler. Soil water retention was measured using the method described by (Wang & Benson, 2004) and the data were fit to the Van Genuchten soil water retention model (equation 1) (Van Genuchten, 1980).

$$\theta(\psi) = \theta r + \frac{\theta s - \theta r}{[1 + (\alpha|\psi|)]^{1-1/n}} \tag{1}$$

We compared soil organic content to the best fit soil water retention parameters to identify the relationship between organic matter and soil water retention.

Soil organic content was measured as the mass lost on ignition (ASTM Standard D 7348 – 08) after completion of the soil water retention characterization experiments. Soil texture, or the mineral fractions of sand, silt, and clay, was calculated from the distribution of particle sizes. We measured the particle size distribution curves for each soil sample following the ASTM guideline D422-63 Standard Test Method for Particle-Size Analysis of Soils. Following the USDA soil textural classification system, we defined the particle size limits for sand (2 mm to >0.05 mm), silt (≤0.05 mm to ≥0.002 mm), and clay (<0.002 mm). Roots and other visible organic matter were removed before particle size analysis procedure was completed.

Measurements of soil water retention were used to estimate the amount of water made available to plants for each soil sample, which varied in soil organic content. The capacity of water storage is represented with a metric called Available Water Capacity (herein referred to as AWC), which has been used to represent the amount of water available to plants (Van Diepen, 1993; Katterer et al., 2006). AWC is calculated as the difference in moisture between the Field Capacity pressure (Ψ_{FC} = 3.36 m, or -33 kPa) and the Wilting Point pressure (Ψ_{WP} = 153 m, or -1500 kPa).

Numerical Modeling of Variably Saturated Groundwater Flow and Root Water Uptake

A more complete way to evaluate the spatiotemporal impact of soil water retention on plants across a range of soil organic matter content is through numerical model simulation. We used a 1-D variably-saturated groundwater flow model developed in COMSOL following the approach of Lowry & Loheide, (2010) to simulate the response of soil moisture and transpiration to a water table decline characteristic of that observed in Tuolumne Meadows and other examples in the literature (Loheide and Gorelick, 2007; Hammersmark et al., 2010). The model domain represents the observed dual domain soil stratigraphy and consists of a 0.7 m thick upper-layer of organic mineral soil on top of 2.3 m of sand and gravel (Figure 1a). The 3 m soil column is discretized into 0.01 m elements. The governing equation is Richards Equation (Richards, 1931), and root distribution function, boundary conditions, initial conditions, hydraulic conductivity, and reduction functions for evaporation and transpiration the same as those used by (Lowry & Loheide, 2010). Based on the work of (Metselaar & Van Lier, 2007), the transpiration reduction function accounts for the water limiting conditions that cause water stress. This function sets RWU equal to the potential value, and reduces the rate curvilinearly to zero between the pressure heads $\Psi_{\text{Onset of Water Stress}} = -19$ m and $\Psi_{\text{WP}} = -153$ m. The Van Genuchten soil water retention model parameters are specified separately for both the upper and bottom layers.

To validate the model we simulated the soil moisture response (Figure 1b, dotted lines) using the groundwater well hydrograph observed in the meadow as the lower boundary condition (Figure 2). For the validation, upper soil layer parameters for thickness and the Van Genuchten soil water retention model parameters n, α, saturated water content (θs), and residual water content (θr) were measured directly from a 10 cm deep sample taken at the location of the soil probes. Hydraulic conductivity for both layers was defined by literature values for silt (upper layer) and loamy sand (lower layer) (Carsel & Parrish, 1988). Van Genuchten retention model parameters for the lower layer were fit to match the recorded data while remaining consistent with values for a coarse sand (Carsel & Parrish, 1988). From depths 0.7 m to 0.8 m, θs=0.40 [L^3/ L^3], θr=0.04 [L^3/ L^3], n=1.89, and α=13.5. From depths 0.8 m to 3.0 m, θs=0.32 [L^3/ L^3], θr=0.05 [L^3/ L^3], n=2.48, and α=16.4.

To assess the sensitivity of transpiration to soil water retention, we performed a scenario analysis. For each scenario, the soil water retention parameters for the upper layer were set to a particular soil water retention curve from a spectrum that is consistent with the range of organic content found in the meadow. The transpiration was simulated for a 180 day growing

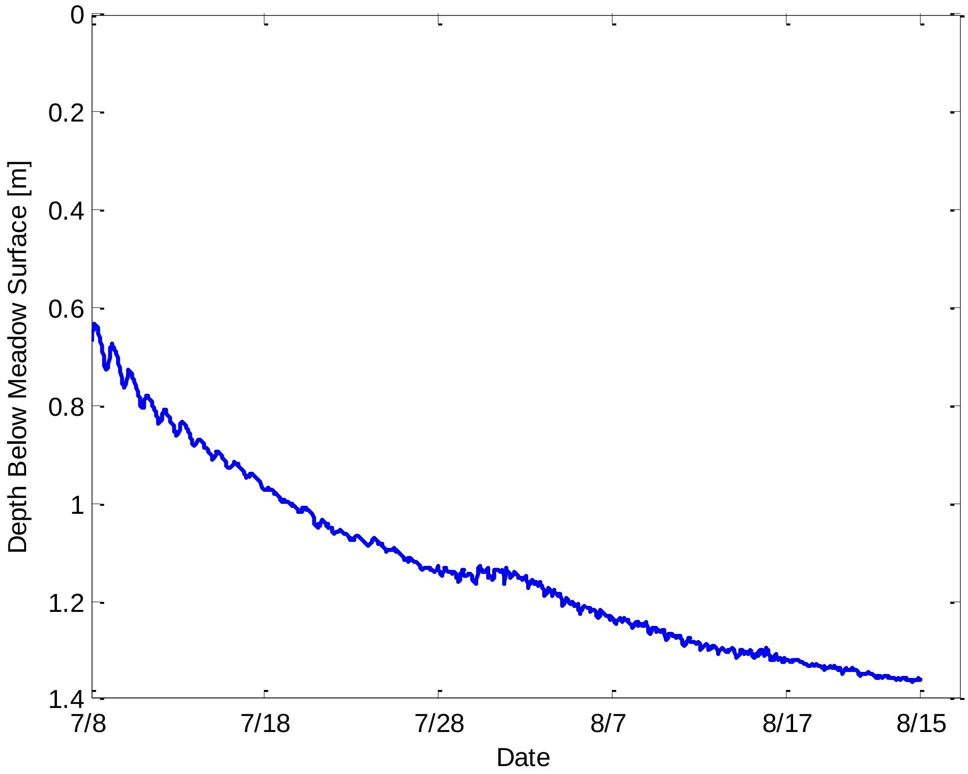

Figure 2: *The well recorded at the soil moisture nest over the period of recorded soil moisture used in the model validation.*

season that is representative of Tuolumne Meadows through a decreasing water table depth hydrograph. The hydrograph begins with saturated conditions to represent the annual spring flood and declines exponentially (equation 2), which is similar to examples in the literature for wet meadows in the Sierra Nevada (Loheide and Gorelick, 2007; Hammersmark et al., 2010). It is defined by:

$$Hp = (3 - WT_{max}) + WT_{max}e^{(-\lambda * t)} \tag{2}$$

where Hp is the specified pressure head bottom boundary, WT_{max} is the maximum depth (m) to which the water table will asymptotically approach, λ is the water table decay constant, and t is time. We use WT_{max} = 2.9 m and $\lambda = 0.05$. To complete the scenario analysis, we varied soil water retention parameters of the top soil layer according to a range of organic contents observed in the meadow to assess transpiration sensitivity to changes in soil hydraulic properties (θs from 0.44 [L^3/ L^3] to 0.68 [L^3/ L^3] and α from 1.31 to 0.50).

RESULTS

Qualification: Soil Water Retention Varies with Soil Organic Content

Our measurements of soil organic content and soil water retention throughout the meadow showed substantial variability in both organic content and in soil water retention curves. Figure 3 presents the soil water retention curves, with the color of each curve representing the amount of organic material found in the sample. Curves with less organic matter (more red) tend to have less moisture at saturation and lose more water with increasing suction, while curves with more organic matter (more blue) tend to have more moisture at saturation and retain it longer under increasing suction. This indicates that soil water retention varies with organic content.

Quantification: Variability in Θs and α With Organic Content and Their Control on Retention

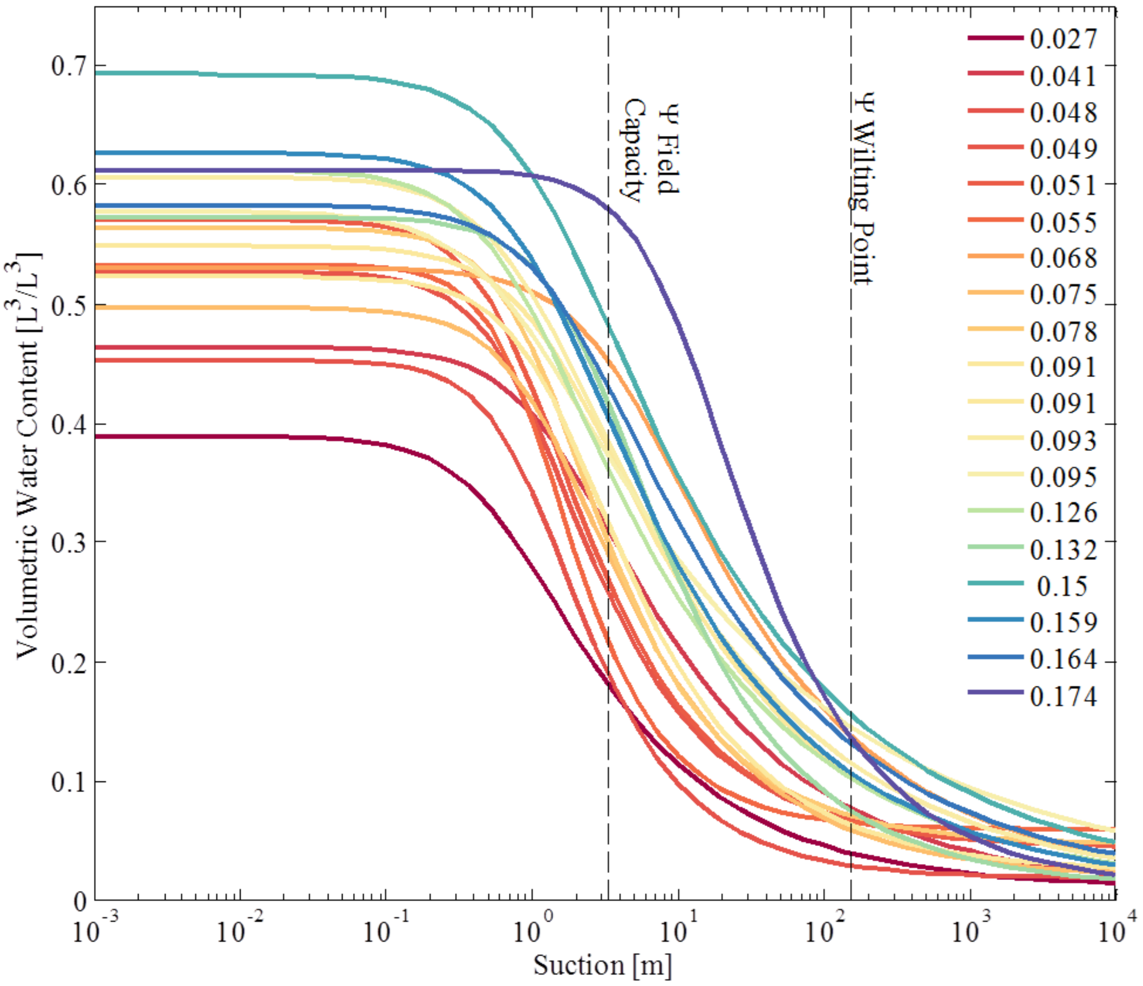

Figure 3: *Soil water retention curves measured in Tuolumne Meadows are colored according to the amount of organic material in the sample. Curves with low organic content (more red) have less moisture at saturation and lose it with smaller increases in suction. Curves with more organic matter (more blue) have more moisture at saturation and retain it longer under increasing pressure. Moisture lost between* $\Psi_{Field\ Capacity}$ *and* $\Psi_{Wilting\ Point}$ *is considered Available Water Capacity (AWC).*

To quantify the relationship between soil organic content and soil water retention, we compared the organic content values to the best fit Van Genuchten parameters of each curve. The volumetric water content at saturation (θs), which represents the maximum water content that the soil can hold, increases with organic content (Figure 4a). The values of θs increase with organic content from 0.389 [L^3/ L^3] to 0.693 [L^3/ L^3] (R^2 = 0.625). The Van Genuchten parameter α controls the suction required to initiate the release of moisture and how readily moisture is released with increased suction. The values of α range from 0.10 m^{-1} to 1.56 m^{-1}. The values decrease with increasing organic content (Figure 4c) (R^2 = 0.232). A nearly zero slope between organic content and parameters *n* and *θr* suggest these parameters do not vary substantially with organic content (R^2 = 0.16, m= -0.14; and R^2 = 0.20, m= -0.16 respectively).

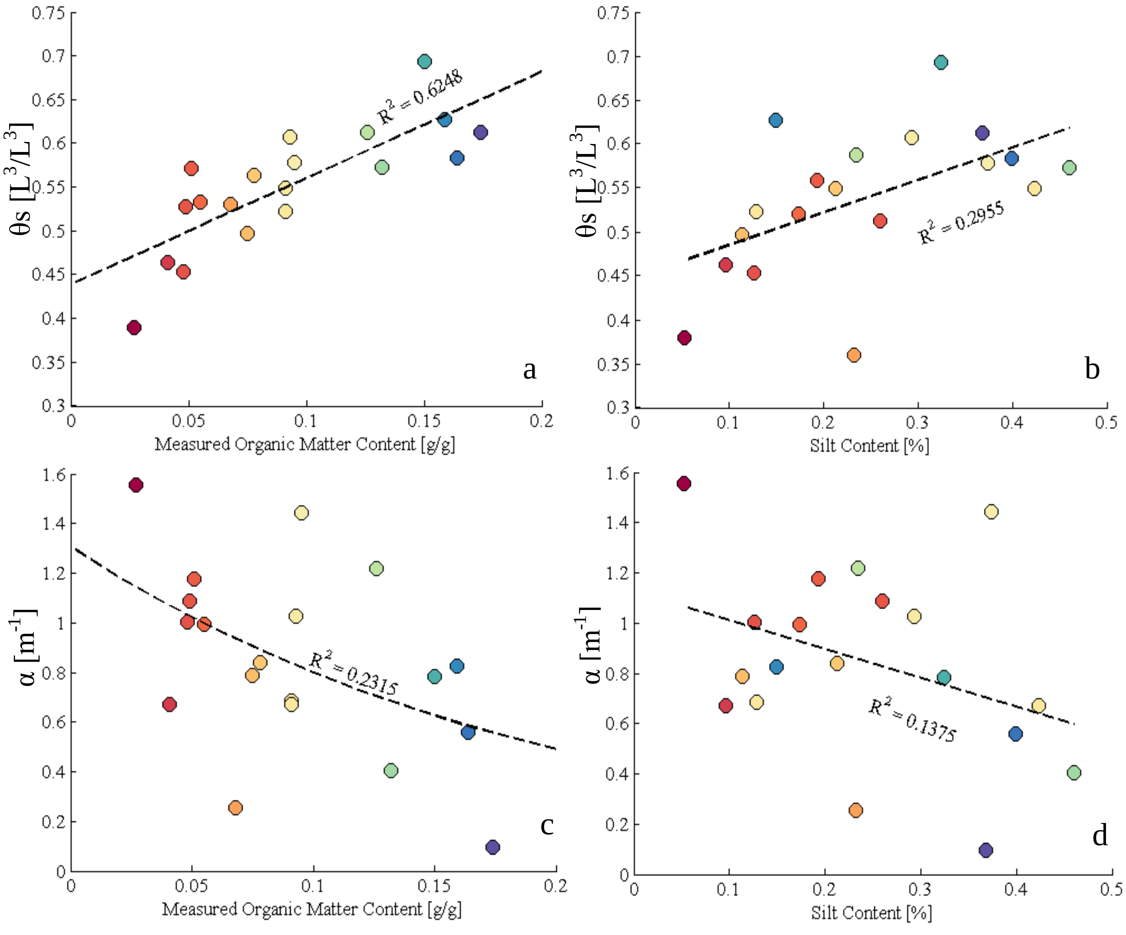

Figure 4: *(a) The correlation between the Van Genuchten parameter θs and organic content. (b) The correlation between θs and silt content. (c) The correlation of the Van Genuchten parameter α and organic content. (d) The correlation between α and silt content.*

Qualification: Soil Texture is Similar in Clay Content, and Varies in Sand and Silt Content

The fractions of sand, silt, and clay were determined from the particle size distributions of each sample. The soil textural triangle (Figure 5) shows these fractions for each sample, with the color of each dot representing the amount of organic material. Variability clay content is small, and fractions of clay range from 3.3% to 13.5%. Therefore, the majority of variability in texture is explained as a nearly linear tradeoff between silt content and sand content. Silt content ranges from 5.3% to 46.0% and sand content ranges from 40.6% to 88.5%. The USDA soil classification system classifies these samples as either loamy sand, sandy loam, or loam.

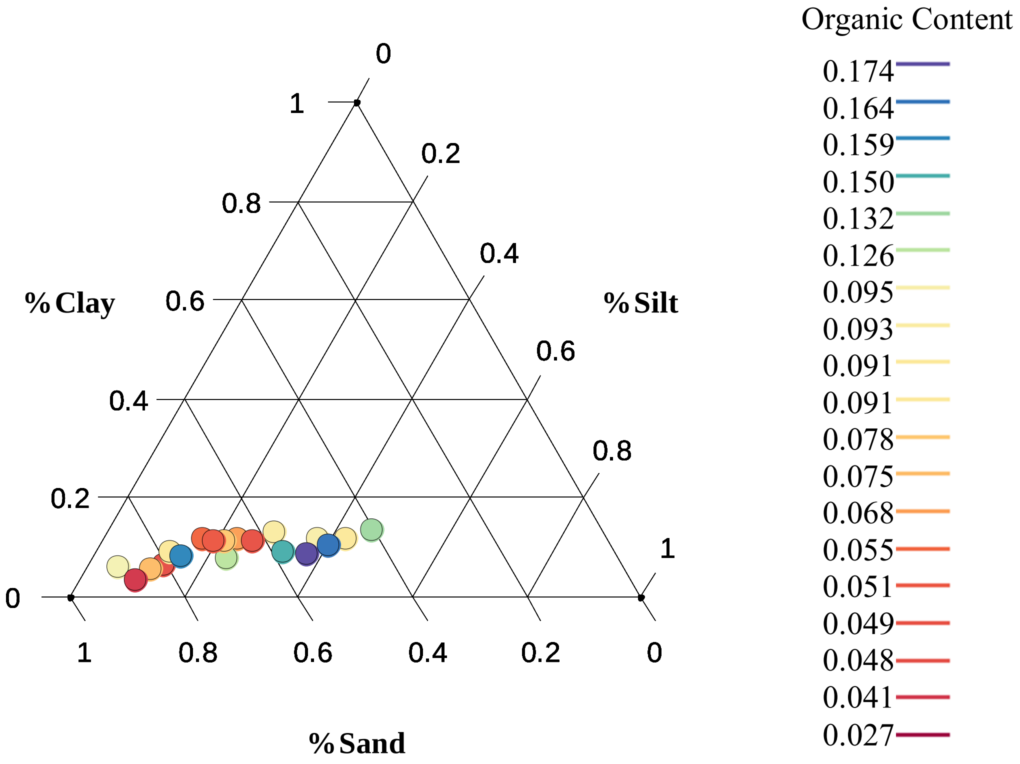

Figure 5: *The soil texture for each soil sample is represented by a dot in the soil textural triangle. The color of the dot indicates the organic content of the sample.*

The results from the comparison of soil textural fractions to Van Genuchten soil hydraulic parameters show similar but opposite relationships of sand and silt fractions with soil water retention. The trends are similar but opposite because the tradeoff between sand content and silt content is nearly linear due to a lack of variability in clay content. The trends of retention parameters with silt content are shown here because they are slightly more significant than the trends with sand content. θs increases with increasing silt content ($R^2 = 0.30$, Figure 4b) and α decreases with increasing silt content ($R^2 = 0.14$, Figure 4d). The Van Genuchten parameters n and θr do not vary substantially with silt ($R^2 = 0.126$ for n, and $R^2 = 0.004$ for θr). As described in the second and third paragraphs of the Discussion section, we attribute the variability in retention parameters to organic content rather than to texture.

The Spectrum of Curves That Describe the Water Retention of Soil from 0% to 20% Organic Content

We used these trends of θs and α with organic content to create a spectrum of soil water retention curves that describe how soil water retention changes with organic content (Figure 6). The spectrum shows that retention curves with low organic content (more red) have less moisture at saturation and release it more completely with increasing suction. Curves with more organic matter (more blue) have more moisture at saturation and retain more water under increasing suction. For each curve, θs and α vary according to the trend lines in Figure 5a and Figure 5c respectively. The influence of the θs parameter is shown in the increasing moisture values at the smallest value of suction. The influence of the α parameter is shown in

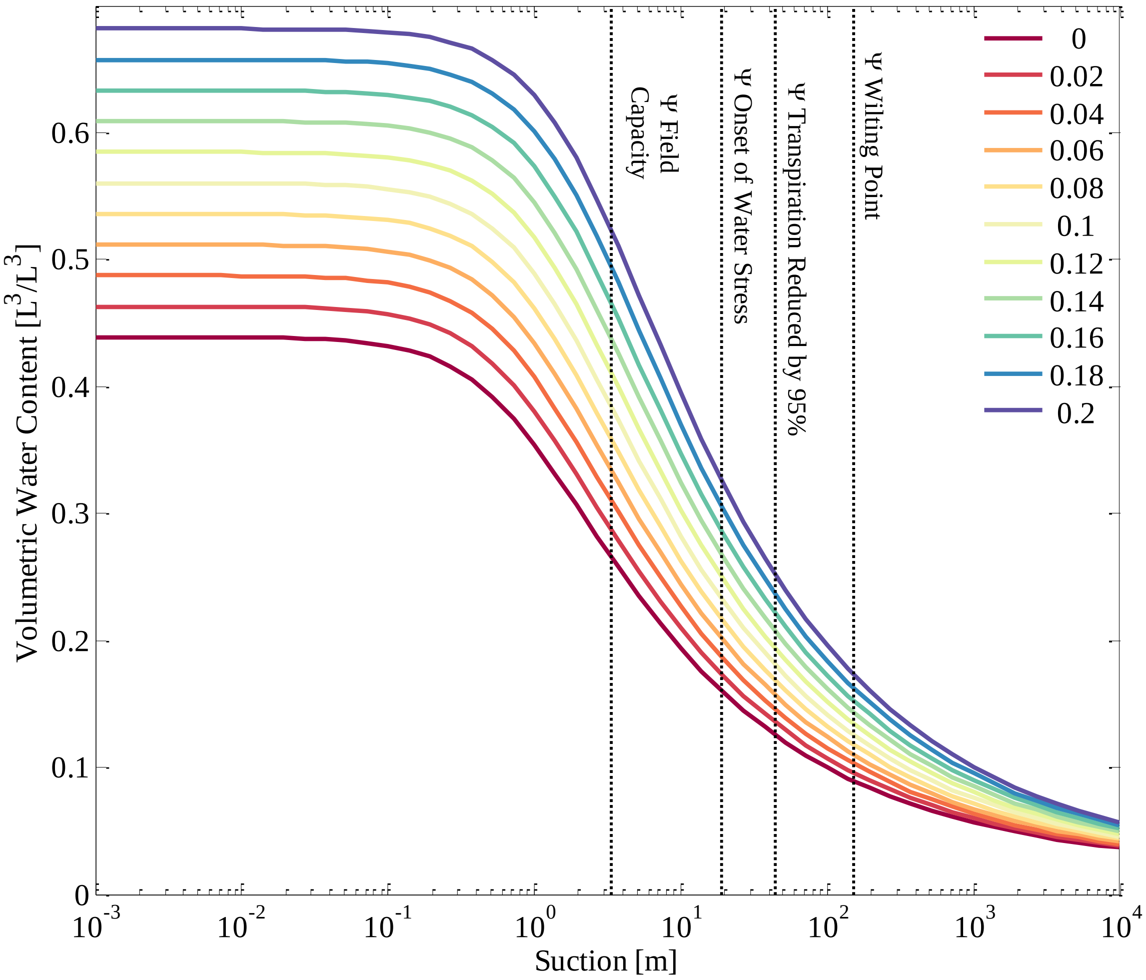

Figure 6: *Soil water retention curves are predicted between 0% and 20% organic content, and are colored according to the organic content. Plants begin to experience water stress at* $\Psi_{\text{Onset of Water Stress}}$ *= -19 m due to a reduction in transpiration. Transpiration continues to decrease with increasing suction and reaches 5% of the potential rate at* Ψ *= -44 m. Transpiration is equal to zero at the wilting point, or* Ψ_{WP} *= -153 m.*

the delayed moisture decrease, or the delayed downturn of the curves, with increasing organic content. Another influence of the α parameter is the reduced amount of moisture released with increased suction, which generates more space between the curves at suction values larger than the value at the initial downturn. Because the Van Genuchten parameters n

and θr do not vary significantly with organic content, this spectrum was generated with values consistent with the range measured in the meadow. In all curves, n is equal to 1.34 [dimensionless] and θr is equal to 0.02 [L^3/ L^3].

Representing the Water Capacity of the Retention Curve

The AWC values from the soils found in Tuolumne Meadows increase dramatically over the range of sampled organic content (Figure 7, colored dots). A linear trend (Figure 7, long dashed line) shows an increase of 120% in AWC from 0.17 [L^3/ L^3] to 0.37 [L^3/ L^3] over the range of sampled organic content. We also show the AWC values calculated from the spectrum of modeled retention curves (Figure 7, short dashed line). This modeled AWC

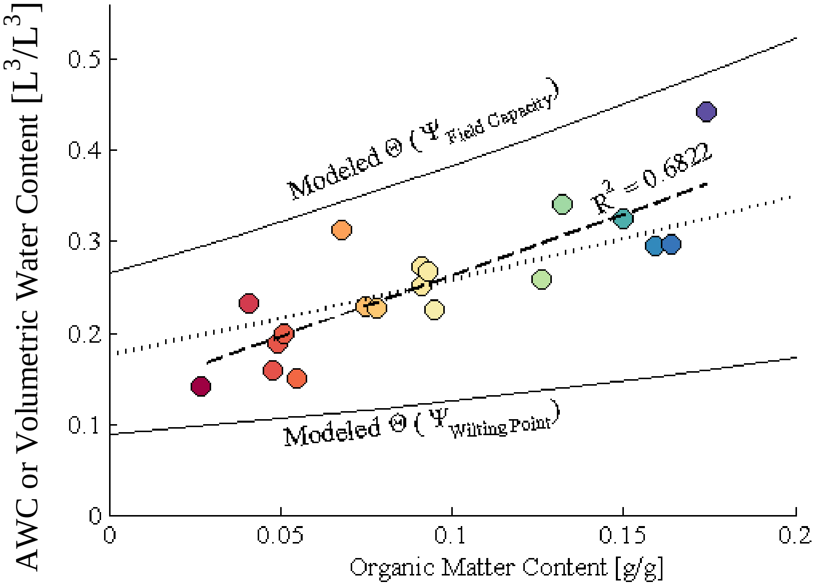

Figure 7: *The amount of water available to plants, or Available Water Capacity (AWC), increases with increasing organic content. AWC is calculated as the difference in moisture between* Ψ_{FC} *and* Ψ_{WP}. Ψ_{FC} *and* Ψ_{WP} *are shown graphically in Figure 3 and Figure 6. Colored circles are AWC values calculated from the measured water retention curves in Figure 3. These measured data are fitted with the long-dash linear trend (*R^2*=0.6822). The AWC values corresponding to the spectrum of modeled curves are shown two ways: (1) by the short dash line, and (2) by the space between the lines representing* θ (Ψ_{FC}) *and* θ (Ψ_{WP}).

trend line is less sensitive to organic matter because the trend lines for α and θs reduce the influence of the extreme values of the measured data. The moisture values of Ψ_{FC} and Ψ_{WP} both increase with organic matter, but the Ψ_{FC} line increases with a larger slope. Therefore, the corresponding AWC values, which represent the differences between these curves, also increase. The soil water retention curves in soils with more organic matter have higher AWC values because they tend to start with more water (have a larger θs) which is retained at Ψ_{FC} (due to smaller α values). Higher organic soils also retain more water at Ψ_{WP}, which means that a larger amount of water is left inaccessible to plants. This result, however, does not correspond to lower AWC values because the increase in moisture at Ψ_{FC} is much larger.

The Results of the Model Validation

The 1-D model accurately simulates the soil moisture dynamics observed in the meadow. The Delta-T soil moisture probes (Figure 1a) recorded data (Figure 1b, solid lines) that match well with the simulated soil moisture records at the same depths (Figure 1b dashed lines). The Nash Sutcliffe model efficiency was used to evaluate the model performance. Values can range from 1 to -∞, where value of 1 indicates a perfect model prediction and a value of 0 indicates that the model predictions are as accurate as the mean of the observed data. The Nash Sutcliffe model efficiency results for each probe depth (from shallow to deep) are 0.9071, 0.4278, 0.4333, 0.9837, and 0.9476. Both observed and simulated soil moisture records show retention in the upper layer that persists long after the water table drops below. This stored soil moisture is primarily depleted through evaporation (from the surface) or root water uptake (throughout the domain) with minimal downward percolation into the sand and gravel layer. The records from the gravel (75cm and 100cm depths) show almost immediate drainage as soon as the water table drops below those sensor depths.

The Scenario Analysis Shows that Changes in Retention Influence Transpiration

The results from the numerical modeling scenario analysis show the effects of water retention on seasonal transpiration. Examples of simulated transpiration are shown for each of the modeled retention curves (Figure 8), which represent a range of organic content from 0% to 20%. In general, soils with more organic matter retain more water later into the growing season and delay transpiration reductions caused by water stress. Transpiration rates for all curves are equal to the maximum rate at the beginning of the season due the saturated initial conditions associated with the spring melt. Rates begin to vary later into the season as some roots in the root profile begin to experience water stress and reduced RWU. The initial reduction seen within a few days of day 35 in all scenarios occurs when the sand layer becomes depleted due to drainage and initiation of water stress occurs. Large reductions in transpiration occur first in the soils with the least organic matter (most red) near day 70 of the growing season. The delayed reduction in soils with increasing organic content shows that soils with more organic matter keep transpiration high later into the growing season.

Increased Retention in the Top Layer Quickens the Onset of Water Stress in the Lower Layer

The scenario analysis shows that increased retention in the upper layer delays the major reductions in transpiration caused by the onset of water stress until later in the growing season. Close inspection of the transpiration rates shows that this interaction is complex and nonlinear. On day 33, the transpiration rate of most organic soil is the first to experience a

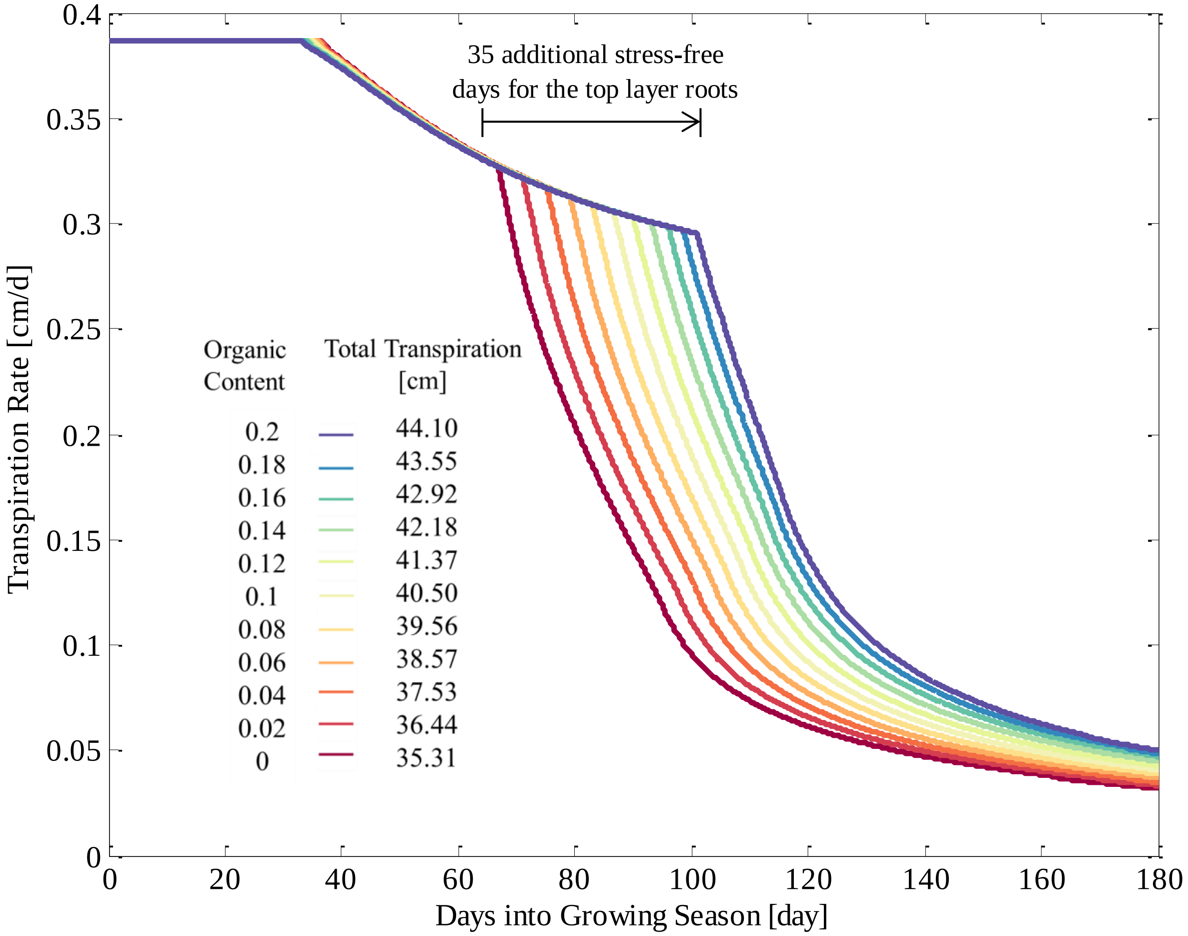

Figure 8: *Soils with more organic matter retain more water later into the growing season and delay transpiration reductions caused by water stress. Model simulations of transpiration rate are colored according to the organic content of the top soil layer used in the simulation. The simulations all show a gradual decrease in transpiration as larger portions of the root zone experience increasing amounts of water stress, but simulations with high organic soil (more blue) show this effect is delayed.*

decrease due to water stress (Figure 8, purple curve). This occurs because the more retentive upper layer minimizes water drainage into the gravel, leading to water stress for roots below the top soil layer. An examination of the pressure head with depth on day 33 (Figure 9b) shows that water stress first occurs directly below the transition between soil layers (>0.8m) where pressure head first reaches $\Psi_{\text{Onset of Water Stress}}$. Root water compensation is not considered in the 1-D model, so plants cannot preferentially draw water from the excess moisture stored in the upper layer or from the groundwater below when one portion of the root zone becomes water limited. Although the most organic soil is the first to show this phenomenon, all soils experience this within 3.5 days. This minor difference in onset of transpiration reduction is soon outweighed by a major difference in transpiration caused by water stress in the upper soil layer.

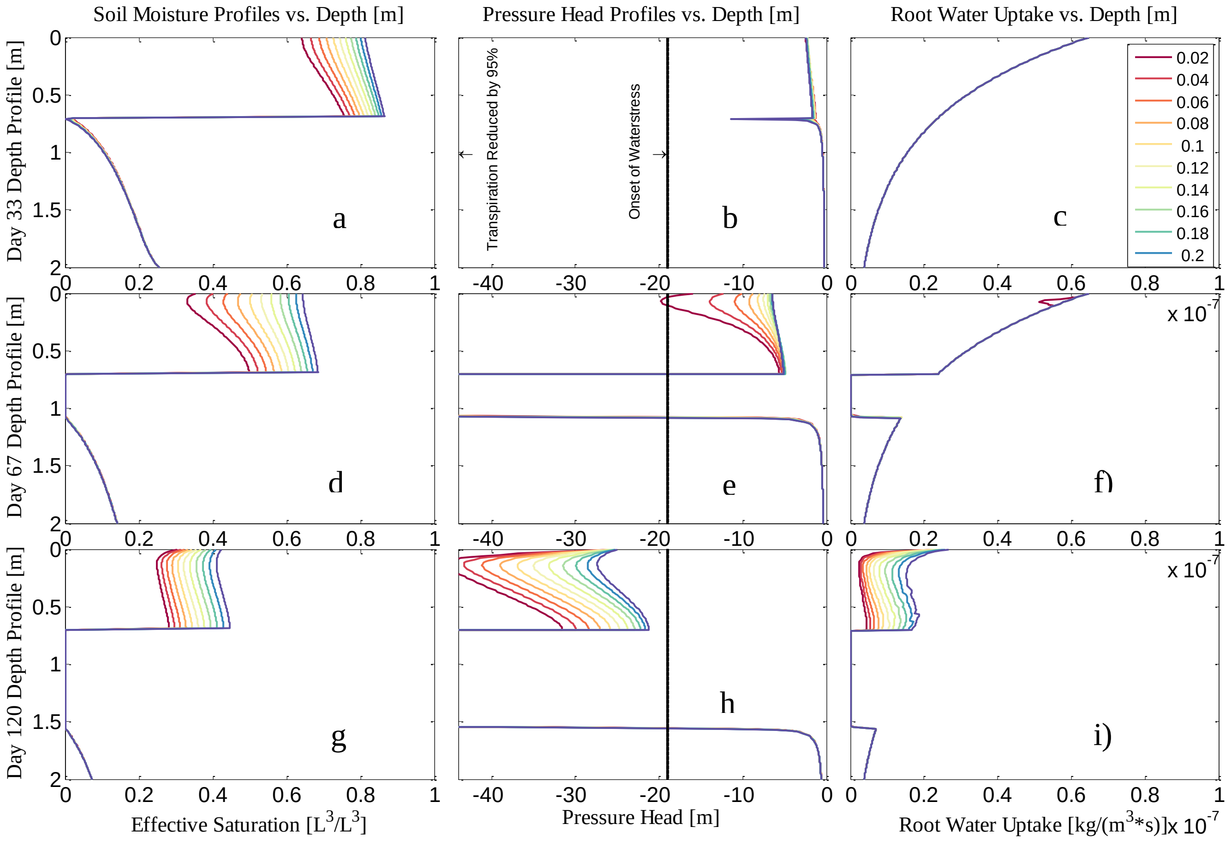

Figure 9: *The depth profiles of soil moisture, pressure head, and root water uptake (RWU) on days 33, 67, and 120 of the model simulations are shown for each scenario, and colored according to the associated soil organic content.*

Increased Retention in the Top Layer Delays Water Stress in the Top Layer

The soil with the least organic matter (dark red) is the first to experience a severe decrease in transpiration. On day 67, the roots in this soil have extracted enough moisture from the upper layer to induce water stress in some portion of the layer. This occurs because the pressure head at which water stress begins has been reached on the soil water retention curve in a portion of the root zone. This is visible on the pressure head depth profile where the dark red curve drops below the pressure head associated with the onset of water stress (Figure 9e, dark red curve). The soil water retention curves with less organic matter have smaller θs values so the roots are able to more quickly deplete moisture reserves in the soil and reach $\Psi_{\text{Onset of Water Stress}}$. As RWU continues to extract moisture, pressure head also decreases and more of the root zone experiences increasing water stress, thus rapidly reducing transpiration. This effect does not occur in soil with 2% organic content until day 71, or four days later. The most organic soil experiences this upper layer water stress a full 35 days after the soil with zero organic content. Water stress is eventually experienced across all upper layer root zones (Figure 9h) and all soils show reductions of transpiration due to water stress.

Increased Retention Contributes Water to Transpiration During the Late Summer

Increased soil water retention provides a substantial amount of water to plants. There is a difference in total transpiration of 8.80 cm between the soil with the most organic matter and that with the least. This stems primarily from the higher θs moisture values (origin of curves in Figure 6), which indicate more water can eventually be transpired by roots during the season. We determine the transpiration rate difference for each scenario by subtracting the transpiration associated with zero organic content from the transpiration of the soil of interest

(Figure 10). The results of this analysis show that the largest differences in transpiration, or the largest contributions from increased organic content, occur late in the season after day 66. Peak contributions occur between day 66 and day 101.

The Marginal Benefit of Increased Organic Content is Larger in Less Organic Soils

The largest difference in cumulative transpiration between scenarios occurs in the soils with

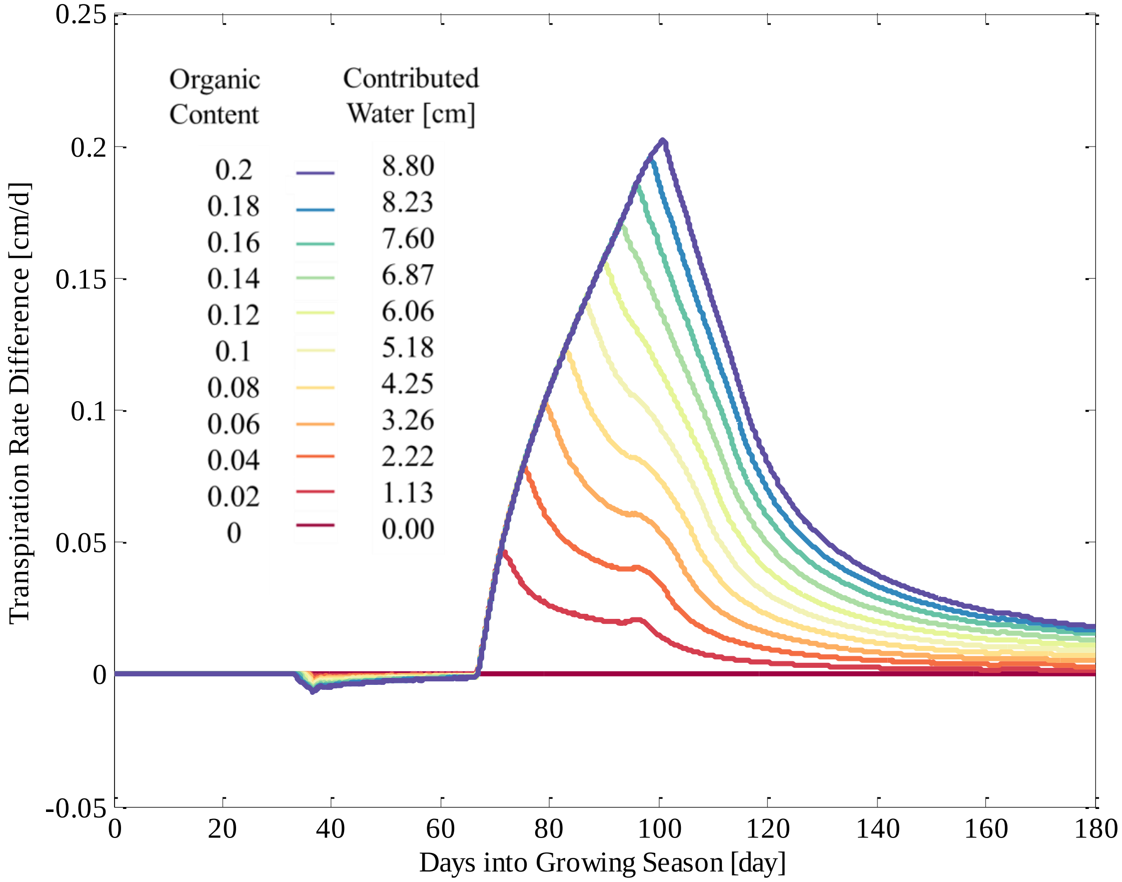

Figure 10: *The transpiration rate difference for each scenario is found by subtracting the transpiration of a soil with zero organic content from the transpiration of the soil of interest. Soils with more organic matter contribute more water to transpiration. The effect is particularly significant during the driest part of the season when plants are most stressed.*

the least organic content (see “Contributed Water” values in Figure 10). The water contributed to transpiration for each 2% increase in organic content is used to calculate the marginal benefit of organic matter across the range of modeled organic content. Figure 11 shows the marginal benefit of additional available water for a 1% increase in organic content. This figure shows the value of organic matter is highest in soils with the least organic content.

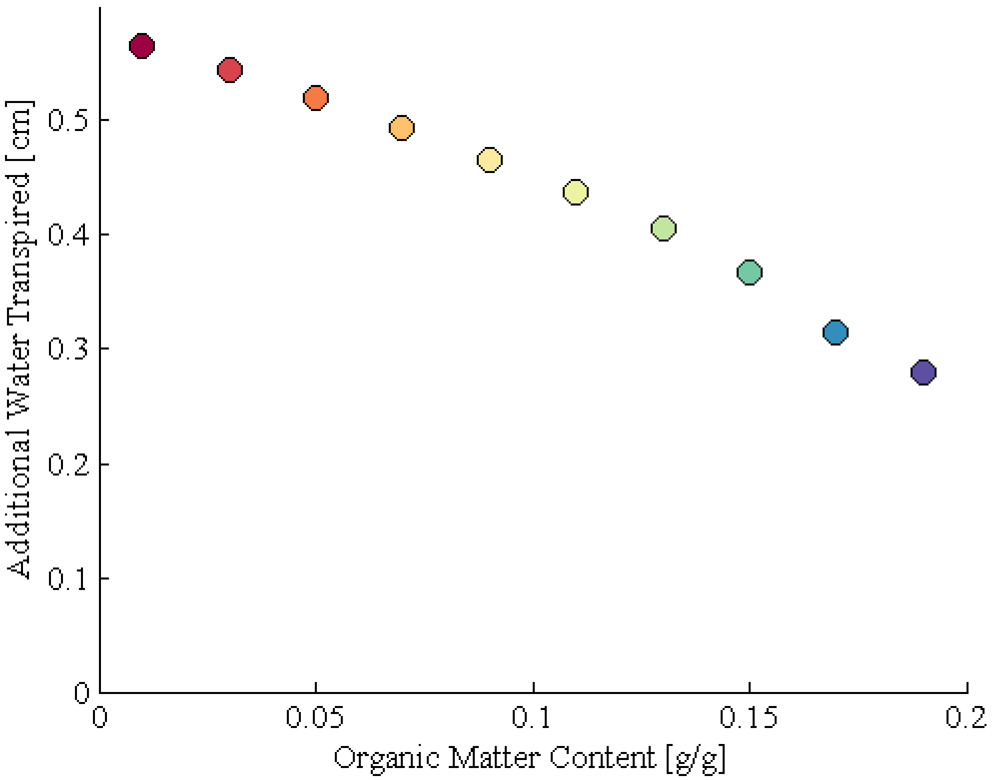

Figure 11: *The marginal increase in total transpiration from an increase in organic content decreases with increasing organic content. The benefit of additional organic matter is the largest in low organic soils, which means they are most vulnerable to impact.*

DISCUSSION

The θs and α Correlations Imply Soil Water Retention is Lost with Organic Content

The Van Genuchten soil water retention parameters θs and α depend significantly on soil organic content. θs can have implications for determining the total amount of water available to plants because it controls the highest moisture content value of the soil water retention curve. The strong correlation of θs with organic matter suggests that a loss of organic matter affects the total amount of water that can be stored in the soil. The relationship with α is more complex: it suggests that a loss of organic matter decreases the suction required to initially release moisture and decreases how much moisture is lost with incremental increasing suction. Together, these trends suggest that losses or gains of organic matter substantially affect the amount of water that can be stored in the soil and the ability of soil to retain moisture. A loss of organic matter in Tuolumne Meadows may negatively affect soil water retention and decrease the amount of water retained from spring snowmelt to support plants through the dry growing season.

The dependency of soil water retention on soil texture observed in Tuolumne Meadows supports the conclusion of Jamison (1953) that organic matter can have a strong influence in sandy soils with low clay content. Also, our findings remain consistent with the general trends of widely used pedotransfer functions (Schaap et al., 2001; Vereecken et al., 1989). Carsel and Parrish (1988), however, presented probability density functions for parameters of soil moisture relationships to capillary head that predicted the θs values for loamy sand (M=0.41 [L^3/ L^3], SD=0.09), sandy loam (M=0.41 [L^3/ L^3], SD=0.09), and loam (M=0.43

[L^3/ L^3], SD=0.10) that do not represent the full range of the values we observed for the same textural classifications. The prediction of θs values by Saxton (2006), which allows for the inclusion of organic content as a predictor variable up to 8%, more closely represent our observed range (θs = 0.38 [L^3/ L^3] for loamy sand with 0% organic content and θs = 0.65 [L^3/ L^3] for a loam with 8% organic content. Because the θs parameter has the largest effect on the shape of the retention curve, it is likely that the soil in Tuolumne Meadows is highly retentive not just from texture, but rather organic content. Also, due to the consistency with the Saxton (2006) model, it is reasonable to expect the textural contribution to θs to range from 0.38 [L^3/ L^3] to 0.40 [L^3/ L^3]. This is the range predicted by Saxton (2006) for the textural range we observed with 0% organic content, and is consistent with the range predicted by Carsel and Parish (1988). In Tuolumne Meadows, the contribution of organic content to retention is particularly clear due to the lack of variability in clay content, which can have similar effects on soil water retention as soil organic content (Ebrahimi et al., 2014; Kern, 1995). The demonstration of the strong dependency of soil water retention on organic content is particularly valuable because soil texture cannot be influenced by ecosystem management actions as readily as soil organic matter.

Similar to θs, the α values predicted for loamy sand (M=12.4, SD=4.3), sandy loam (M=7.5, SD=3.7), and loam (M=3.6, SD=2.1) are substantially different than values we measured, which range from 0.1 to 1.3. Because the observed α values are outside the range of expected values, and represent more retentive soils, we attribute this increased retention (low α) to organic matter. The differences in predicted α values and θs values for the range of soil textures encountered in Tuolumne Meadows suggests that soil texture is not the primary driver of variability in retention characteristics. For this reason, we assume constant textural types, and attribute observed difference in water retention characteristic to organic matter variability.

The Timing of the Contributed Water Increases the Value of Organic Content to Plants

The results of the 1-D model demonstrate the implications for plant communities caused by altered soil hydraulic properties and reveal the times when the impacts are most influential. The increased soil water retention provides a service to plants in addition to increased total water capacity. Changes in retention affect the timing and duration of water availability. This critical effect provides additional water in the upper soil layer and delays the onset of water stress in the top soil layer by as much as 35 days (arrow annotation in Figure 8). These additional 35 stress-free days for roots in the top soil layer occur at a critical time in the growing season. Limited precipitation in the Sierra Nevada Mountains during the summer requires plants to use sources of water other than precipitation during this time. Therefore, the slower decrease in transpiration delays when a 95% reduction in transpiration is reached and would likely allow plants more time to produce biomass such as roots, leaves, or seeds before the onset of senescence. This improves the fitness of plants, increases the chance of reproductive success, and provides greater biomass contributions of carbon input to the soil which helps to maintain soil organic content. Therefore, organic content offers an environmental service to plants by relieving the water stress in hot, dry summers, providing for the moist conditions required by riparian ecosystems, and promoting the maintenance of soil organic matter.

The Differences in the Marginal Benefit of Organic Matter Imply Resiliency and Vulnerability

The finding that organic matter content affects plant water availability suggests that riparian ecosystem management strategies could focus on managing soil moisture by influencing soil organic matter. The loss or gain of a percent organic matter has a differential effect depending on whether the soil initially has a high or low organic content. The marginal impact of altering organic matter on transpiration (Figure 11) can be used as a guideline for anticipating the effectiveness of management strategies attempting to remediate organic matter in soils in a manner similar to the way the concept of groundwater subsidies as introduced by Loheide and Lowry (2010) can be used to anticipate the effects of changing groundwater regimes on plant water use. The largest marginal contributions to transpiration occur in the least organic soils, so these soils stand to suffer the most when organic matter is lost. Sub-alpine meadows, or portions of meadows, with low organic matter are therefore the most vulnerable to severe changes in plant function and productivity if organic matter is lost (Norton et al., 2011). This means that equal losses in organic matter across the meadow could have serious consequences for the low organic matter places, while the organic rich places remain less disturbed. On the other hand, locations with high organic matter that experience a loss are more resilient since they are likely to retain the moisture required for productive wet meadow plants (like sedges) that can build and maintain soil organic matter.

Numerous efforts have been made to quantify hydrologic niches of vegetation based on groundwater depth regimes with the use of water table based metrics that include depth to water table (Berlow et al., 2002; Loheide & Gorelick, 2007) , frequency of high water levels

(Henszey et al., 2004) and sum-exceedance thresholds for water table depth which describe oxygen stress and water stress (Lowry et al., 2011; Silvertown et al., 1999). Less focus has been directed toward the development of soil moisture based metrics even though it is recognized that these groundwater related metrics are only a proxy for hydrologic conditions in the root zone such as water availability and redox conditions which affect plant physiology. Soil moisture is a more direct measurement of the physical phenomenon regulating root water uptake (Rodriguez-Iturbe, et al., 2007) and has been shown to better predict plant distributions than water table based metrics (Booth & Loheide, 2012a), but may be less frequently employed in groundwater dependent ecosystems due to the challenges of soil moisture data collection. Our finding of substantial variability in plant water availability related to variability in organic content even under conditions with the same groundwater regime, suggests that hydrologic niches that are articulated in terms of groundwater metrics are only transferable to the extent that similar soil organic matter contents would exist. The improved development of quantifiable and measureable environmental metrics for use in predictive ecological models can provide valuable insight to researchers and practitioners responsible for restoration planning by reducing the uncertainty of estimated ecosystem responses (Palmer & Bernhardt, 2006; Wohl, 2005; Bernhardt et al., 2005).

CONCLUSION

In this study, we sought to answer to the question *how much does soil water retention depend on soil organic content, and what is the impact to transpiration if soil organic content changes*. Our measurements of soils in Tuolumne Meadows revealed that soil water retention depends substantially on organic matter. Moreover, the predicted contribution to retention from texture alone does not account for the full range of retention we observe, so additional retention can be attributed to organic matter. The measured retention curves indicate that increased retention makes more water available to plants (increased AWC). By comparing simulated transpiration rates under different soil retention scenarios, we showed how plants are impacted by changes in organic matter. The scenario analysis showed the additional available water is used during the dry second half of the summer, meaning that increased organic matter not only affects the amount of water available to plants, but the timing and duration of it as well. The difference in transpiration rates is an indicator of the marginal benefit of organic matter, and reveals that transpiration is most sensitive to changes in organic content for plants in soils with the least organic matter.

A strong correlation between soil water retention and soil organic matter indicates that the loss of organic matter can result in decreased transpiration. Results demonstrate the importance of organic matter in providing water for transpiration throughout the dry season which has implications for (1) identifying restorations strategies that promote plant productivity and increased inputs to belowground organic matter (2) identifying areas with highest vulnerability or ammendability (3) identifying processes that inhibit and encourage meadow recovery. Management strategies should include efforts to preserve and promote organic matter, particularly in locations with the least organic soils.

ACKNOWLEDGEMENTS

This paper is based on research funded by the National Park Service under Study# YOSE-00502. Any opinions, findings, conclusions or recommendations expressed in this material are those of the authors and do not necessarily reflect the views of the National Park Service. We would like to Carolyn Voter and Sam Zipper for their helpful comments during the development of this manuscript. We would also like to thank Chris Lowry for his continued effort to help us adapt the initial design of his 1-D variably saturated groundwater flow model for a different application. The field work and data collection required by this research would not have possible without the help of Evan Wolf and David Cooper. We are very grateful to Jim Roche, Sue Beatty, and the rest of the National Park Staff for providing the resources necessary to complete this work, and for insightful conversations regarding the needs and interests of the project.

REFERENCES

Allen-Diaz, B. (1991). Water-Table and Plant-Species Relationships in Sierra-Nevada Meadows. *American Midland Naturalist*, *126*(1), 30–43. doi:10.2307/2426147

Arya, L., & Paris, J. (1981). A Physicoempirical Model to Predict the Soil-Moisture Characteristic from Particle-Size Distribution and Bulk-Density Data. *Soil Science Society of America Journal*, *45*(6), 1023–1030.

Berlow, E. L., D'Antonio, C. M., & Reynolds, S. A. (2002). Shrub expansion in Montane meadows: The interaction of local-scale disturbance and site aridity. *Ecological Applications*, *12*(4), 1103–1118. doi:10.2307/3061039

Bernhardt, E. S., Palmer, M. A., Allan, J. D., Alexander, G., Barnas, K., Brooks, S., … Sudduth, E. (2005). Ecology - Synthesizing US river restoration efforts. *Science*, *308*(5722), 636–637. doi:10.1126/science.1109769

Booth, E. G., & Loheide, S. P. (2012a). Comparing surface effective saturation and depth-to-water-level as predictors of plant composition in a restored riparian wetland. *Ecohydrology*, *5*(5), 637–647. doi:10.1002/eco.250

Booth, E. G., & Loheide, S. P. (2012b). Hydroecological model predictions indicate wetter and more diverse soil water regimes and vegetation types following floodplain restoration. *Journal of Geophysical Research-Biogeosciences*, *117*, G02011. doi:10.1029/2011JG001831

Carsel, R., & Parrish, R. (1988). Developing Joint Probability-Distributions of Soil-Water Retention Characteristics. *Water Resources Research*, *24*(5), 755–769. doi:10.1029/WR024i005p00755

Choate, J. (1972). Effects of Stream Channeling on Wetlands in a Minnesota Watershed. *Journal of Wildlife Management*, *36*(3), 940–&. doi:10.2307/3799451

Davidson, E. A., Samanta, S., Caramori, S. S., & Savage, K. (2012). The Dual Arrhenius and Michaelis-Menten kinetics model for decomposition of soil organic matter at hourly to seasonal time scales. *Global Change Biology*, *18*(1), 371–384. doi:10.1111/j.1365-2486.2011.02546.x

Ebrahimi, E., Bayat, H., Neyshaburi, M. R., & Abyaneh, H. Z. (2014). Prediction capability of different soil water retention curve models using artificial neural networks. *Archives of Agronomy and Soil Science*, *60*(6), 859–879. doi:10.1080/03650340.2013.837219

Gupta, S., & Larson, W. (1979). Estimating Soil-Water Retention Characteristics from Particle-Size Distribution, Organic-Matter Percent, and Bulk-Density. *Water Resources Research*, *15*(6), 1633–1635. doi:10.1029/WR015i006p01633

Hammersmark, C. T., Dobrowski, S. Z., Rains, M. C., & Mount, J. F. (2010). Simulated Effects of Stream Restoration on the Distribution of Wet-Meadow Vegetation. *Restoration Ecology*, *18*(6), 882–893. doi:10.1111/j.1526-100X.2009.00519.x

Hammersmark, C. T., Rains, M. C., Wickland, A. C., & Mount, J. F. (2009). Vegetation and Water-Table Relationships in a Hydrologically Restored Riparian Meadow. *Wetlands*, *29*(3), 785–797.

Henszey, R. J., Pfeiffer, K., & Keough, J. R. (2004). Linking surface- and ground-water levels to riparian grassland species along the Platte River in central Nebraska, USA. *Wetlands*, *24*(3), 665–687. doi:10.1672/0277-5212(2004)024[0665:LSAGLT]2.0.CO;2

Katterer, T., Andren, O., & Jansson, P.-E. (2006). Pedotransfer functions for estimating plant available water and bulk density in Swedish agricultural soils. *Acta Agriculturae Scandinavica Section B-Soil and Plant Science*, *56*(4), 263–276. doi:10.1080/09064710500310170

Kern, J. (1995). Evaluation of Soil-Water Retention Models Based on Basic Soil Physical-Properties. *Soil Science Society of America Journal*, *59*(4), 1134–1141.

Kozak, J. A., & Ahuja, L. R. (2005). Scaling of infiltration and redistribution of water across soil textural classes. *Soil Science Society of America Journal*, *69*(3), 816–827. doi:10.2136/ssaj2004.0085

Loheide, S. P., & Booth, E. G. (2011). Effects of changing channel morphology on vegetation, groundwater, and soil moisture regimes in groundwater-dependent ecosystems. *Geomorphology*, *126*(3-4), 364–376. doi:10.1016/j.geomorph.2010.04.016

Loheide, S. P., & Gorelick, S. M. (2007). Riparian hydroecology: A coupled model of the observed interactions between groundwater flow and meadow vegetation patterning. *Water Resources Research*, *43*(7), W07414. doi:10.1029/2006WR005233

Lowry, C. S., & Loheide, S. P. (2010). Groundwater-dependent vegetation: Quantifying the groundwater subsidy. *Water Resources Research*, *46*(6), n/a–n/a. doi:10.1029/2009WR008874

Lowry, C. S., Loheide, S. P., Moore, C. E., & Lundquist, J. D. (2011). Groundwater controls on vegetation composition and patterning in mountain meadows. *Water Resources Research*, *47*, W00J11. doi:10.1029/2010WR010086

Luo, T. X., Li, W. H., & Zhu, H. Z. (2002). Estimated biomass and productivity of natural vegetation on the Tibetan Plateau. *Ecological Applications*, *12*(4), 980–997. doi:10.2307/3061031

Metselaar, K., & van Lier, Q. de J. (2007). The shape of the transpiration reduction function under plant water stress. *Vadose Zone Journal*, *6*(1), 124–139. doi:10.2136/vzj2006.0086

Moyano, F. E., Manzoni, S., & Chenu, C. (2013). Responses of soil heterotrophic respiration to moisture availability: An exploration of processes and models. *Soil Biology & Biochemistry*, *59*, 72–85. doi:10.1016/j.soilbio.2013.01.002

Nemes, A., & Rawls, W. J. (2006). Evaluation of different representations of the particle-size distribution to predict soil water retention. *Geoderma*, *132*(1-2), 47–58. doi:10.1016/j.geoderma.2005.04.018

Norton, J. B., Jungst, L. J., Norton, U., Olsen, H. R., Tate, K. W., & Horwath, W. R. (2011). Soil Carbon and Nitrogen Storage in Upper Montane Riparian Meadows. *Ecosystems*, *14*(8), 1217–1231. doi:10.1007/s10021-011-9477-z

Olness, A., & Archer, D. (2005). Effect of organic carbon on available water in soil. *Soil Science*, *170*(2), 90–101. doi:10.1097/01.ss.0000155496.63323.35

Palmer, M. A., & Bernhardt, E. S. (2006). Hydroecology and river restoration: Ripe for research and synthesis. *Water Resources Research*, *42*(3), W03S07. doi:10.1029/2005WR004354

Rawls, W. J., Pachepsky, Y. A., Ritchie, J. C., Sobecki, T. M., & Bloodworth, H. (2003). Effect of soil organic carbon on soil water retention. *Geoderma*, *116*(1-2), 61–76. doi:10.1016/S0016-7061(03)00094-6

Rodriguez-Iturbe, I., D’Odorico, P., Laio, F., Ridolfi, L., & Tamea, S. (2007). Challenges in humid land ecohydrology: Interactions of water table and unsaturated zone with climate, soil, and vegetation. *Water Resources Research*, *43*(9), W09301. doi:10.1029/2007WR006073

Saxton, K. E., & Rawls, W. J. (2006). Soil water characteristic estimates by texture and organic matter for hydrologic solutions. *Soil Science Society of America Journal*, *70*(5), 1569–1578. doi:10.2136/sssaj2005.0117

Schaap, M. G., Leij, F. J., & van Genuchten, M. T. (2001). ROSETTA: a computer program for estimating soil hydraulic parameters with hierarchical pedotransfer functions. *Journal of Hydrology*, *251*(3-4), 163–176. doi:10.1016/S0022-1694(01)00466-8

Sigua, G. C., Coleman, S. W., & Albano, J. (2009). Beef cattle pasture to wetland reconversion: Impact on soil organic carbon and phosphorus dynamics. *Ecological Engineering*, *35*(8), 1231–1236. doi:10.1016/j.ecoleng.2009.05.004

Silvertown, J., Dodd, M. E., Gowing, D. J. G., & Mountford, J. O. (1999). Hydrologically defined niches reveal a basis for species richness in plant communities. *Nature*, *400*(6739), 61–63. doi:10.1038/21877

Six, J., Conant, R. T., Paul, E. A., & Paustian, K. (2002). Stabilization mechanisms of soil organic matter: Implications for C-saturation of soils. *Plant and Soil*, *241*(2), 155–176. doi:10.1023/A:1016125726789

Six, J., Feller, C., Denef, K., Ogle, S. M., Sa, J. C. D., & Albrecht, A. (2002). Soil organic matter, biota and aggregation in temperate and tropical soils - Effects of no-tillage. *Agronomie*, *22*(7-8), 755–775. doi:10.1051/agro:2002043

Sollins, P., Homann, P., & Caldwell, B. A. (1996). Stabilization and destabilization of soil organic matter: Mechanisms and controls. *Geoderma*, *74*(1-2), 65–105. doi:10.1016/S0016-7061(96)00036-5

Vangenuchten, M. (1980). A Closed-Form Equation for Predicting the Hydraulic Conductivity of Unsaturated Soils. *Soil Science Society of America Journal*, *44*(5), 892–898.

Vereecken, H., Maes, J., Feyen, J., & Darius, P. (1989). Estimating the Soil-Moisture Retention Characteristic from Texture, Bulk-Density, and Carbon Content. *Soil Science*, *148*(6), 389–403.

Wang, X. D., & Benson, C. H. (2004). Leak-free pressure plate extractor for measuring the soil water characteristic curve. *Geotechnical Testing Journal*, *27*(2), 163–172.

Wohl, E. (2005). Compromised rivers: Understanding historical human impacts on rivers in the context of restoration. *Ecology and Society*, *10*(2), 2.

Zhuang, J., Jin, Y., & Miyazaki, T. (2001). Estimating water retention characteristic from soil particle-size distribution using a non-similar media concept. *Soil Science*, *166*(5), 308–321. doi:10.1097/00010694-200105000-00002

Chapter 3

The Clay Pad and Erosion Chain Method for Measuring Sedimentation Processes for the Characterization of Biogeomorphic Succession along the Tuolumne River Riparian Corridor

ABSTRACT

It is known that vegetation along riparian corridors interacts with water and sediment flows to increase sediment deposition for the production of new landforms which allow for the establishment of additional vegetation. This process is called biogeomorphic succession, and is thought to be a powerful control on channel shape in natural alluvial channels. In turn, the shape of the river channel in groundwater dependent meadows determines groundwater levels and the corresponding water availability for vegetation throughout the meadow. Tuolumne Meadows in Yosemite National Park is a groundwater dependent wet meadow where concerns than an abundance of deer are responsible for decreased declining willow

cover and channel widening This presents a threat to the water availability of native wet meadow vegetation.

For the purpose of providing a scientific basis for the management strategies, we characterize biogeomorphic succession in riparian areas along Tuolumne River from 2012 to 2013. With the use of inert clay pads and erosion chains, we measure sedimentation and erosion around willows in areas that vary in four meaningful biogeomorphic ways: (1) grazing accessibility by deer, (2) location on a river bank or a gravel bar, (3) position relative to nearby willows (upstream, downstream, or adjacent), and (4) distance to the river. In total, this study made use of 72 clay pads to measure sedimentation around 24 willow plant/clusters on banks and bars under excluded and non-excluded conditions. Results show that organic duff material builds preferentially on banks, while mineral sediments build preferentially downstream of willows closer to the river in exclosed plots on bars. We provide the detailed procedure required to repeat the experiment for a continuation of the study.

INTRODUCTION

Sub-alpine wet meadows in California's Sierra Nevada Mountain Range are considered groundwater dependent ecosystems (Allen-Diaz, 1991) and are some of the most degraded of Sierra Nevadan habitats (SNEP, 1996). The groundwater dependency of Tuolumne Meadows, one of the largest sub-alpine meadows in Yosemite National Park, is characterized by a meandering river channel that is in strong hydrologic connection with the meadow aquifer (Loheide & Lundquist, 2009; Lowry, Deems, Loheide, & Lundquist, 2010). Impacts to wet meadow ecosystems that affect geomorphic conditions of the channel, such as stream incision and channel widening, are common causes of altered hydrologic regimes (Booth and Loheide, 2010). Changes in stream stage propagate throughout the meadow aquifer, causing changes in ground water levels that lead to meadow-wide losses of native, wet meadow vegetation, increases in xeric vegetation, and sagebrush and conifer encroachment (Cooper et al., 2006; Loheide et al. 2009: Loheide and Gorelick, 2007). Shifts in the distributions of plant communities caused by altered water levels can lead to impacts on ecological functions and services within the meadow, like the regulation of floods, nutrient cycling and habitat preservation (Lowry et al., 2010).

Riparian vegetation, however, has also been shown to have an influence on channel geomorphology. In a Mediterranean-mountainous watershed in France, Corenblit et al. (2009) showed that riparian vegetation can to have a geomorphological influence on the landscape by trapping suspended fine sediment and thereby facilitating vegetation recruitment. This process, called biogeomorphic succession, is mediated by vegetation like shrubs and pioneer tree groups that act as ecosystem engineers to construct fluvial habitat and riparian landforms (Corenblit et al., 2011);. A proposed mechanism for this phenomenon from a study of four temperate gravel bed rivers is that islands of pioneer vegetation trap sediment on the downstream side which coalesce to form larger established islands (Gurnell et al., 2006). The study also showed that pioneer vegetation builds landforms of different types in different locations depending on the elevation of the landform and intensity of the hydrological conditions. Species on gravel bars are active engineers during low flow years while species on banks and flood plans are active during high flow years, and the location of the transition between these areas is a function of the hydrologic conditions (Gurnell et al., 2012). This is consistent with a study completed in the Rocky Mountains which found that potential establishment sites for willows occur along abandoned channels and drained beaver ponds and are formed as a function of high flow frequency (Cooper, Dickens, Hobbs, Christensen, & Landrum, 2006). Biogeomorphic is not just a function of elevation, however, but also distance from the river. Sedimentation rates in the River Tech were found to vary significantly along a transverse gradient from the river (Corenblit et al., 2009). Therefore, biogeomorphic succession is dynamic process that is a function of sediment and water flows, distance from the river, and elevation relative to flood stages which helps to control channel shape (Corenblit et al., 2010; Gurnell et al., 2012).

In the Sierra Nevada, a wide range of human activities affect riparian vegetation either through direct removal or by altering the factors controlling the distribution and structure of riparian vegetation (SNEP, 1996). Reduced riparian vegetation can increase erosion (Behnke and Raleigh, 1979; Platts, 1991; Dudley and Dietrich, 1995), particularly in meadows where the hydrologic impact is amplified due to reduced river stages that propagate throughout the groundwater table (Odion et al, 1990). But grazing pressure is not the only factor at play, because riparian areas previously impacted by intense grazing do not recover through reduced grazing alone (Marshall et al., 2013). In fact, increased grazing pressure has been shown to increase above ground biomass (Johnston, Cooper, & Hobbs, 2007), implying that grazed vegetation offers more resistance to flow and increased potential to trap sediment. So although there seems to be a relationship between riparian vegetation channel shape and stability, it is unclear exactly how grazing affects the ability of vegetation to build new landforms. .

In Tuolumne Meadows, an apparent overabundance of deer and the subsequent overgrazing has raised the concerns about the future of willow communities in riparian areas. To better understand the implications of decreased willow recruitment on the health of this groundwater dependent ecosystem, we assessed biogeomorphic succession over the course of two years through a characterization of sedimentation along the riparian corridor. We framed the research around the question d*oes failed willow recruitment reduce trapping of fine sediment on gravel bars*. In the context of the complexity of biogeomorphic succession described in the literature, we characterize sedimentation by examining the influence of four biogeomorphic factors. First, we observed sedimentation around willows that are grazed by deer and those that are not. Second, we examined sedimentation on an equal number of banks and bars because biogeomorphic succession may behave differently on banks with established willow populations verses gravel bars with limited willow establishment. Third, we observed sedimentation on three sides of a willow to assess the role of flow direction on trapping sediment. Finally, we examined pairs of willows along a transverse gradient from the river, either near or far, to assess the importance of proximity to the river.

In this study, our goal is to provide evidence for or against the relative importance of failed willow recruitment in maintaining meadows in a degraded state. In the following sections we describe in detail the procedure we developed and demonstrate its ability to track biogeomorphic succession in Tuolumne Meadows. We show that the method is capable of measuring small amounts of sedimentation and differentiating between deposits of different type. Unfortunately, the two years over which this study was implemented were characterized by abnormally low annual precipitation, so the corresponding low spring melt peak flows limited our ability to observe active sedimentation processes. Using the limited data available, we formulate conclusions that provide a case for a continued effort to observe biogeomorphic succession in Tuolumne Meadows for the purpose of producing evidence to help improve management efforts of this valuable ecosystem.

METHODS

To investigate the influence of riparian vegetation on sediment deposition and erosion, we observed sedimentation rates at three sites along Tuolumne River (Figure 1) over the course of the 2012 and 2013 seasons. At each site, we delineate a 7 m x 14 m study plot on a gravel

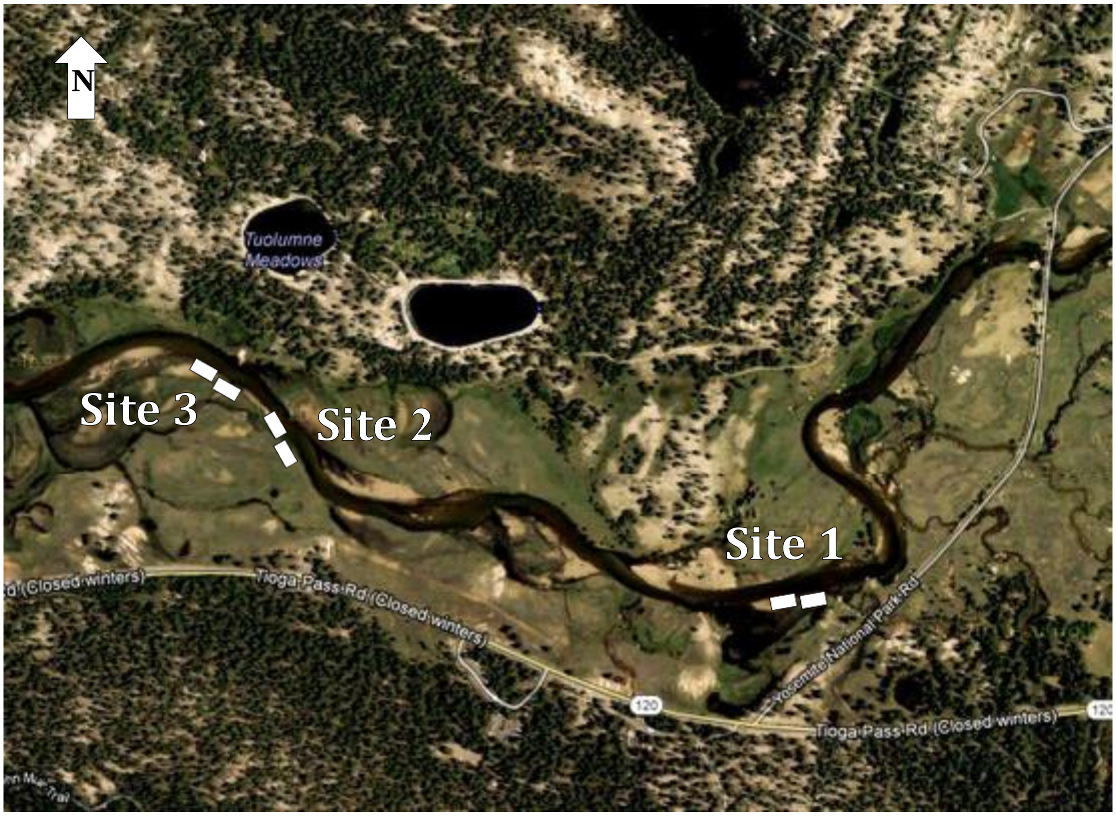

Figure 1: *Three study sites are located along the Tuolumne River in Tuolumne Meadows. Each site has a plot on a gravel bar and on a river bank, indicated in this map as pairs of white rectangles. All sites are located on the south site of the river, and are in areas designated non-wilderness areas.*

bar with limited willow establishment and on a river bank with a well-established willow population. Each bank or bar plot was delineated at each of the three sites. Each plot consists of a control subplot and an exclosure subplot, which is the fenced off area in Figure 2. Two willow plants were identified within each subplot around which we installed three clay pads. This study made use of 72 clay pads to measure sedimentation around 24 willow plant/clusters on banks and bars under excluded and non-excluded conditions. We use a 12" length of beaded chain to monitor erosion. A chain is installed vertically in the ground

Figure 2: *The four t-posts and black plastic fencing material is used to prevent mule deer from grazing the willows in the exclosure subplot shown on the gravel bar of site 1. The control subplot is the unfenced area directly downstream of the exclosure subplot.*

in the middle of the downstream edge of every clay pad. The chain is installed by attaching it to the end of a flat-edged 18” section of #4 rebar and hammering it into the ground. If erosion occurs, the depth of erosion is equal to the length of exposed erosion chain, which can still be measured even in cases in which it is subsequently buried by deposition.

CLAY PAD INSTALLATION AND SAMPLING

The most accurate way to measure short term erosion is with the use of clay pads (Kroes and Hupp, 2010). After the absorption of soil moisture powdered clay pad serves as a fixed horizon from which small depths ($\pm 1\ mm$) of sedimentation can be measured (Baumann, Day, & Miller, 1984). The clay pads are made of powdered white feldspar clay and are sized 30 cm x 30 cm and from 1 cm to 2 cm thick. To measure sedimentation around a willow, the pads were placed directly upstream, downstream, and on one of the lateral sides of each willow. Prior to installation, the area was cleared of vegetation and debris. A small amount of material was excavated to the depth of 1 – 2 cm. Clay powder was then added in layers until the surface elevation of the clay pad was equal to the elevation of the land surface. A spray bottle was used to moisten each layer of clay powder (approx. 500 mL water per pad) as it was being installed so that it adhered the ground and to itself. Each pad was constructed with three to five layers of clay. Photographs were taken of the area after the installation is complete to complement the results of the depth measurements. This installation process is photographically documented in Appendix A of this thesis.

After the peak spring stage retreated below the elevation of the clay pads, measurements of the sedimentation on top of the clay pads were made. Clay pads that were intact and recorded no deposition were left undisturbed to record sedimentation after the next flooding event. If sedimentation was visible on the surface of the pad, a coring device (clear plexi-glass tube with 15 mm diameter) was used to take a core sample. The white clay horizon is observable through the tube sidewall, and a measurement of deposited sediment was made with a tape measure. Plugs were replaced after the measurement was taken to minimize disturbance and allow for another year of measurement. The deposition depth on a clay pad is the average of three randomly placed cores over the surface of the clay pad. When sedimentation was measured on a clay pad, the accreted sediment was collected from half of the surface (the side nearest the stream) and the other half (the one farthest from the stream) was left undisturbed. Clay pads that have accreted material from previous years require that a random triplicate sample be taken from each half of the pad. This enables the observation of sedimentation dynamics between the most recent flood in addition to the accumulated sediment from all years past.

The riparian corridor along the Tuolumne River in Tuolumne Meadows is a popular place for wildlife and visitors to the national park. During the course of our study, some clay pads were stepped on or otherwise destroyed by humans or animals, which disturbed the clay surface and left behind sediment that was not representative of biogeomorphic succession. Damaged clay pads were restored by clearing the non-representative material, then adding thin layers of feldspar clay powder until the surface elevation of the clay pad was equal to the land surface. Additionally, the vegetation cleared during the installation of the clay pad occasionally regrew through the surface of the pad. This vegetation growth was left undisturbed so that the clay pad surface remained representative of the sample area around the willow. A photo of a damaged pad is in Appendix A of this thesis.

RESULTS

The two years over which this study occurred experienced unusually low annual precipitations which produced peak discharges of 1,840 cfs in 2012 and 1,740 cfs in 2013

(CA.gov ID TUM). The mean peak discharge from 2006 to 2011 was 4,318 cfs. No erosional chain was exposed in either year, so erosion was never observed. Sedimentation was observed on 23/65 measured pads in 2012 and on 8/62 measured pads in 2013. In the following sections, we present the results of our deposition measurements in terms of counts (number of occurrences), depths and material type. These data are compared among the four biogeomorphic factors of interest: (1) grazed verses ungrazed willows (exclosed subplots or control subplots), (2) bank plots verses bar plots, (3) pads upstream, downstream, or adjacent of a willow, and (4) willows near to the stream or far from the stream.

The accreted material observed on the clay pads is classified into one of three categories based on an onsite visual assessment. Duff (Figure 3a) is generally composed of conifer needles and cone fragments, but may consist of any small woody debris that fit within the core sampler. Sand (Figure 3b) is visually classified as any particles between 2 mm and 0.05 mm in diameter. Silt (Figure 3c) is visually classified as particles less than 0.05 mm and is brownish or dark brown in color. Some clay pads appeared to be washed away because all the feldspar clay is missing (aside from some small residual amounts) and the excavation made during the original installation appears intact (Figure 4). The surrounding bed material seemed undisturbed because the edges of the excavation are unaltered. The erosion chains were not exposed in these sites, so a measurement of erosion cannot be made. Therefore, these pads have no measurement and were removed from the data.

Figure 3: *The deposited material observed on the surface of the clay pads was classified into three different types: duff (a) is generally composed of conifer needles and cone fragments, but may consist of any small woody debris that fit within the core sampler, sand (b) is visually classified as any particles between 2 mm and 0.05 mm in diameter, and silt (c) is visually classified as particles less than 0.05 mm and is brownish or dark brown in color.*

The occurrences of sedimentation on a clay pad are denoted by brown, orange, blue, or white boxes in Figure 5 for 2012 and Figure 6 for 2013. The total number of observations between treatment types is tabulated in Table 1B. The largest consistent count differences between biogeomorphic factors were between near-stream willows and far-stream willows (9 in 2012 and 8 in 2013). There was also a difference between bar plots and bank plots (5 in 2012 and 8 in 2013). The difference in number of observations was smaller and less consistent between

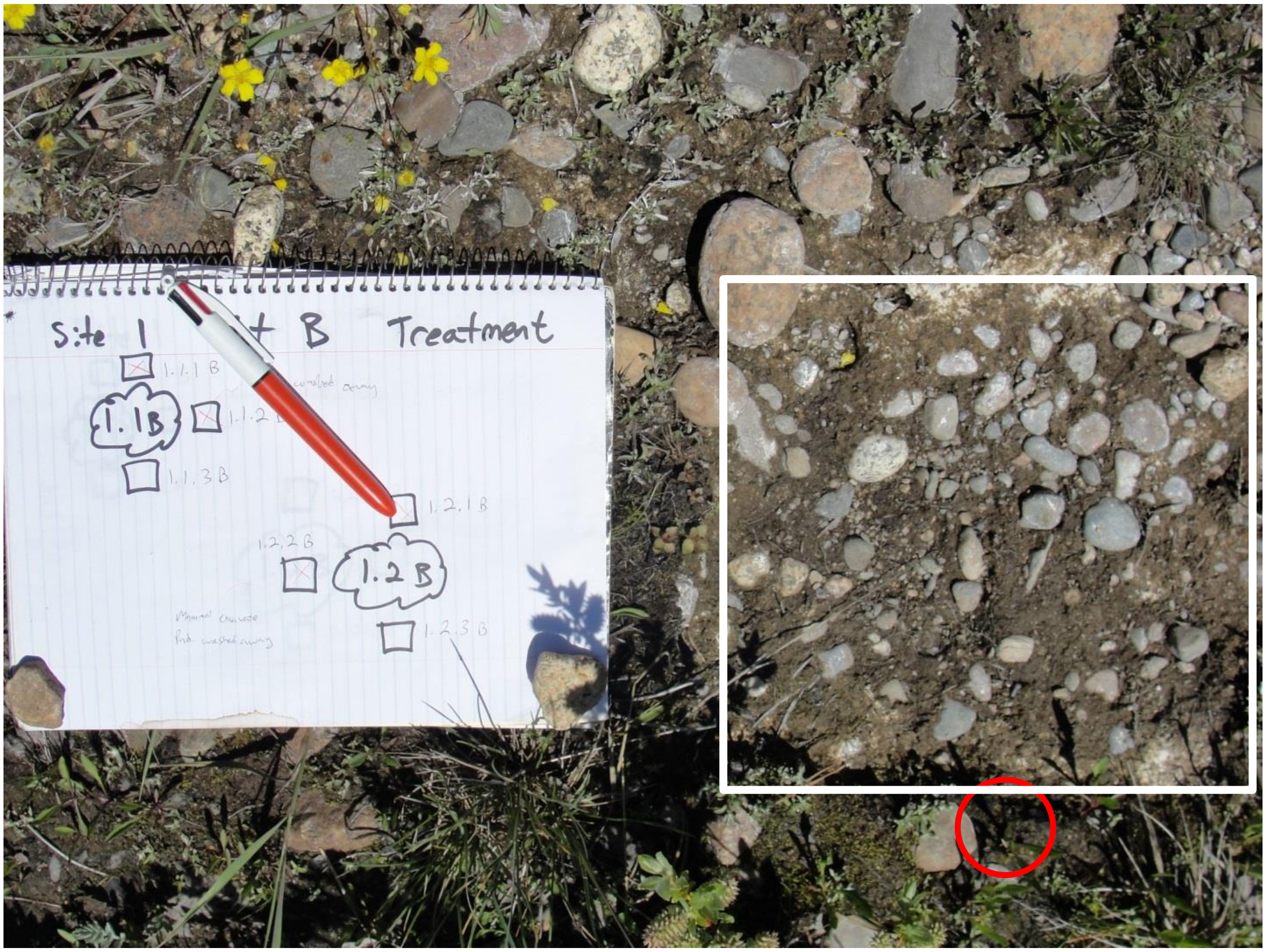

Figure 4: *This clay pad has been washed away and the original excavation made in the bed material during installation (outlined in white) appears undisturbed. The erosion chain installed in red circle was not revealed, so a measurement of erosion cannot be made.*

exclosed plots verses control plots (-1 in 2012 and 4 in 2013) and upstream pads verses downstream pads (-4 in 2012 and 0 in 2013).

Because the clay pad method provides a clear horizon to observe the sedimentation profile, we able to accurately measure the depth of deposited material for every observation. The

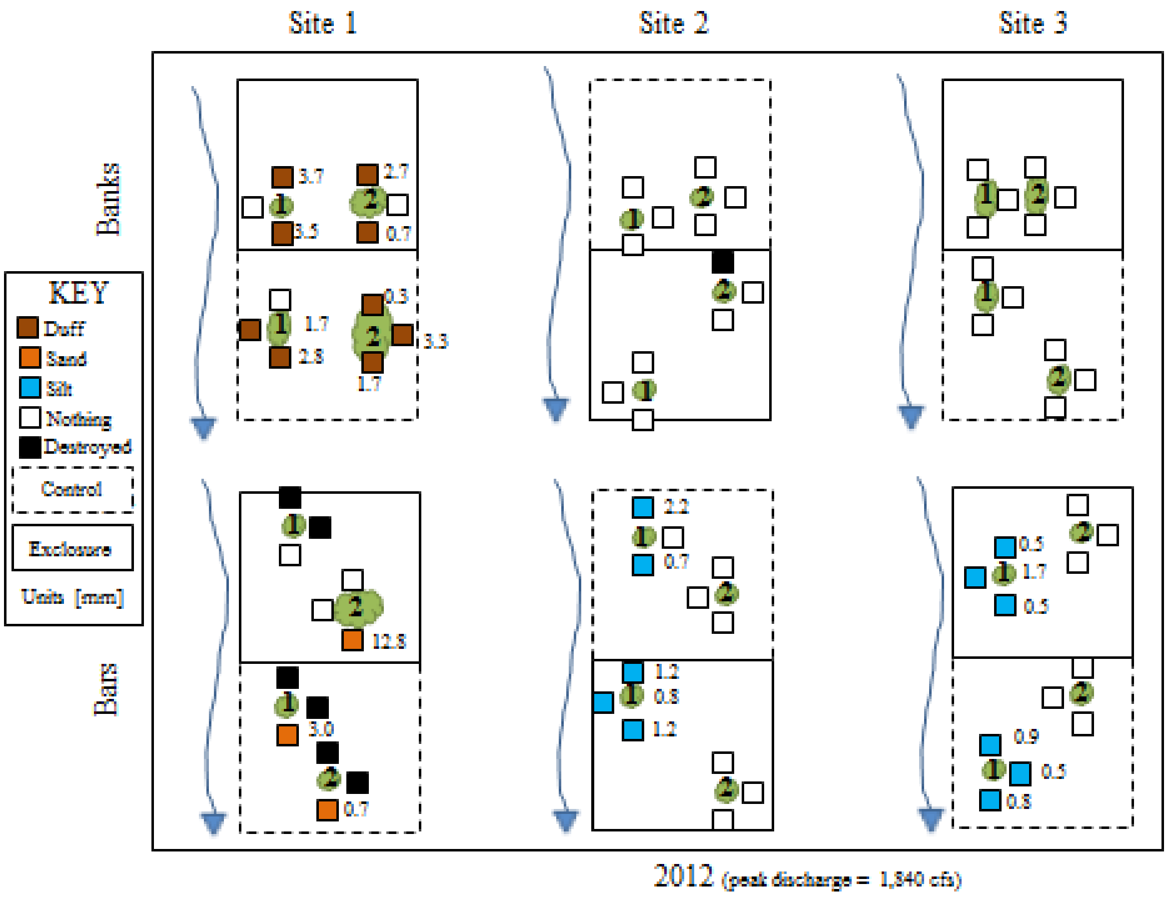

Figure 5: *The results recorded after the spring melt of 2012 for all three sites are shown in the diagram above. In this diagram, the sites are separated into different columns, with bank sites above and bar sites below. The exclosure subplot is indicated as a solid box, while the control subplot is a dashed box. The observed deposition on a clay pad is colored according to the material type (duff, sand, or silt) and the observed depth is indicated alongside. Clay pads with no deposition have no color and no depth number. Willows in each plot are numbered either 1 (near-stream) or 2 (far-stream). Not to scale.*

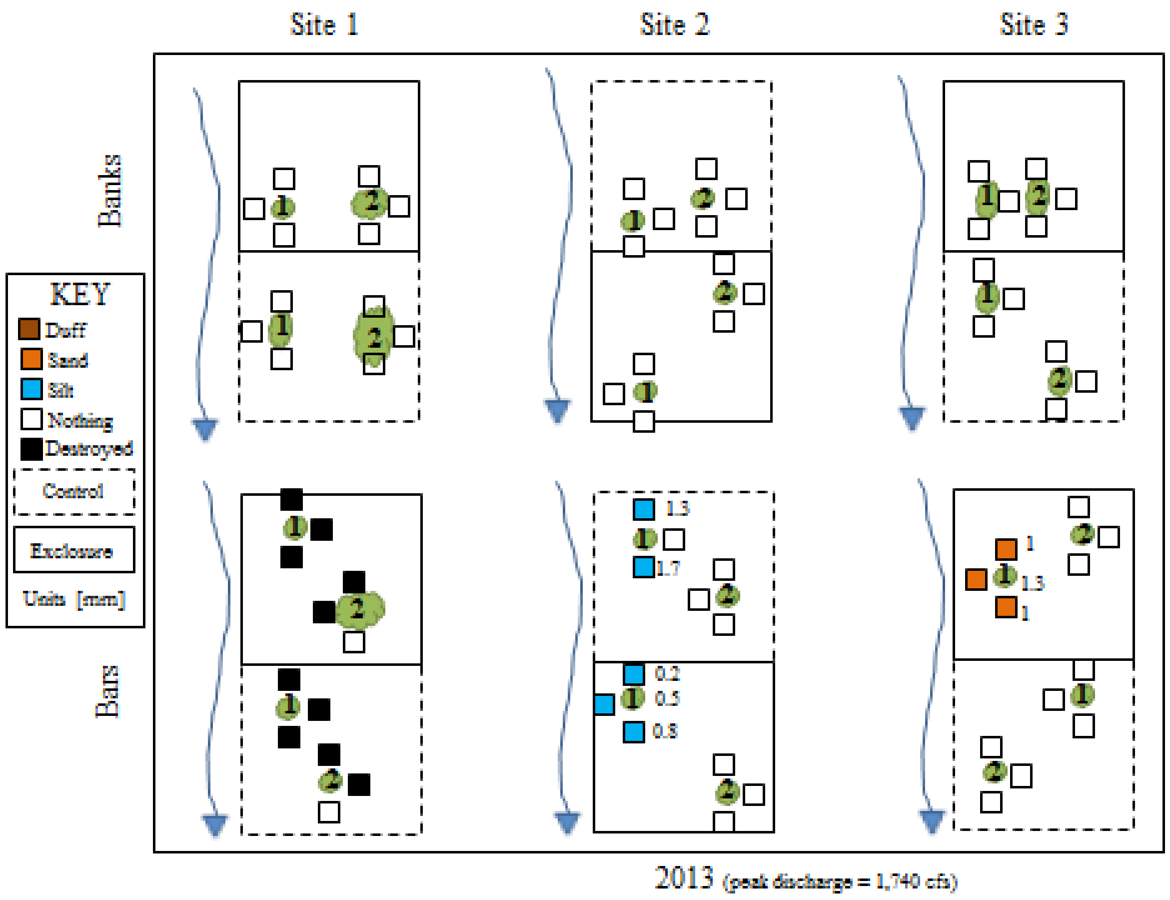

Figure 6: *The results recorded after the spring melt of 2013 for all three sites are shown in the diagram above. In this diagram, the sites are separated into different columns, with bank sites above and bar sites below. The exclosure subplot is indicated as a solid box, while the control subplot is a dashed box. The observed deposition on a clay pad is colored according to the material type (duff, sand, or silt) and the observed depth is indicated alongside. Clay pads with no deposition have no color and no depth number. Willows in each plot are numbered either 1 (near-stream) or 2 (far-stream). Not to scale.*

	Avg. Depth / Std. Dev. [mm]		Count Number / Total Pad Number	
	2012	2013	2012	2013
Treatment	0.79/2.27	0.13/0.34	11/33	6/31
Control	0.51/0.95	0.08/0.35	12/32	2/31
Bank	0.57/1.16	0/0	9/35	0/36
Bar	0.73/2.17	0.22/0.47	14/30	8/26
Upstream	0.46/1.00	0.10/0.33	7/20	3/20
Adjacent	0.29/0.76	0.08/0.29	5/21	2/20
Downstream	1.18/2.69	0.15/0.42	11/24	3/22
Stream-side	0.68/1.07	0.22/0.47	16/32	8/30
Far-side	0.62/2.22	0/0	7/33	0/32

Table 1: *(A) The average depth (mm) and standard deviation (mm) for are shown for the clay pads in each factor pair. (B) The number of observations is shown over the total number of clay pads in each factor pair.*

average depth of each triplicate core sample for every observation is shown next to each clay pad in Figure 5 for 2012 and Figure 6 for 2013. White pads without a number represent a measurement of zero. The average depths of deposited material range from 0.2 mm to 12.8 mm. To identify the influence of the biogeomorphic factors of interest, we present the average depth for each factor along with the standard deviation in Table 1A. The average depth was larger in exclosed subplots (0.79 mm in 2012, 0.13 mm in 2013) than in control subplots (0.51 mm in 2012, 0.08 mm in 2013). The average deposition depth was larger on bar plots (0.73 mm in 2012, 0.22 mm in 2013) than on bank plots (0.57 mm in 2012, 0 mm in 2013). The average deposition depth was larger around the near-stream willows (0.68 mm in 2012, 0.22 mm in 2013) than around the far-stream willows (0.62 mm in 2012, 0 mm in 2013). In 2012, the deposition was much larger on downstream pads (1.18 mm) than on upstream pads (0.46 mm). In 2013, the difference between upstream and downstream pads was not as large (0.10 mm upstream and 0.15 mm downstream), but deposition was still greater on downstream pads. The standard deviations of each distribution are larger than the averages, which mean that the distributions are heavily skewed towards zero due to the numerous zero measurements. We do not have precise stage data relative to the surface of each pad, so we are unable to differentiate between no submergence (which we can neglect), and submergence without sedimentation (which we cannot neglect). Because there were no definite observational clues indicating the high water level, we assume that all clay pads were submerged and subjected to conditions that generate biogeomorphic activity.

A standard paired t-test was used to determine if the sedimentation differences between factor pair population means were not a result of randomness, at least 95% of the time. The difference between the mean of the factor pair populations is considered significant if the p-value is equal to or less than 0.05. The p-values for each factor pair are shown in Table 2A for both years. The 2012 results show that the differences between all factor pair populations are insignificant at the 95% confidence level. The relationship that is least likely due to random variation is the variability in average sedimentation depth between clay pads that are upstream of a willow verses those that are downstream (p = 0.216). In 2013, there is a significant difference between bank and bar plots (p = 0.0082) largely because no sedimentation was observed on bank plots. Similarly, there is a significant difference between near-stream and far-stream willows (p = 0.008) largely because no sedimentation was observed around far-stream willows.

	A	**B**	**C**	**D**
Biogeomorphic Factor	**All Sites** 2012/2013	**Site 1 Only** 2012/2013	**Site 2& 3** 2012/2013	**Bar Plots Only** 2012/2013
Exclosed vs. Control subplots	0.474/0.465	0.50/-	0.95/0.53	0.474/0.473
Bank vs. Bar Plots	0.697/0.0082	0.79/-	0.001/0.005	-/-
Upstream vs. Downstream Pads	0.216/0.185	0.19/-	0.68/0.70	0.27/0.19
Near-stream vs. Far-stream Willows	0.88/0.008	0.60/-	0.001/0.005	0.95/0.006

Table 2: *The p-values are shown for each factor pair for (A) all data, (B) data only from site 1, and (C) data only from bar plots. A p-value equal to or less than 0.05 means that there is less than a 5% chance that the difference in the means of the factor pair populations is a result of random variation.*

Complex interactions between sediment, water flow, and willows increase the difficulty of identifying the signal of influential factors. To make a population of data produced by multiple factors more meaningful, it can be stratified according to differentiating information (Thompson, 1992). We incorporate this statistical technique by stratifying the population of depth data into a site 1 only population, sites 2 and 3 and an individual population, and a bar plot only population. The justification for this is site 1 appears to be different than site 2 and site 3 because it contained all pads that were eroded and held the only depositions of duff. When we test the influence of the four biogeomorphic factors on the site 1 population, we see no significant difference between means (Table 2b). In 2013, the difference between means for the bar site population is significant for near-stream verses far-stream willows ($p = 0.006$) because sedimentation was not observed on any far stream willows. Similarly, significant different exist with bank verses bar and near-stream verses far-stream in the site 2 and 3 population simply because no sedimentation was observed in the banks or far-stream willows in both years.

The biogeomorphic factors controlling deposition may have a different influence on the deposition of duff than on mineral sediments because duff is generally less dense. Therefore, we consider duff and mineral sediment as separate categories and test for a significant difference between observed counts and expected counts with a chi-square statistic (X^2). This statistic evaluates how likely it is that any difference between observed and expected counts arose by chance. Expected counts are the number of events that should occur if the categories are independent of the factors. In other words, if deposition occurs on either area of opposing biogeomorphic factors, then we expect that there is no difference if the deposited material is duff or mineral sediment. We test for differences between the duff and mineral categories with each biogeomorphic factor, and can reject null hypothesis that the depositions are independent if the X^2 value is greater than or equal to 3.84, assuming one degree of freedom and a 0.05 significance level. The results for both years show that there is a significant

Count

	Duff	Mineral
Exclosed Subplots	4/4.9	13/12.1
Control Subplots	5/4.1	9/9.9
	X^2 =	0.6
Bank Plots	9/2.6	0/6.4
Bar Plots	0/6.4	22/15.6
	X^2 =	31.0
Upstream Pads	3/2.9	7/7.1
Downstream Pads	4/4.1	10/9.9
	X^2 =	0.01
Near-stream Willows	4/7.0	20/17.0
Far-stream Willows	5/2.0	2/5.0
	X^2 =	7.9

Table 3: *The chi-squared statistic (X^2) calculated for categories of duff and mineral content is italicized for each biogeomorphic factor below each box. The X^2 statistic is the sum of normalized squared differences between the expected count (denominator) and the observed count (numerator). The expected count is the number of events that should occur if the categories are independent of the factors. A X^2 value larger than the critical value means the categories are not independent of the factors. Observations from 2012 and 2013 are considered together. The critical X^2 value is 3.84 for all cases because they all have one degree of freedom.*

difference between duff and mineral sediment with all four biogeomorphic factors considered (Table 3). The X^2 statistics for bank verses bar and near-stream verses far-stream are larger than 3.84. Therefore, if deposition occurs in areas differing in these biogeomorphic factors, the likelihood of duff or mineral sediment deposition is significantly different. On the other hand, the deposition of either duff or mineral content is equally likely on upstream verses downstream areas or exclosed verses control areas. The chi-square statistic cannot determine the level of dependence of the categorical variables on the factors, but only if there is a significant dependence or not. Therefore, these results do not show that any particular biogeomorphic factor is more influential than any other.

DISCUSSION

Field observations showed numerous different sedimentation patterns which suggest that the sedimentation processes along the Tuolumne River riparian corridor are produced by highly complex interactions of multiple biogeomorphic factors. A collection of these images can be found in Appendix A of this thesis. Examples include sedimentation and erosion downstream of willow on a gravel bar (Figure A1.9), a large deposit of sand downstream of a willow (Figure A1.10), a pioneer group of heavily grazed willows (Figure A1.11), a heterogeneous deposit of sand, duff, and gravel around a cluster of willows on a gravel bar (Figure A1.12), and a distinct flow pattern of erosion and woody debris downstream of a large lone willow on a gravel bar (Figure A1.13).

The limited sediment deposition data and the lack of erosion data suggest that the unusually low flows did not mobilize substantial amounts of sediment. It is uncertain whether or not peak stage was high enough to reach all of the clay pads, so are unable to discern if non-existent sedimentation on a pad is truly zero sedimentation (that cannot be neglected), or just lack of submergence (that can be neglected). We assume that zero deposition on a clay pad is representative of submergence without sedimentation and include it in calculations of averages and the t-test analysis. The large number of zero readings skews the average depth distributions towards zero for all factor pair populations. Future efforts can implement strategies to discern between submergence without sedimentation and non-submergence. Possible methods could include time lapse cameras, or crest-stage gages. Pressure transducers used as stage gages are problematic because interactions with bank ice prevent installation close to the site (they must be installed in the active channel a significant distance away), and large lateral distances do not allow for precise measurements relative to subtle variations in clay pad surface elevation.

Sufficient non-zero depth data is needed to determine the influence of a single biogeomorphic factor on sedimentation depth. The sedimentation depth for 2012 and 2013 consists mostly of zeros. Therefore, the t-test did not show a significant influence of any biogeomorphic factor on sedimentation depth. Some observations of individual clay pads appear to be a result of a meaningful biogeomorphic factor, such as the thick sand deposit behind an exclosed site 1 bar willow in 2012. This observation is in accordance with the biogeomorphic mechanism proposed by Gurnell (2012) where deposition behind pioneer vegetation increases downstream and coalesces to form larger landforms. The difference between the average depth of sedimentation in exclosures verses in control plots is not statistically significant, but the trend shows that the average depth is nearly twice as large in the treatment plots for both years. The current data only account for two seasons of non-grazed willow growth, and the influence of the exclosures may act over a longer time scale. Vegetated areas expand into low flow margins during consecutive low flow years (Bertoldi, Drake, & Gurnell, 2011), and the additional growth required to affect sedimentation depth in a statistically significant way may take more than two years. The difference in willow size and density will likely increase as the experiment continues (Johnston et al., 2007). It is likely that the framework shown here can be applied to a larger data set developed over more and wetter years to show meaningful biogeomorphic relationships that can provide evidence for or against the relative importance of failed willow recruitment in maintaining meadows in a degraded state.

A trend shows the average depth on bars is larger than on banks for both years, suggesting that bars are the active sedimentation areas during low flow years (Wolf, Cooper, & Hobbs, 2007). Consecutive low flow years may generate small annual depths of sedimentation that, over time, create opportunities where willow establishment will more likely be successful (Gage & Cooper, 2004b). This observation is consistent with others where rapid expansions of vegetated areas into low flow channel margins occur during periods without large floods ((Bertoldi, Gurnell, & Drake, 2011; Bertoldi, Drake, & Gurnell, 2011). A series of low flow years may allow recently germinated willows to become established such that they can resist the erosive forces of high peak discharge wet years (Gage & Cooper, 2004a); (Woods & Cooper, 2005). This suggests that repeated low flow years may encourage willow establishment.

By considering the occurrences of sedimentation, we count only events where non-zero deposition occurred. The chi-square analysis of deposition occurrence shows that deposition is significantly different between duff and mineral content for two of the biogeomorphic factors considered. Duff material builds up preferentially on banks and mineral sediment builds preferentially on bars. Similarly, duff is more likely to deposit on far-stream willows, while mineral sediment is more likely to deposit on near stream willows This supports the model proposed by Gurnell et. al. (2012) in that willows established on bars induce sedimentation that raises the elevation the elevation to transform the landform into a bank. Our results suggest that the higher elevation banks farther from the river are more likely to receive highly organic depositions of duff.

Despite the limited data due to limited sedimentation transport during low flow years, this clay pad method enables us to observe very small depositions (±1mm) that would otherwise be neglected by other survey based methods (Corenblit et al., 2009). These small depositions of silt and sand can add up significantly over time, which can lead to increased establishment of new willow populations (Wolf et al., 2007) and changes in the morphology of the channel.

Therefore, even minor depositions are important to the morphology of the river, and should be understood for the purpose of managing the geomorphology of the river. Clay pads also enable us to differentiate between factors that control the deposition of highly organic material (duff) and mineral sediments. A more developed record of the preferential deposition of these types of materials will provide insight into the origin of the highly organic top soil layer seen throughout the meadow. Characterizing the deposition of sand and silt is key for understanding the controls on channel morphology because these are the materials that compose the bed of the river channel.

CONCLUSION

We adapted the clay pad method for the measurement of sedimentation along the Tuolumne River and implemented it over two dry years. We showed this method can identify very small depositions (± 1 mm) and differentiate between the deposition of duff, silt, and sand. With limited data available, this method determined that there is a difference in where duff and mineral sediments are deposited. Results show that duff builds preferentially on banks farther from the river, while mineral sediment builds preferentially on bars closer to the river. We provide the detailed procedure required to repeat the experiment for a continuation of the study.

Additionally, we provide a statistical framework to determine the influence of four biogeomorphic factors on sedimentation around willows: (1) the influence of grazing by deer

(2) the location of willows on a bank verses a bar, (3) the deposition upstream of a willow verses downstream, and (4) the distance of a willow to the river. Understanding the influence of these biogeomorphic factors can characterize biogeomorphic succession in Tuolumne Meadows to better answer the question *does failed willow recruitment reduce trapping of fine sediment on gravel bars.*

REFERENCES

Allen-Diaz, B. (1991). Water-Table and Plant-Species Relationships in Sierra-Nevada Meadows. *American Midland Naturalist*, *126*(1), 30–43. doi:10.2307/2426147

Baumann, R., Day, J., & Miller, C. (1984). Mississippi Deltaic Wetland Survival - Sedimentation Versus Coastal Submergence. *Science*, *224*(4653), 1093–1095. doi:10.1126/science.224.4653.1093

Bertoldi, W., Drake, N. A., & Gurnell, A. M. (2011). Interactions between river flows and colonizing vegetation on a braided river: exploring spatial and temporal dynamics in riparian vegetation cover using satellite data. *Earth Surface Processes and Landforms*, *36*(11), 1474–1486. doi:10.1002/esp.2166

Behnke, R.J., and R.F. Raleigh. 1979. Grazing and the riparian zone: Impact and management perspectives. General Technical Report WO-12. Washington, DC: U.S. Forest Service.

Bertoldi, W., Gurnell, A. M., & Drake, N. A. (2011). The topographic signature of vegetation development along a braided river: Results of a combined analysis of airborne lidar, color air photographs, and ground measurements. *Water Resources Research*, *47*, W06525. doi:10.1029/2010WR010319

Cooper, D. J., Dickens, J., Hobbs, N. T., Christensen, L., & Landrum, L. (2006). Hydrologic, geomorphic and climatic processes controlling willow establishment in a montane ecosystem. *Hydrological Processes*, *20*(8), 1845–1864. doi:10.1002/hyp.5965

Corenblit, D., Baas, A. C. W., Bornette, G., Darrozes, J., Delmotte, S., Francis, R. A., … Steiger, J. (2011). Feedbacks between geomorphology and biota controlling Earth surface processes and landforms: A review of foundation concepts and current understandings. *Earth-Science Reviews*, *106*(3-4), 307–331. doi:10.1016/j.earscirev.2011.03.002

Corenblit, D., Steiger, J., Gurnell, A. M., Tabacchi, E., & Roques, L. (2009). Control of sediment dynamics by vegetation as a key function driving biogeomorphic succession within fluvial corridors. *Earth Surface Processes and Landforms, 34*(13), 1790–1810. doi:10.1002/esp.1876

Corenblit, D., Steiger, J., & Tabacchi, E. (2010). Biogeomorphologic succession dynamics in a Mediterranean river system. *Ecography*, *33*(6), 1136–1148. doi:10.1111/j.1600-0587.2010.05894.x

Dudley, T.L., and W.E. Dietrich. 1995. Effects of cattle grazing exclosures on the recovery of riparian ecosystems in the southern Sierra Nevada. Technical Completion Report UCAL-WRC-W-831. Davis: University of California, Water Resources Center.

Gage, E. A., & Cooper, D. J. (2004a). Constraints on willow seedling survival in a Rocky Mountain montane floodplain. *Wetlands*, *24*(4), 908–911. doi:10.1672/0277-5212(2004)024[0908:COWSSI]2.0.CO;2

Gage, E. A., & Cooper, D. J. (2004b). Controls on willow cutting survival in a montane riparian area. *Journal of Range Management*, *57*(6), 597–600. doi:10.2307/4004014

Gurnell, A. M., Bertoldi, W., & Corenblit, D. (2012). Changing river channels: The roles of hydrological processes, plants and pioneer fluvial landforms in humid temperate, mixed load, gravel bed rivers. *Earth-Science Reviews*, *111*(1-2), 129–141. doi:10.1016/j.earscirev.2011.11.005

Gurnell, A. M., Morrissey, I. P., Boitsidis, A. J., Bark, T., Clifford, N. J., Petts, G. E., & Thompson, K. (2006). Initial adjustments within a new river channel: Interactions between fluvial processes, colonizing vegetation, and bank profile development. *Environmental Management*, *38*(4), 580–596. doi:10.1007/s00267-005-0190-6

Johnston, D. B., Cooper, D. J., & Hobbs, N. T. (2007). Elk browsing increases aboveground growth of water-stressed willows by modifying plant architecture. *Oecologia*, *154*(3), 467–478. doi:10.1007/s00442-007-0854-4

Loheide, S. P., & Lundquist, J. D. (2009). Snowmelt-induced diel fluxes through the hyporheic zone. *Water Resources Research*, *45*, W07404. doi:10.1029/2008WR007329

Lowry, C. S., Deems, J. S., Loheide, S. P., & Lundquist, J. D. (2010). Linking snowmelt-derived fluxes and groundwater flow in a high elevation meadow system, Sierra Nevada Mountains, California. *Hydrological Processes*, *24*(20), 2821–2833. doi:10.1002/hyp.7714

Marshall, K. N., Hobbs, N. T., & Cooper, D. J. (2013). Stream hydrology limits recovery of riparian ecosystems after wolf reintroduction. *Proceedings of the Royal Society B-Biological Sciences*, *280*(1756), 20122977. doi:10.1098/rspb.2012.2977

Odion, D.C., T.L. Dudly, and C.M. D'Antonio. 1990. Cattle grazing in southeastern Sierra meadows: Ecosystem change and prospects for recovery. In Plant biology of eastern California, edited by C.A. Hall and V. Doyle-Jones, 277-92. Los Angles: University of California, White Mountain Research Station.

Platts, W.S. 1991. Livestock grazing. In Influences of forest and rangeland management on salmonoid fishes and their habitats, edited by W.R. Meehan, 389-423. Special Publication 19. Bethesda, MD: American Fisheries Society.

Wolf, E. C., Cooper, D. J., & Hobbs, N. T. (2007). Hydrologic regime and herbivory stabilize an alternative state in yellowstone national park. *Ecological Applications*, *17*(6), 1572–1587. doi:10.1890/06-2042.1

Woods, S. W., & Cooper, D. J. (2005). Hydrologic factors affecting initial willow seedling establishment along a subalpine stream, Colorado, USA. *Arctic Antarctic and Alpine Research*, *37*(4), 636–643. doi:10.1657/1523-0430(2005)037[0636:HFAIWS]2.0.CO;2

Chapter 4

Thesis Conclusion

The research presented in this thesis attempted to determine the importance of soil organic matter and riparian willows to the health of the Tuolumne Meadows ecosystem. The two main objectives of this research were to (1) evaluate the dependency of soil water retention on soil organic matter and determine the impact to plants under changes in organic matter and (2) to examine the role of riparian willows in trapping sediment to create landforms in the Tuolumne River. In light of the work that was detailed in the two previous chapters, we can make the following claims:

1. The loss of soil organic matter reduces soil water retention and decreases the water available to plants for transpiration. The impact of decreased soil water retention on plants is greatest late in the growing season when plants experience increased water stress, thus limiting the opportunity for biomass growth and reproductive success. The marginal benefit (or cost) of organic matter is greatest in soils with the least

organic content, which makes vegetation in these soils most vulnerable to increased degradation.

2. The effect of willows on sedimentation processes is different for organic duff material than it is for mineral sediments. Duff deposition occurs more frequently around willows that are on banks and are farther from the river, while mineral sediment deposition occurs more frequently around willows on bars closer to the river. Repeated implementation of our procedure will likely clarify the effect of willow growth on sedimentation processes through the identification of statistically significant relationships derived from deposition depths.

In remaining portion of this chapter, we briefly review the details of the two studies that support these claims and discuss the future research directions relevant to each study.

Study One

THE LINKED EFFECTS OF SOIL HYDRAULIC PROPERTIES AND SOIL ORGANIC MATTER ON ROOT WATER UPTAKE

The work in the second chapter of this thesis was motivated by the question *how much does soil water retention depend on soil organic content, and what is the impact to plants if soil organic content changes*. By measuring soil water retention curves and soil organic content at distributes sites across the meadow, we found that soil water retention is strongly dependent on soil organic matter. A correlation between soil organic content and the Van Genuchten retention parameters θs and α suggested that losses of organic matter will decrease the porosity of soil and increase the ease at which water is drained. We saw that these two effects combine to reduce the Available Water Capacity (AWC) of the soil, which is a meaningful metric that describes the amount of water available for use by plants. A textural analysis of the soils shows that θs and α also vary with silt content, but the observed range of θs is larger than the expected range that is predicted to be caused by texture alone over the measured range of silt content (Saxton & Rawls, 2006; Carsel & Parrish, 1988). The additional retention found in Tuolumne Meadows soil can be attributed to organic matter. Therefore, a loss of organic matter will have a significant impact on the ability of soil to retain water.

To demonstrate the impact of soil organic matter loss on plants we simulated seasonal transpiration under different levels of soil water retention. We used a physically-based hydrological numerical model to show the degree to which root water uptake is affected by changes in soil water retention. The results demonstrated that the increased water retention by soil organic matter contributes as much as 8.8 cm to transpiration during the dry second half of summer when plants experience increased water stress. Moreover, the largest difference in cumulative transpiration for a marginal difference in organic content is in soils with the least organic matter. Because plants in the least organic soils lose more water with an equivalent loss of organic content, they are the most vulnerable to continued degradation.

The amount of carbon in the soil is a balance between the supply of organic material by plants and the loss of organic matter due to soil respiration (Six, Feller, et al., 2002). This study suggests that soil organic matter loss may decrease plant productivity, which suggests that the input rate of plant-based carbon could also decrease. Because soil respiration is higher in conditions that are less persistently saturated (Moyano et al., 2013; Davidson et al., 2012), increased dryness due to decreased soil water retention may perpetuate the loss of organic matter through increased respiration. It would be instructive to see how the rates of carbon input by plants and carbon output through respiration interact under changes in soil water retention because the balance of these rates can determine how resistant a meadow is to degradation, or how amendable it is to restoration activities.

Study Two

THE CLAY PAD AND EROSION CHAIN METHOD FOR MEASUREING SEDIMENTATION PROCESSES FOR THE CHARACTERIZATION OF BIOGEOMORPHIC SUCCESSION ALONG THE TUOLUMNE RIVER RIPARIAN CORRIDOR

Biogeomorphic succession is the interaction of riparian vegetation with water and sediment flows to generate new landforms and opportunities for additional vegetation establishment. Thus, riparian willows may play an important biogeomorphic role to decrease channel widening caused by hydrologic impacts to the meadow. The work completed in Chapter 3 of this thesis was motivated by the question *does failed willow recruitment reduce trapping of* *fine sediment on gravel bars*. We attempted to address this question by measuring sedimentation on inert clay pads around willows in riparian areas along the Tuolumne River. Although the unusually low peak stream flows during 2012 and 2013 limited our opportunity to observe sedimentation events, we collected sufficient data to show that the procedure is robust. Additionally, we were able to precisely measure small deposition events ($\pm 1\ mm$) and differentiate between the deposition of sand, silt, and organic duff. We found that the deposition of duff is more likely to occur around willows that are on banks, while mineral sediments are more likely to deposit around willows close to the river on gravel bars. Individual observations of mineral deposition downstream of willows on gravel bars is consistent with other studies which show a similar downstream effect (Gurnell et al., 2012). Our results suggest that riparian willows assist with mineral sediment build up of gravel bars, which may eventually become banks that receive depositions of highly organic duff. Thus, we provide a partial answer to the stated question by showing the deposition of mineral sediments occurs more frequently on gravel, and the consistency of this result with other developed studies suggests that willows play a critical role in maintaining meadow health.

A more compete answer to the question could be made by showing statistically significant relationships between the depth of sedimentation on clay pads and the biogeomorphic factors of interest. The depth relationships we produced were statistically insignificant, and this is likely caused by a limited number of non-zero depth data. Future efforts can exclude some clay pads with no observed deposition by identifying those that were never submerged. Additionally, a continuation of this study will likely generate more data over wetter years that could reveal relationships between willow recruitment, sedimentation depth, and biogeomorphic factors that are statistically significant.

The progress made towards the achievement of objectives (1) and (2) through the completion of these two studies can help direct ecosystem management strategies because it is likely that any change in water availability for meadow vegetation under continued degradation will be due to some combination of soil organic matter loss and channel erosion.

REFERENCES

Carsel, R., & Parrish, R. (1988). Developing Joint Probability-Distributions of Soil-Water Retention Characteristics. *Water Resources Research*, *24*(5), 755–769. doi:10.1029/WR024i005p00755

Davidson, E. A., Samanta, S., Caramori, S. S., & Savage, K. (2012). The Dual Arrhenius and Michaelis-Menten kinetics model for decomposition of soil organic matter at hourly to seasonal time scales. *Global Change Biology*, *18*(1), 371–384. doi:10.1111/j.1365-2486.2011.02546.x

Gurnell, A. M., Bertoldi, W., & Corenblit, D. (2012). Changing river channels: The roles of hydrological processes, plants and pioneer fluvial landforms in humid temperate, mixed load, gravel bed rivers. *Earth-Science Reviews*, *111*(1-2), 129–141. doi:10.1016/j.earscirev.2011.11.005

Moyano, F. E., Manzoni, S., & Chenu, C. (2013). Responses of soil heterotrophic respiration to moisture availability: An exploration of processes and models. *Soil Biology & Biochemistry*, *59*, 72–85. doi:10.1016/j.soilbio.2013.01.002

Saxton, K. E., & Rawls, W. J. (2006). Soil water characteristic estimates by texture and organic matter for hydrologic solutions. *Soil Science Society of America Journal*, *70*(5), 1569–1578. doi:10.2136/sssaj2005.0117

Six, J., Feller, C., Denef, K., Ogle, S. M., Sa, J. C. D., & Albrecht, A. (2002). Soil organic matter, biota and aggregation in temperate and tropical soils - Effects of no-tillage. *Agronomie*, *22*(7-8), 755–775. doi:10.1051/agro:2002043

Appendix A

Photographic Documentation of the Clay Pad Method to Measure Sedimentation

PHOTOGRAPHIC DOCUMENTATION OF THE CLAY PAD INSTALLATION PROCEDURE

Figure 1: *The material required to install a clay pad are (clockwise from the top): white powder feldspar clay, digging tools, and a pad template, and a spray bottle. In this image, recently installed clay pad is visible on the upstream side of a willow.*

***Figure 2:** A wooden board with the dimensions of the excavation of the pad is used to guide the excavation.*

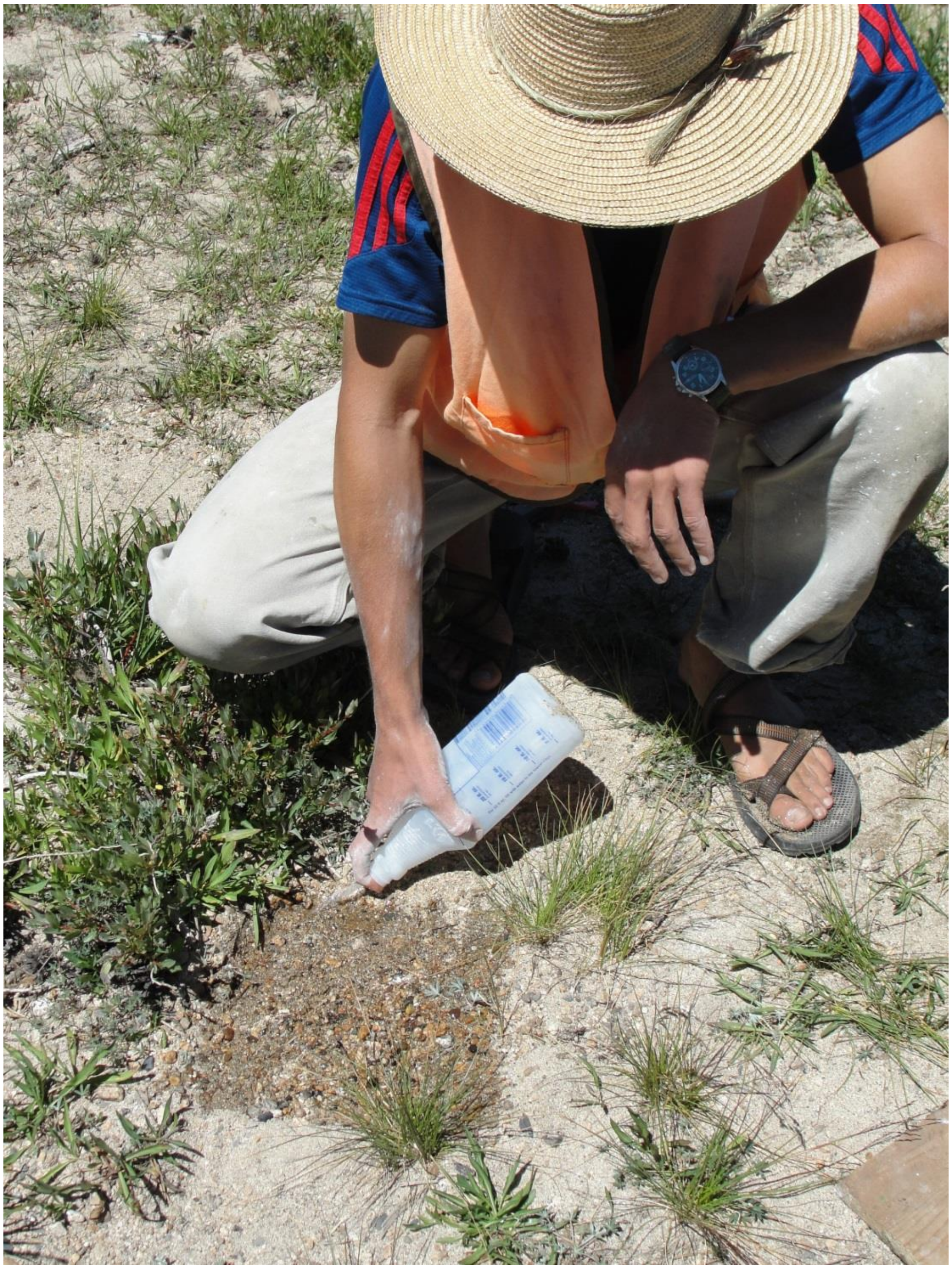

Figure 3: *To install a clay pad, a 12 in square excavation is made 1-2 cm deep. The vegetation is removed. Prior to the adding of clay, the area is wetted to promote cohesion between the clay and the bed material.*

Figure 4: *Clay is added in layers. Each layer is wetted with a spray bottle before the next layer is added. The pad is installed in a total of 3 to 5 layers.*

Figure 5: *A completed clay pad receives a final addition of water to ensure it is completely moistened. Clay that is not moistened will easily be blown away in the wind.*

Figure 6: *A clay pad buried in sand is located with a metal detector. Each pad can be located even if completely buried because the erosion chain installed in the middle of the downstream edge of the pad can be found with a metal detector.*

Figure 7: *The materials required to take measurements from clay pads include: a tape measure, a coring device (plexiglass tube 15 mm in diameter and at least 4 cm long), a stick to push the sample core out of the coring device and back into the clay pad, a cloth to clean the sidewalls of the coring device, and a camera (not shown).*

EVIDENCE OF A DAMAGED CLAY PAD

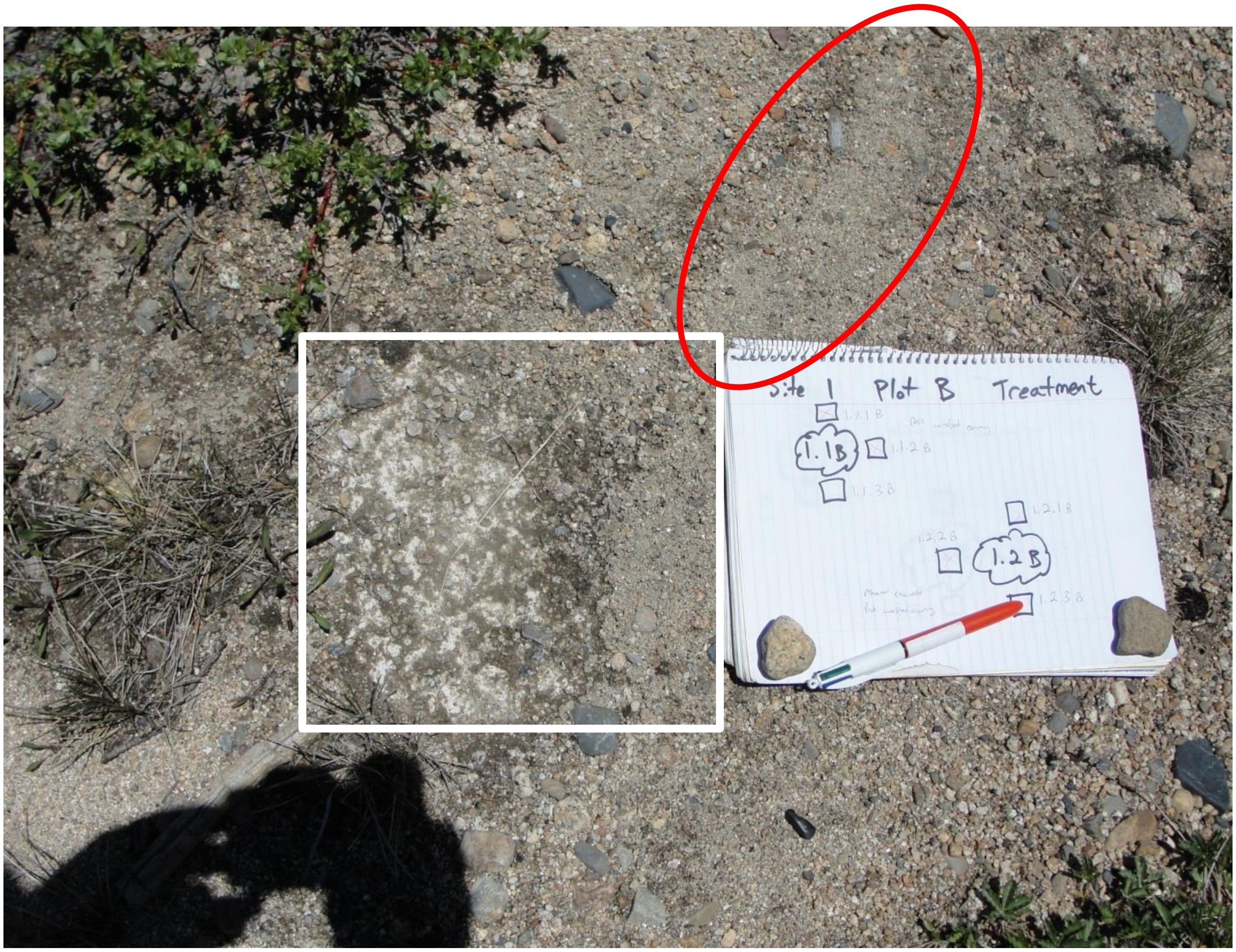

Figure 8: *This pad (white box) was disturbed by what appeared to be a hoof kick (red oval) in 2013. Therefore, the gravel sprinkled on the left side (stream side) is considered non-representative. This pad recorded 12.8 mm of sand deposition in 2012. In 2013, the left side measured zero the right side measured 5.3 mm.*

COMPLEX SEDIMENTATION PATTERNS RESULT FROM INTERACTIONS OF WILLOWS WITH SEDIMENT AND WATER FLOWS

Figure 9: *Sedimentation and erosion downstream of willow on a gravel bar*.

Figure 10: *A large deposit of sand downstream of a willow.*

***Figure 11:** A pioneer group of heavily grazed willows.*

Figure 12: *Heterogeneous deposit of sand, duff, and gravel around a cluster of willows on a gravel bar.*

Figure 13: *a distinct flow pattern of erosion and woody debris downstream of a large lone willow on a gravel bar.*

Figure 14: *The land surface downstream of the established willow is raised, perhaps due to increased deposition (or decreased erosion) of fine grained sediments.*

Figure 15: *Heavily grazed willows can be identified by examining the terminal ends of the branchlets. Ungrazed growth is soft and green, while grazed branchlets appear chopped or torn, and are stiff.*

Figure 16: *Erosion can occur in large periodic events. Here, in a location without supportive willow root growth, we observe chunks of the fine grained meadow top layer (0.5 to 1.5 m wide) that have fallen into the river.*

Figure 17: *Although the banks are heavily undercut in this segment of Unicorn Creek, deeply established willow roots pin the bank in place.*

Figure 18: *Professor Loheide indicates a transition zone between an established bank and a developing gravel bar. Findings in Chapter 3 of this thesis suggest the willows visible on the gravel bar trap sediment to raise the land surface until it becomes a bar.*

Figure 19: *A late spring snow storm allowed for observations of raised stream stages and bank ice formation on the gravel bar of site 1.*

Appendix B

The Method to Correct for Evaporative Losses During the Pressure Plate Test

INTRODUCTION

The leak-free pressure plate test by Wang and Benson (2004) was used to measure the soil water retention curves of the 19 undisturbed soil samples collected from Tuolumne Meadows. The test measures the volume of water extracted from the soil sample by tracking the movement of a meniscus between water and air along a 0.25 cm diameter glass horizontal measurement tube. During the test, water extracted from the sample drains into the horizontal tube and the meniscus moves a measureable amount. We discovered the evaporation loss when we noticed a difference between the estimated volume of extracted water using the meniscus method to the mass loss of soil water before and after the test (Table 1). The following section describes our methods to determine the source of the difference between volume loss and mass loss in the pressure plate test results. A procedure is presented that corrects for this difference to produce a more accurate soil water characteristic curve from those that experience evaporation loss.

The pressure plate test is a method that is designed to be leak free by screwing down precision-machined brass plates against a tightly fitting rubber o-ring to form a seal between the pressure regulator and the porous ceramic plate (Wang and Benson, 2004). The only unsealed opening in the leak free pressure plate test equipment, and therefore the only possible location for evaporation to occur is the opening at the end of the horizontal measurement tube. With the objective to isolate the influence of the opening at the end of the horizontal measurement tube and exclude the influence of all other equipment, we prepared a horizontal measurement tube

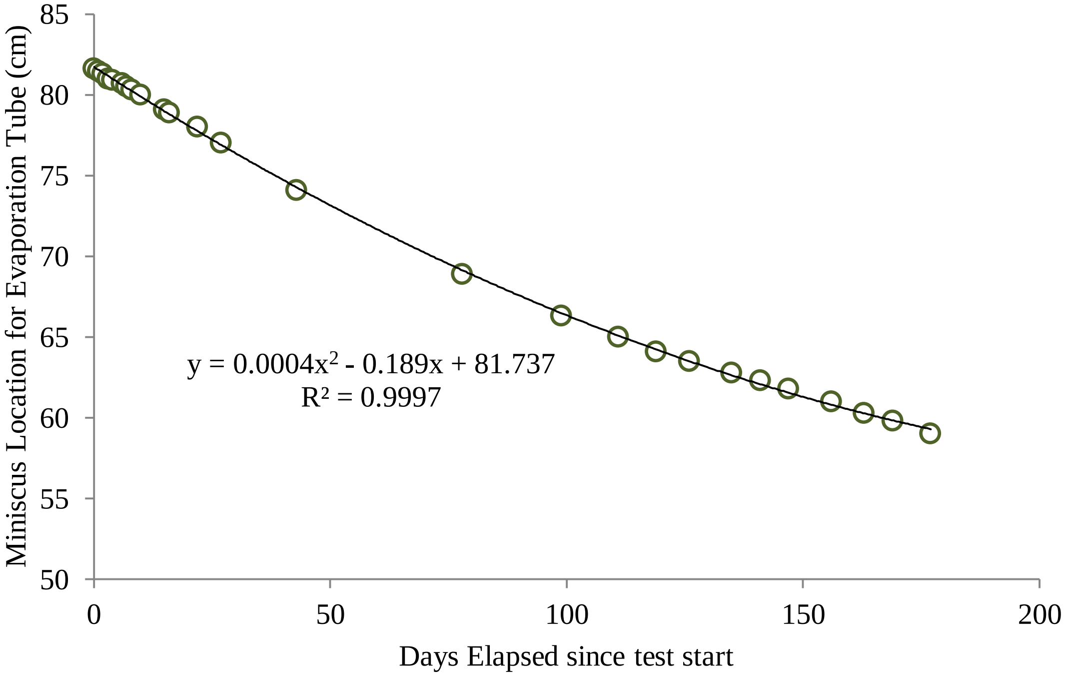

Figure 1: *The movement of the meniscus on an isolated horizontal pressure plate reading tube was recorded over a time period during which pressure plate tests were being conducted on soil samples.*

sealed with a clamp at the end where the pressure plate apparatus is typically connected and open to the atmosphere at the other. Figure 1 shows the movement of the meniscus in this tube over time. The decreasing slope of the Figure 1 trend line implies the rate of movement of the meniscus decreased. We consider the two most likely causes of this is that the rate of movement is dependent on either (1) the distance between the meniscus and the opening at the end of the tube, or (2) the relative humidity of the atmosphere. We performed two additional experiments to determine which effect controls the meniscus movement.

To determine the effect on the meniscus movement of the distance between the meniscus and the opening at the end of the horizontal measurement tube, we measure meniscus movement at 11 different locations on 11 different tubes. Figure 2 shows the location of the meniscus over time for all 11 tubes. The similar slopes of the trend lines in each plot indicate the rate of movement of the meniscus is independent of the distance between the meniscus and the opening at the end of the horizontal measurement tube.

To determine the influence of relative humidity on the rate of movement of the meniscus in Figure 1, we recorded the relative humidity of the room where the while the test took place (Figure 3). The trend line through this data was translated into a function (equation 1) which

$$RH(Jday) = 3.16 \times 10^{-8}x^{4} - 2.8 \times 10^{-5}x^{3} + 6.642 \times 10^{-3}x^{2} - 2.3 \times 10^{-1}x^{-1} + 5.09 \tag{1}$$

Sample (Well #)	Evaporation Loss (difference btw mass loss and vol. loss) (cm^3)	Evaporation Loss After Correction (cm^3)	% error after correction
28	20.68	14.24	23.18
1	4.76	-1.64	-3.50
2	7.08	0.68	1.30
9	10.28	3.88	6.15
8	20.4	13.95	24.29
3	10.92	2.37	4.15
10	11.03	4.71	7.27
27	14.21	7.91	11.41
6	10.07	-1.03	-1.66
14	2.06	0.36	0.50
80	5.91	3.68	6.77
48	-0.68	-2.92	-5.01
35	5.95	3.31	8.22
31	7.06	4.42	7.58
70	3.82	1.02	1.72
38	4.06	1.21	2.19
47	5.03	2.18	3.46
46	5.1	-0.16	-0.33
23	18.71	13.45	20.06

***Table 1**: The difference between the estimated volume of extracted water using the meniscus method to the estimated mass loss of water.*

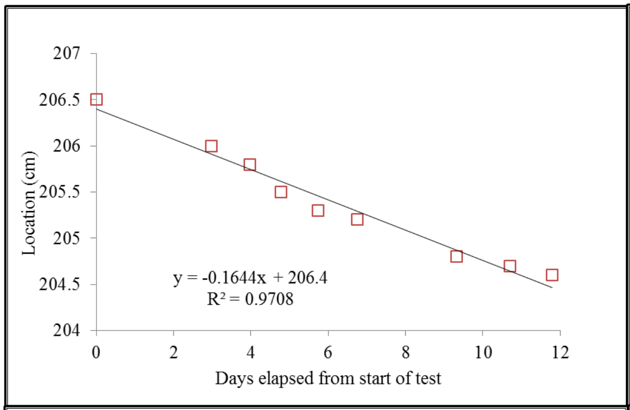
207
206.5
206
205.5
205
204.5
204
Location (cm)
y = -0.1644x + 206.4
R² = 0.9708
0
2
4
6
8
10
12
Days elapsed from start of test

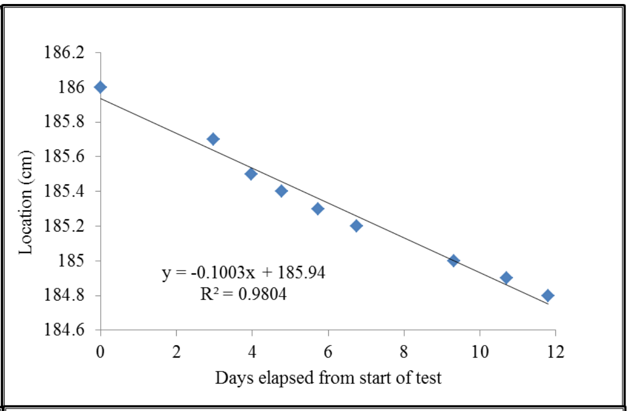
186.2
186
185.8
185.6
185.4
185.2
185
184.8
184.6
Location (cm)
y = -0.1003x + 185.94
R² = 0.9804
0
2
4
6
8
10
12
Days elapsed from start of test

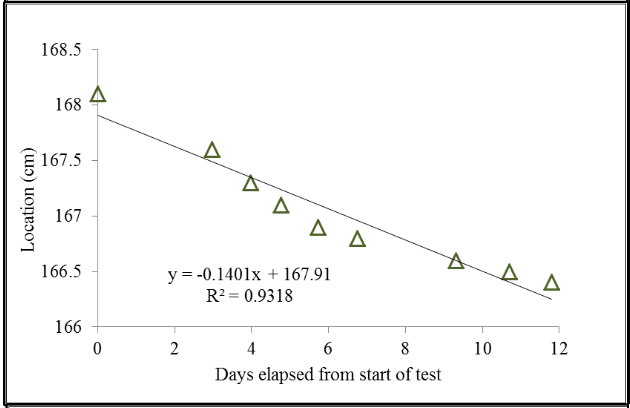
168.5
168
167.5
167
166.5
166
Location (cm)
y = -0.1401x + 167.91
R² = 0.9318
0
2
4
6
8
10
12
Days elapsed from start of test

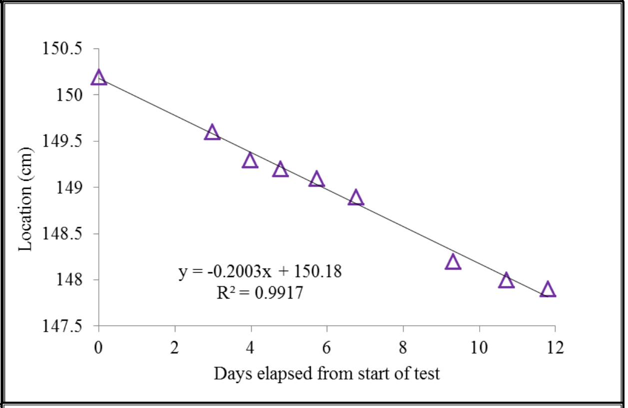
150.5
150
149.5
149
148.5
148
147.5
Location (cm)
y = -0.2003x + 150.18
R² = 0.9917
0
2
4
6
8
10
12
Days elapsed from start of test

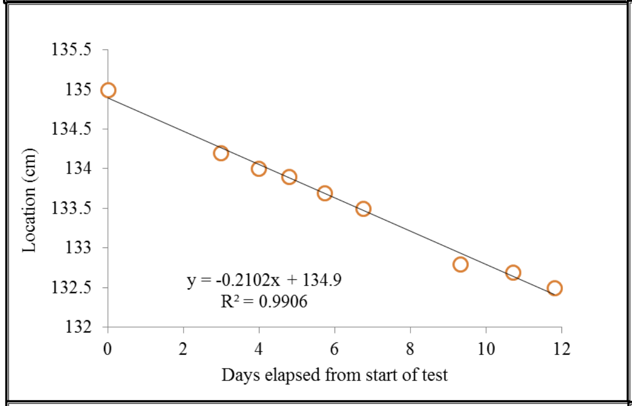
135.5
135
134.5
134
133.5
133
132.5
132
Location (cm)
y = -0.2102x + 134.9
R² = 0.9906
0
2
4
6
8
10
12
Days elapsed from start of test

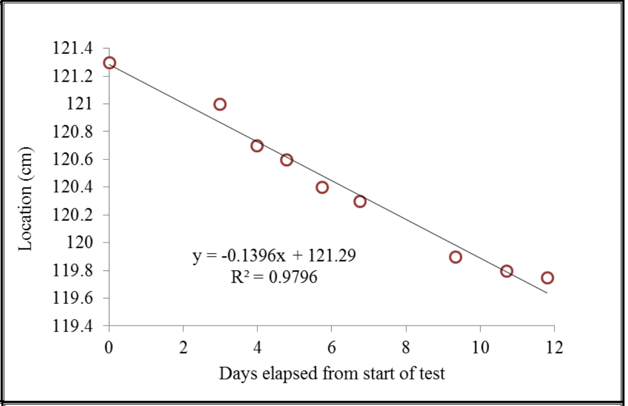
121.4
121.2
121
120.8
120.6
120.4
120.2
120
119.8
119.6
119.4
Location (cm)
y = -0.1396x + 121.29
R² = 0.9796
0
2
4
6
8
10
12
Days elapsed from start of test

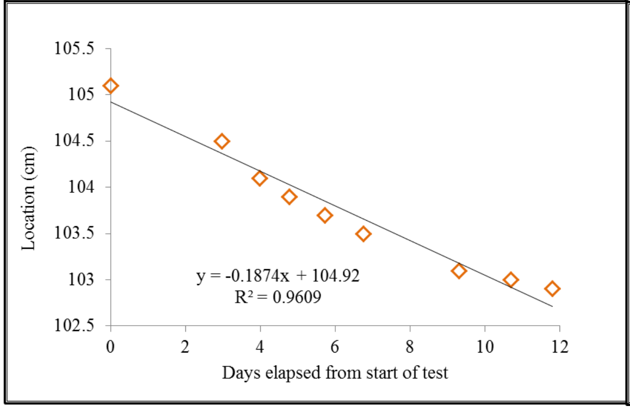
105.5
105
104.5
104
103.5
103
102.5
Location (cm)
y = -0.1874x + 104.92
R² = 0.9609
0
2
4
6
8
10
12
Days elapsed from start of test

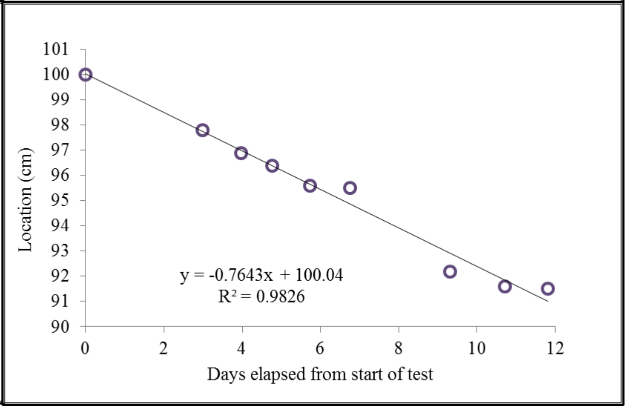
101
100
99
98
97
96
95
94
93
92
91
90
Location (cm)
y = -0.7643x + 100.04
R² = 0.9826
0
2
4
6
8
10
12
Days elapsed from start of test

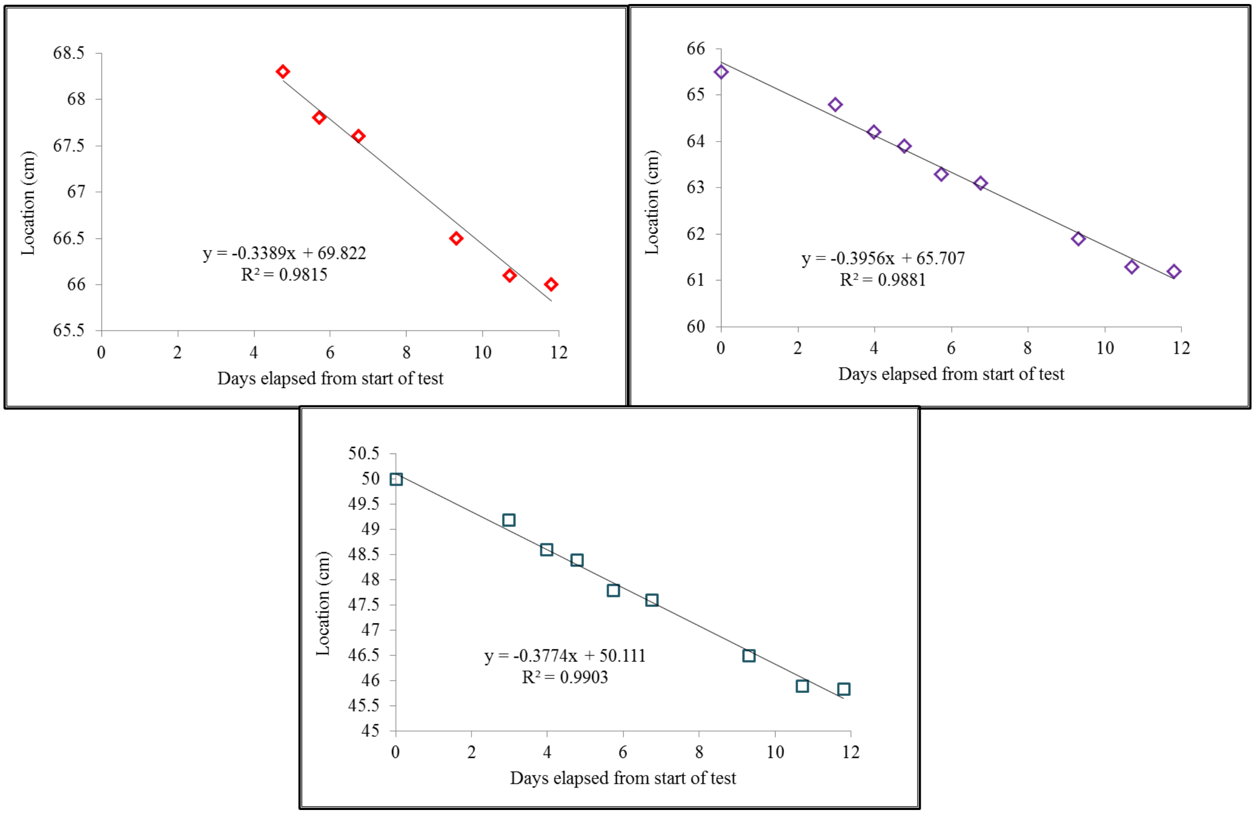

Figure 2: *The location of the meniscus was measured on 11 tubes over 12 days. Each symbol type represents meniscus locations on an individual tube.*

describes the relative humidity for any given Julien Day (Figure 4). We then computed the rate of meniscus movement between each measurement of Figure 1 and plotted them against the relative humidity predicted by eq. (1) for the Julien day of each measurement (Figure 5). The trend line through this data (equation 2) is used to estimate the evaporation rate for the relative

$$EvapRate(RH) = -0.0018x + 0.1918 \qquad (2)$$

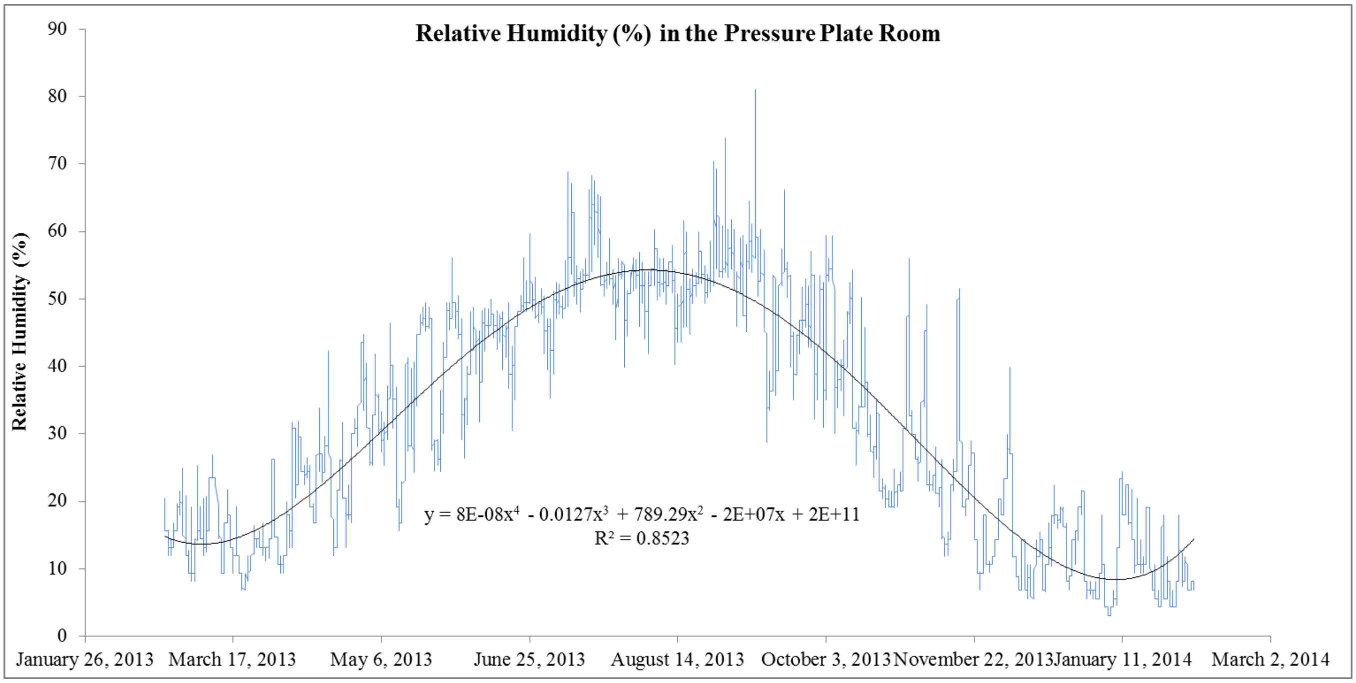

Figure 3: *Relative humidity was recorded in the pressure plate test room while pressure plate tests were conducted.*

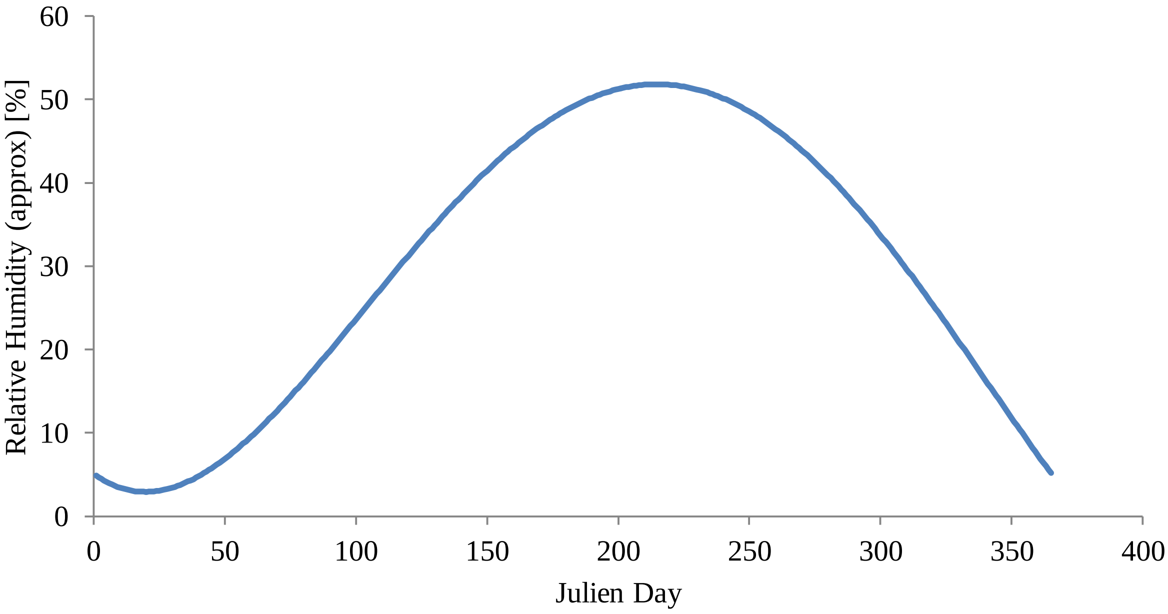

Figure 4: *The fitted polynomial shown in Figure 3 was translated into a function (Equation 2) that determines Relative Humidity for any given Julian Day.*

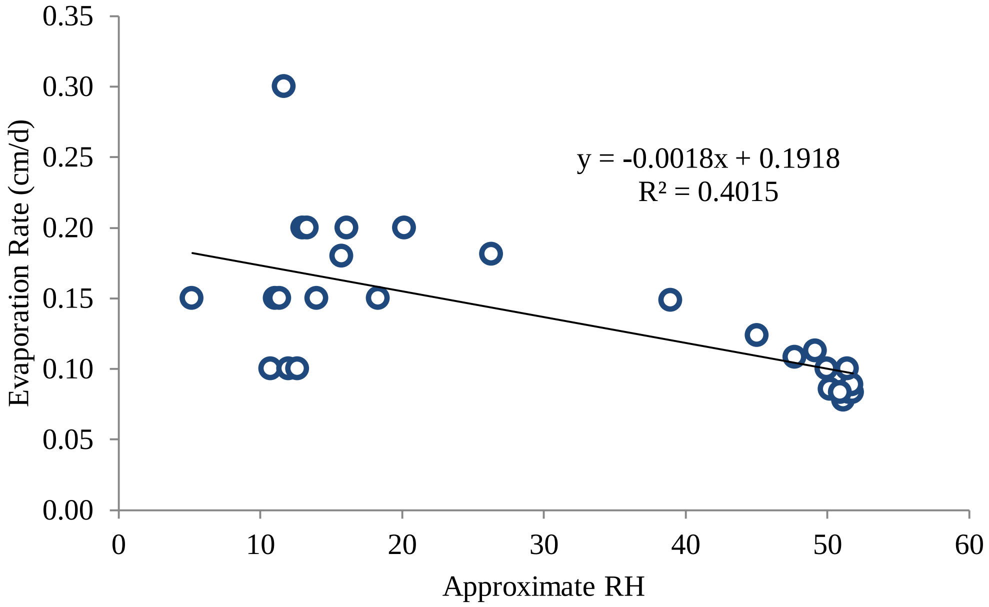

Figure 5: *Equation 2 was used to estimate the relative humidity of all days in Figure 1. The results were fit with a line to produce a function (Equation 3) that determines the evaporation rate for any relative humidity represented by the trend line in Figure 3.*

humidity predicted by eq. 1. The result is a function which predicts the evaporation rate over the Julian year (equation 3) which is plotted in Figure 6.

$$Evap(\,RH(Jday)\,) = -5.688 \times 10^{-11}x^4 + 5.040 \times 10^{-8}x^3 - 1.196 \times 10^{-}x^2 + 4.147 \times 10^{-4}x + 0.1826 \tag{3}$$

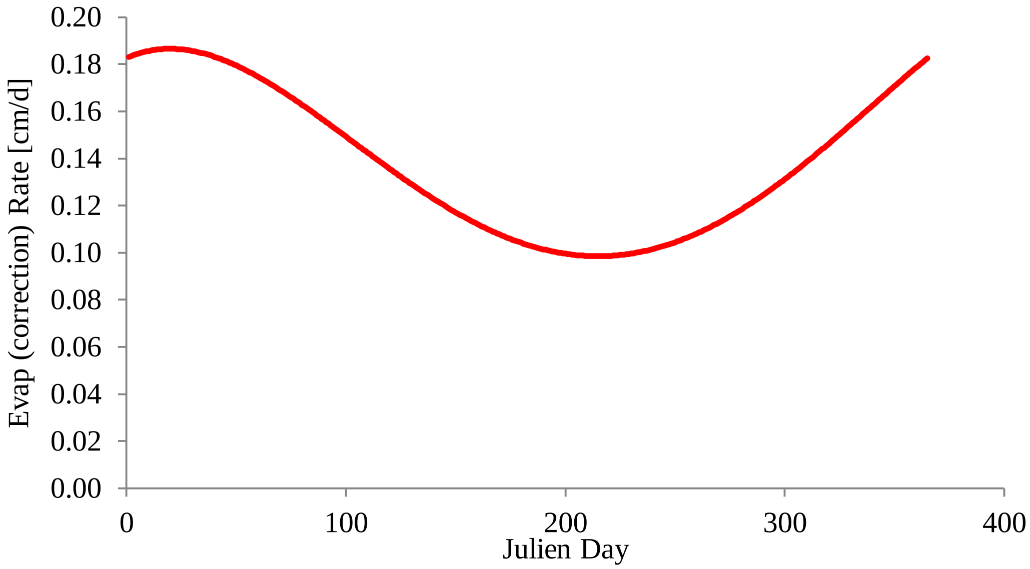

Figure 6: *The evaporation rate over the year is estimated for Figure 4 using Equation 3.*

To correct for evaporation loss for a pressure plate test, the loss calculated by eq. 3 can be implemented into the Wang and Benson (2006) method as follows:

The pressure plate data are plotted with:

$$\theta(\varphi) = \theta s - \frac{\Delta L \times Ac}{V}$$

where θs is the porosity, ΔL is the difference between the meniscus location and the location at the beginning of the test, Ac is the cross-sectional area of the measurement tube (0.2 cm^2), and V is the volume of the sample ring (106.3 cm^3). The evaporation loss distorts the measurement of ΔL, so it must be corrected with

$$\Delta L_{corrected} = \Delta L + \sum EvapCorrection$$

where

$$Evap\ Correction = \frac{1}{2}(\#days\ inbetween) \times \big(Evap(\ current\ Julien\ Day\ ) +$$
$$Evap(\ previous\ Julien\ Day\ )\big)$$

and Evap represents eq. 3. The following collection of curves is the 19 soil water retention curves used in this thesis. The uncorrected values are in the "Uncorrected Values" columns. The corrected values are in the "Measured" columns and are fit with the Van Genuchten (1980) retention model. The sample number is indicated in the legend.

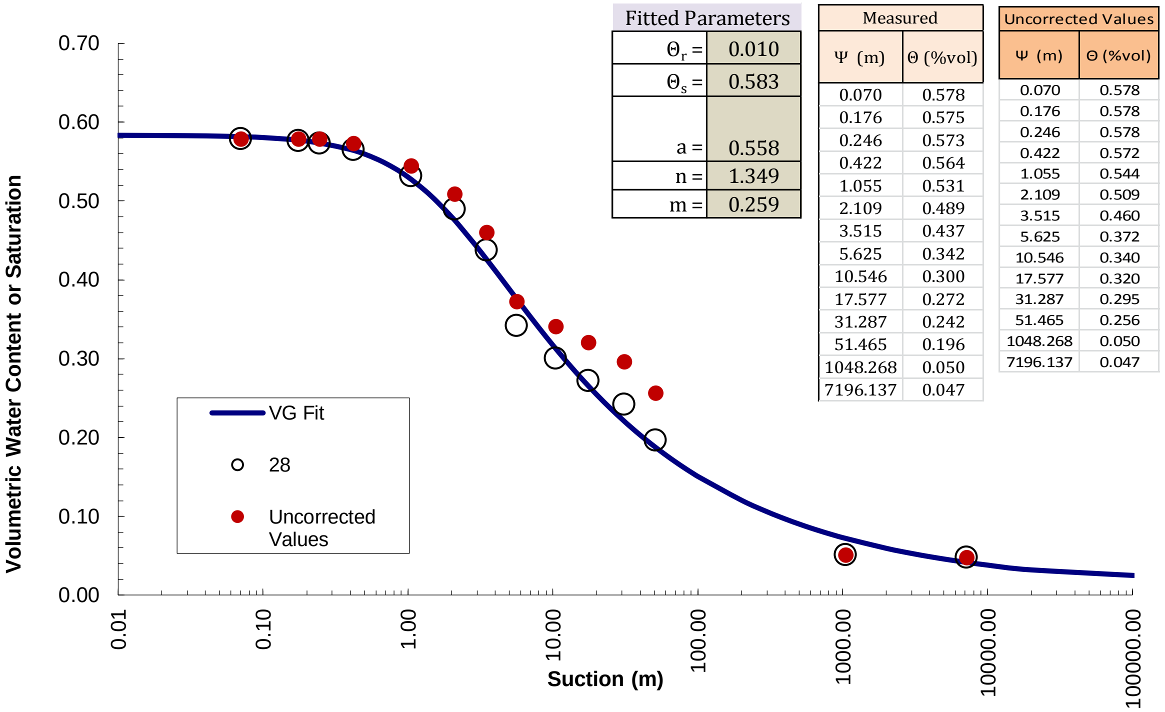

Fitted Parameters	
Θ_r =	0.010
Θ_s =	0.583
a =	0.558
n =	1.349
m =	0.259

Measured	
Ψ (m)	Θ (%vol)
0.070	0.578
0.176	0.575
0.246	0.573
0.422	0.564
1.055	0.531
2.109	0.489
3.515	0.437
5.625	0.342
10.546	0.300
17.577	0.272
31.287	0.242
51.465	0.196
1048.268	0.050
7196.137	0.047

Uncorrected Values	
Ψ (m)	Θ (%vol)
0.070	0.578
0.176	0.578
0.246	0.578
0.422	0.572
1.055	0.544
2.109	0.509
3.515	0.460
5.625	0.372
10.546	0.340
17.577	0.320
31.287	0.295
51.465	0.256
1048.268	0.050
7196.137	0.047

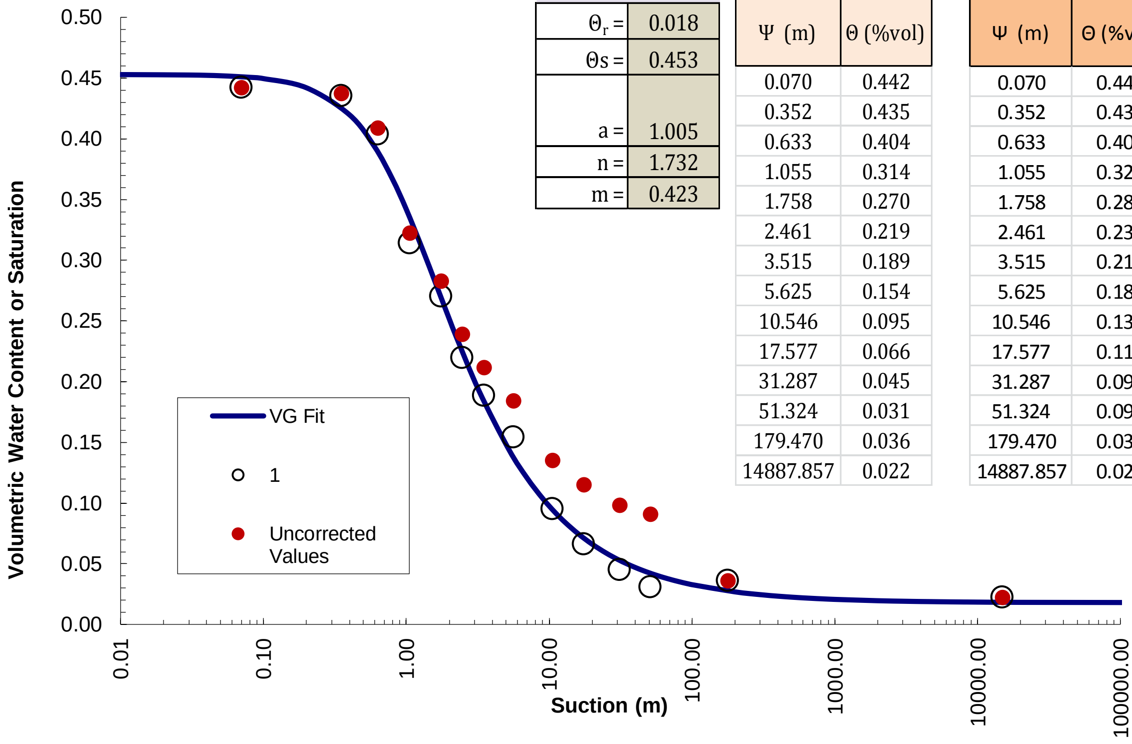

Fitted Parameters	
Θ_r =	0.018
Θs =	0.453
a =	1.005
n =	1.732
m =	0.423

Measured		Uncorrected Values	
Ψ (m)	Θ (%vol)	Ψ (m)	Θ (%vol)
0.070	0.442	0.070	0.442
0.352	0.435	0.352	0.437
0.633	0.404	0.633	0.409
1.055	0.314	1.055	0.322
1.758	0.270	1.758	0.283
2.461	0.219	2.461	0.239
3.515	0.189	3.515	0.212
5.625	0.154	5.625	0.184
10.546	0.095	10.546	0.135
17.577	0.066	17.577	0.115
31.287	0.045	31.287	0.098
51.324	0.031	51.324	0.091
179.470	0.036	179.470	0.036
14887.857	0.022	14887.857	0.022

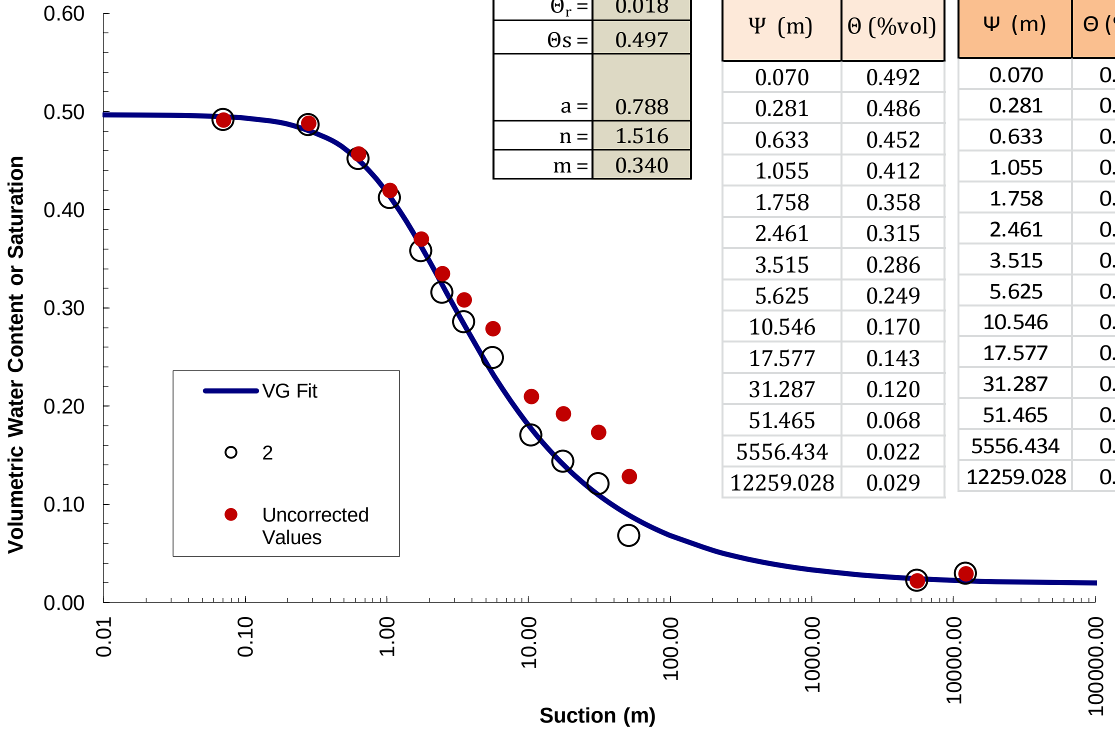

Fitted Parameters	
Θ_r =	0.018
Θs =	0.497
a =	0.788
n =	1.516
m =	0.340

Measured		Uncorrected Values	
Ψ (m)	Θ (%vol)	Ψ (m)	Θ (%vol)
0.070	0.492	0.070	0.492
0.281	0.486	0.281	0.488
0.633	0.452	0.633	0.457
1.055	0.412	1.055	0.420
1.758	0.358	1.758	0.371
2.461	0.315	2.461	0.335
3.515	0.286	3.515	0.308
5.625	0.249	5.625	0.279
10.546	0.170	10.546	0.210
17.577	0.143	17.577	0.193
31.287	0.120	31.287	0.174
51.465	0.068	51.465	0.128
5556.434	0.022	5556.434	0.022
12259.028	0.029	12259.028	0.029

Fitted Parameters	
θ_r =	0.010
θs =	0.573
a =	0.405
n =	1.523
m =	0.344

Measured	
Ψ (m)	Θ (%vol)
0.070	0.594
0.281	0.579
0.633	0.535
1.055	0.506
1.758	0.475
2.461	0.444
3.515	0.419
5.625	0.380
10.546	0.266
17.577	0.206
31.287	0.150
51.465	0.097
392.591	0.056
876.956	0.057
10718.237	0.006

Uncorrected Values	
Ψ (m)	Θ (%vol)
0.070	0.594
0.281	0.581
0.633	0.540
1.055	0.514
1.758	0.488
2.461	0.464
3.515	0.442
5.625	0.410
10.546	0.306
17.577	0.256
31.287	0.203
51.465	0.157
392.591	0.056
876.956	0.057
10718.237	0.006

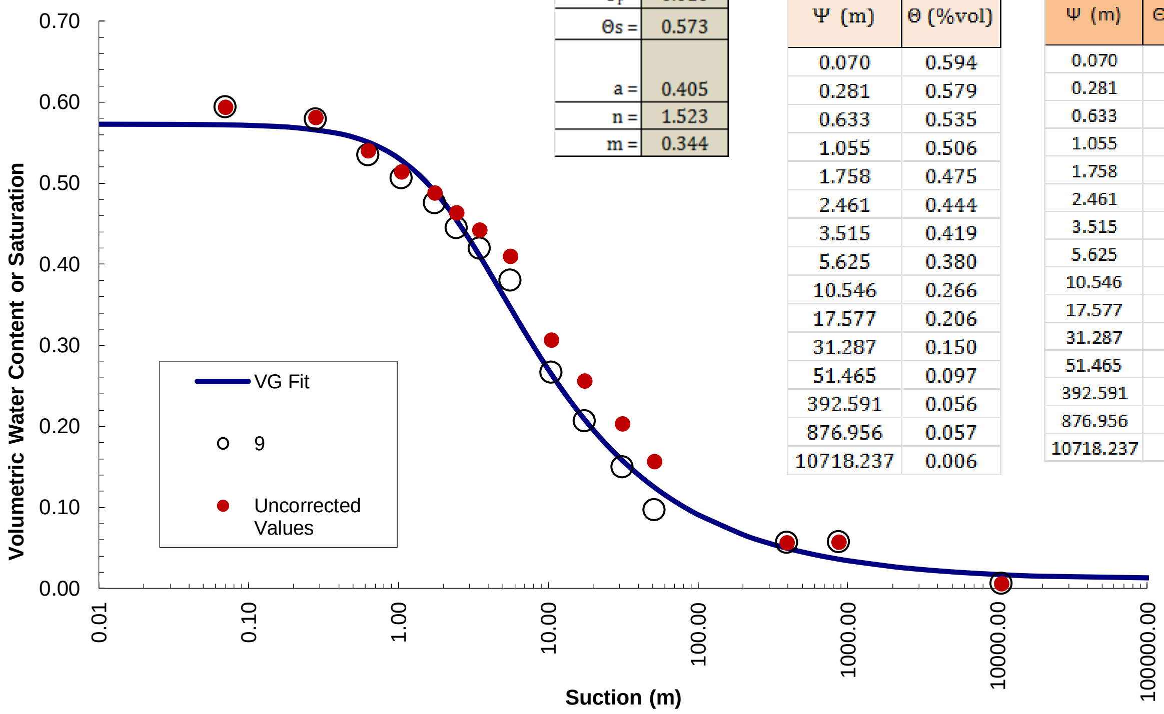

Fitted Parameters	
θ_r =	0.010
θs =	0.549
a =	0.672
n =	1.375
m =	0.273

Measured	
Ψ (m)	Θ (%vol)
0.070	0.540
0.281	0.537
0.352	0.534
0.703	0.503
1.055	0.487
1.758	0.445
3.515	0.373
5.625	0.298
10.546	0.265
17.577	0.227
31.287	0.201
51.465	0.175
351.802	0.042
1818.154	0.043

Uncorrected Values	
Ψ (m)	Θ (%vol)
0.070	0.540
0.281	0.540
0.352	0.539
0.703	0.512
1.055	0.500
1.758	0.465
3.515	0.396
5.625	0.329
10.546	0.306
17.577	0.276
31.287	0.255
51.465	0.235
351.802	0.042
1818.154	0.043

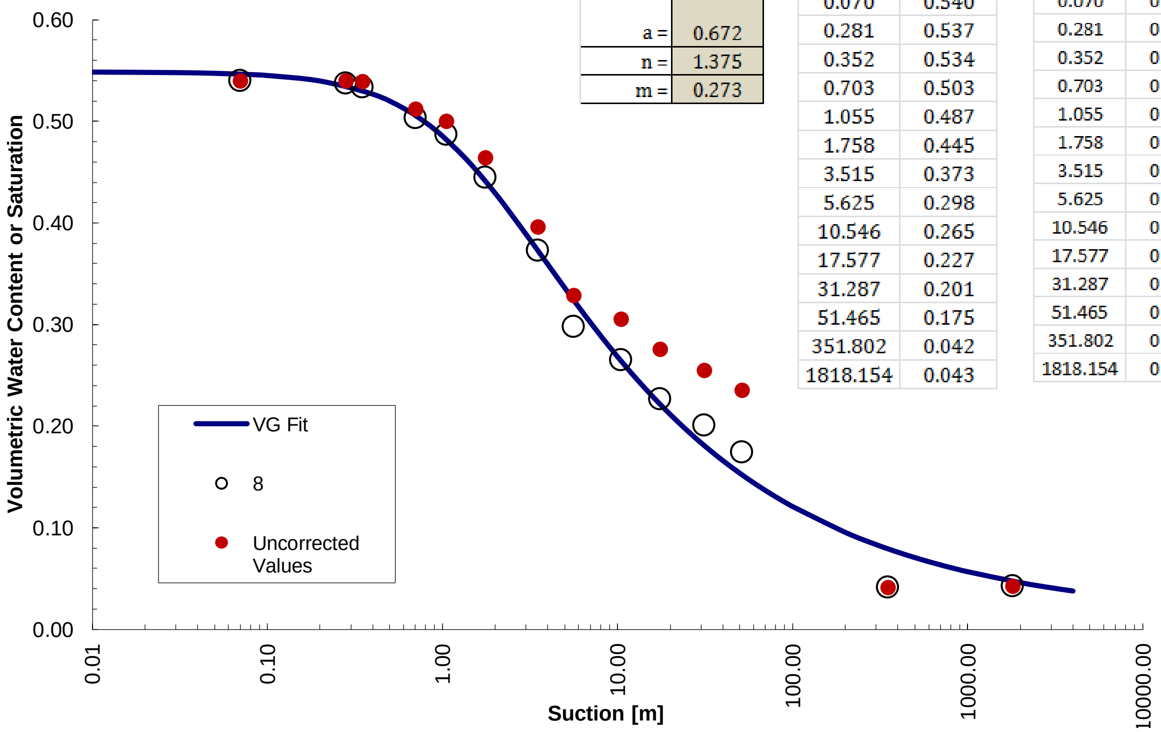

Fitted Parameters	
Θ_r =	0.023
Θs =	0.523
a =	0.687
n =	1.543
m =	0.352

Measured	
Ψ (m)	Θ (%vol)
0.070	0.537
0.176	0.513
0.246	0.508
0.422	0.490
1.055	0.445
2.109	0.366
3.515	0.319
5.625	0.260
10.546	0.186
17.577	0.151
31.287	0.121
51.465	0.083
97.893	0.063
974.849	0.070
9570.037	0.011

Uncorrected Values	
Ψ (m)	Θ (%vol)
0.070	0.537
0.176	0.516
0.246	0.513
0.422	0.498
1.055	0.458
2.109	0.386
3.515	0.343
5.625	0.290
10.546	0.227
17.577	0.200
31.287	0.175
51.465	0.163
97.893	0.063
974.849	0.070
9570.037	0.011

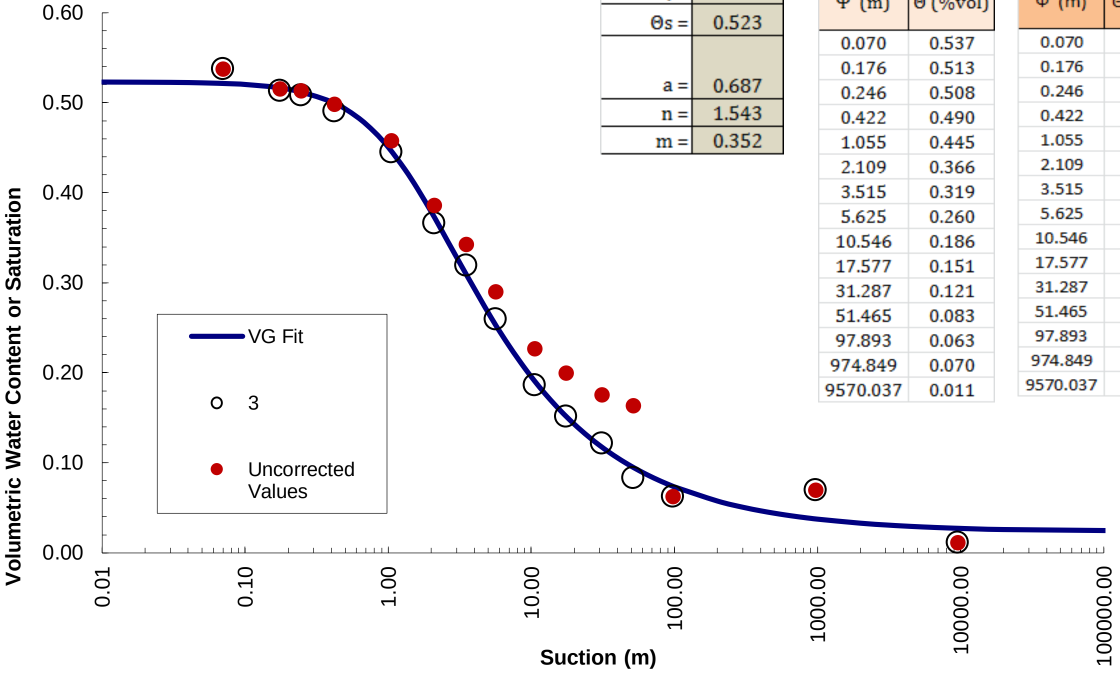

Fitted Parameters	
Θ_r =	0.010
Θs =	0.607
a =	1.025
n =	1.344
m =	0.256

Measured	
Ψ (m)	Θ (%vol)
0.070	0.610
0.352	0.572
1.055	0.501
2.109	0.398
4.289	0.370
7.031	0.323
21.092	0.264
49.215	0.174
93.814	0.100
145.819	0.090
22257.346	0.008

Uncorrected Values	
Ψ (m)	Θ (%vol)
0.070	0.610
0.352	0.575
1.055	0.539
2.109	0.438
4.289	0.411
7.031	0.365
21.092	0.309
49.215	0.233
93.814	0.100
145.819	0.090
22257.346	0.008

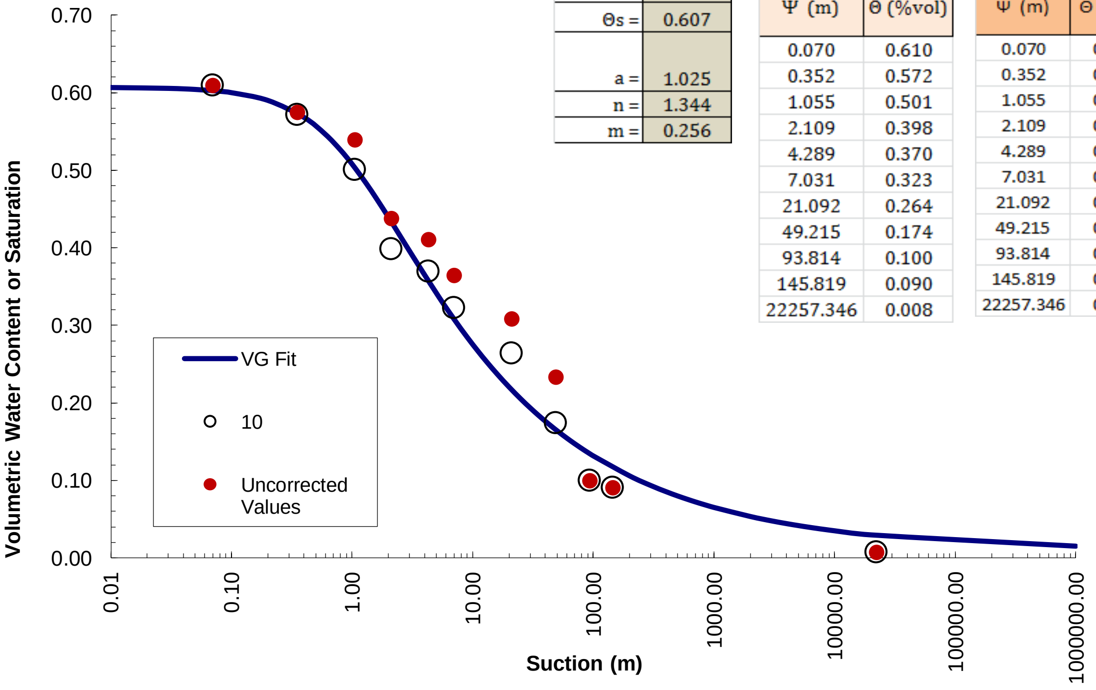

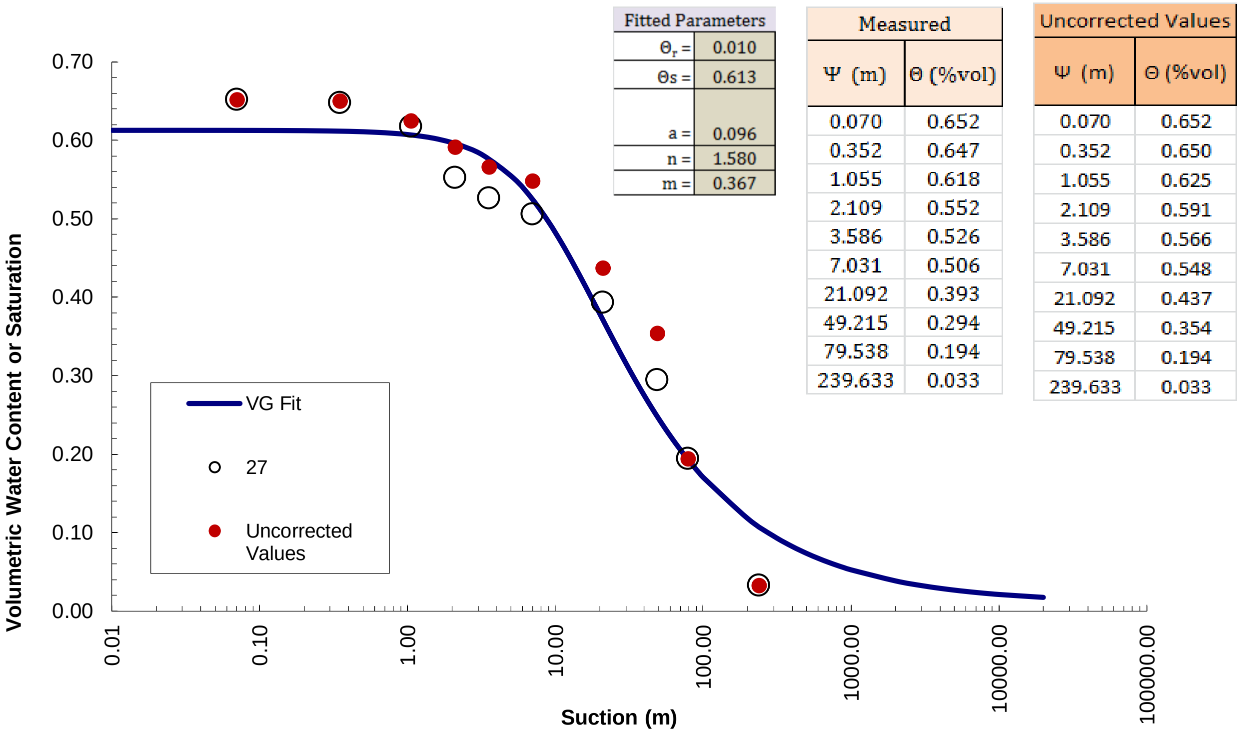

Fitted Parameters	
θ_r =	0.010
θs =	0.613
a =	0.096
n =	1.580
m =	0.367

Measured	
Ψ (m)	Θ (%vol)
0.070	0.652
0.352	0.647
1.055	0.618
2.109	0.552
3.586	0.526
7.031	0.506
21.092	0.393
49.215	0.294
79.538	0.194
239.633	0.033

Uncorrected Values	
Ψ (m)	Θ (%vol)
0.070	0.652
0.352	0.650
1.055	0.625
2.109	0.591
3.586	0.566
7.031	0.548
21.092	0.437
49.215	0.354
79.538	0.194
239.633	0.033

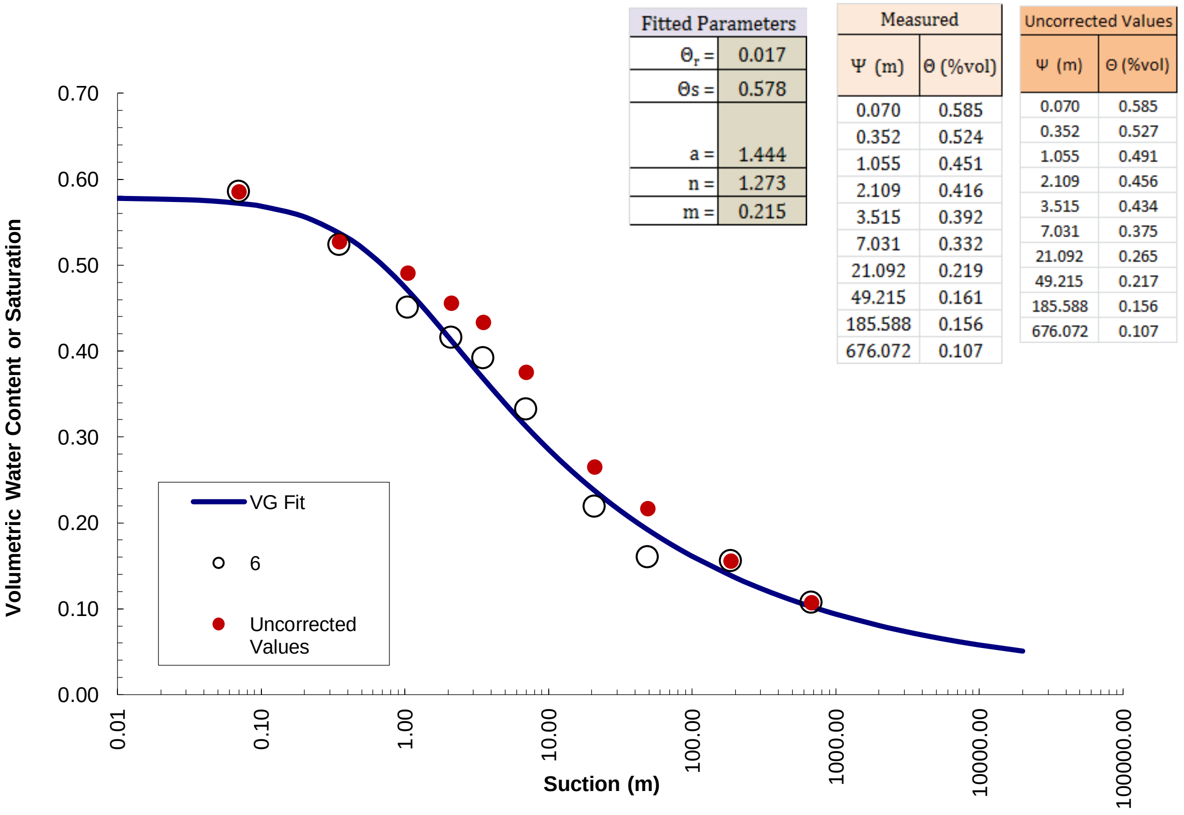

Fitted Parameters	
θ_r =	0.017
θs =	0.578
a =	1.444
n =	1.273
m =	0.215

Measured	
Ψ (m)	Θ (%vol)
0.070	0.585
0.352	0.524
1.055	0.451
2.109	0.416
3.515	0.392
7.031	0.332
21.092	0.219
49.215	0.161
185.588	0.156
676.072	0.107

Uncorrected Values	
Ψ (m)	Θ (%vol)
0.070	0.585
0.352	0.527
1.055	0.491
2.109	0.456
3.515	0.434
7.031	0.375
21.092	0.265
49.215	0.217
185.588	0.156
676.072	0.107

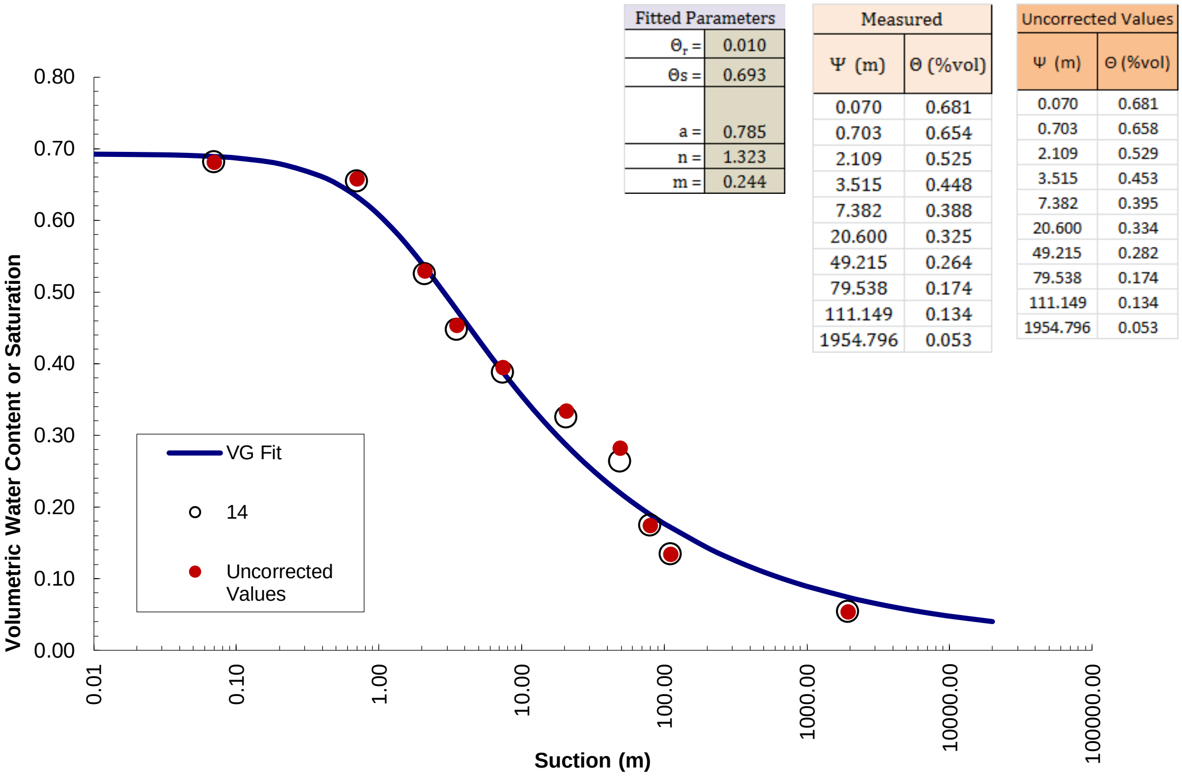

Fitted Parameters	
Θ_r =	0.010
Θs =	0.693
a =	0.785
n =	1.323
m =	0.244

Measured	
Ψ (m)	Θ (%vol)
0.070	0.681
0.703	0.654
2.109	0.525
3.515	0.448
7.382	0.388
20.600	0.325
49.215	0.264
79.538	0.174
111.149	0.134
1954.796	0.053

Uncorrected Values	
Ψ (m)	Θ (%vol)
0.070	0.681
0.703	0.658
2.109	0.529
3.515	0.453
7.382	0.395
20.600	0.334
49.215	0.282
79.538	0.174
111.149	0.134
1954.796	0.053

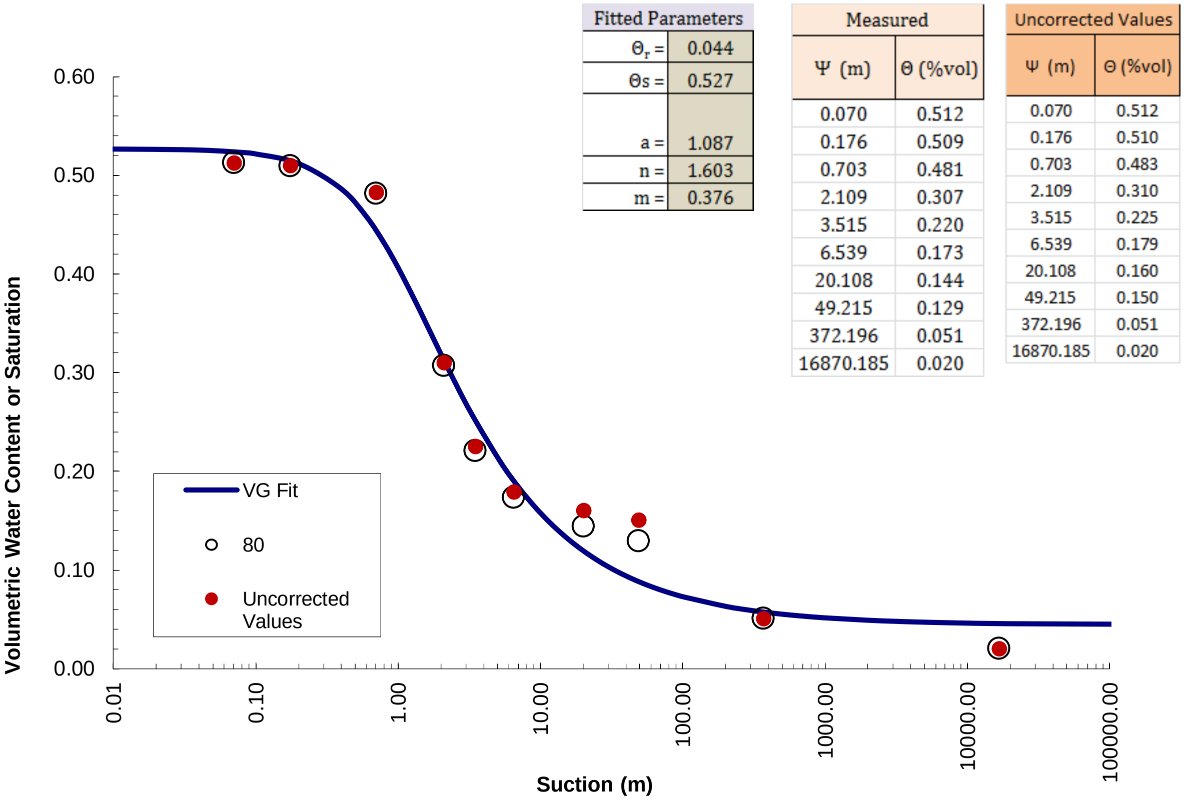

Fitted Parameters	
Θ_r =	0.044
Θs =	0.527
a =	1.087
n =	1.603
m =	0.376

Measured	
Ψ (m)	Θ (%vol)
0.070	0.512
0.176	0.509
0.703	0.481
2.109	0.307
3.515	0.220
6.539	0.173
20.108	0.144
49.215	0.129
372.196	0.051
16870.185	0.020

Uncorrected Values	
Ψ (m)	Θ (%vol)
0.070	0.512
0.176	0.510
0.703	0.483
2.109	0.310
3.515	0.225
6.539	0.179
20.108	0.160
49.215	0.150
372.196	0.051
16870.185	0.020

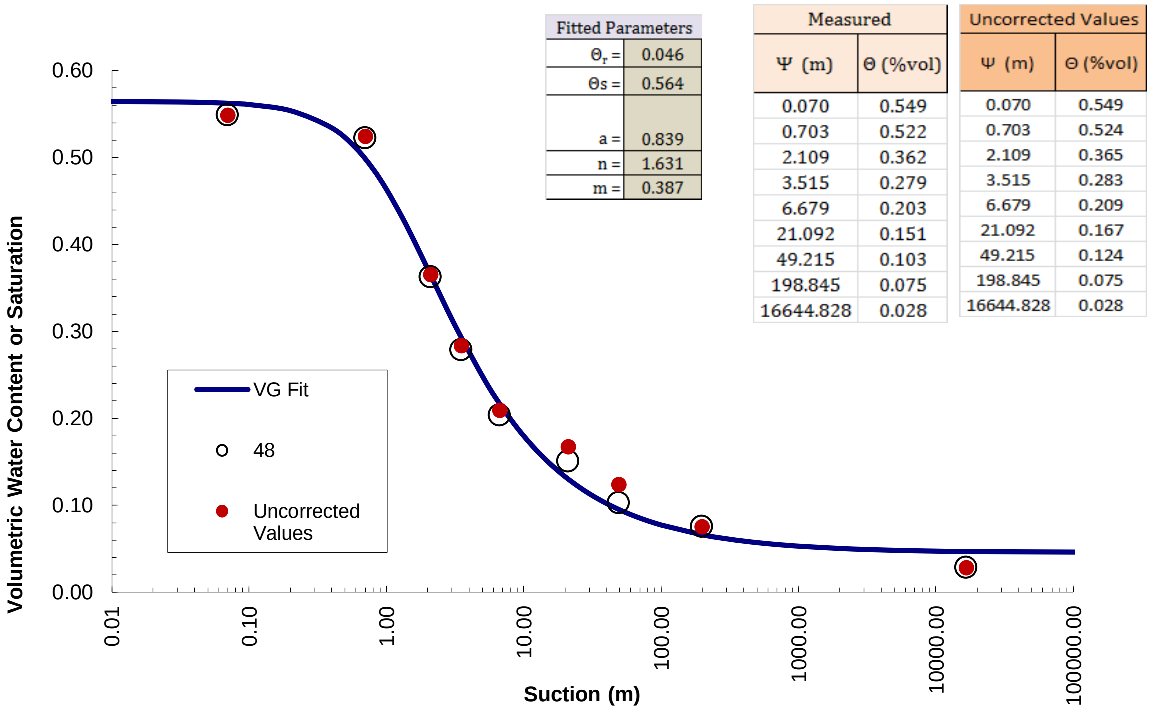

Fitted Parameters	
Θ_r =	0.046
Θs =	0.564
a =	0.839
n =	1.631
m =	0.387

Measured	
Ψ (m)	Θ (%vol)
0.070	0.549
0.703	0.522
2.109	0.362
3.515	0.279
6.679	0.203
21.092	0.151
49.215	0.103
198.845	0.075
16644.828	0.028

Uncorrected Values	
Ψ (m)	Θ (%vol)
0.070	0.549
0.703	0.524
2.109	0.365
3.515	0.283
6.679	0.209
21.092	0.167
49.215	0.124
198.845	0.075
16644.828	0.028

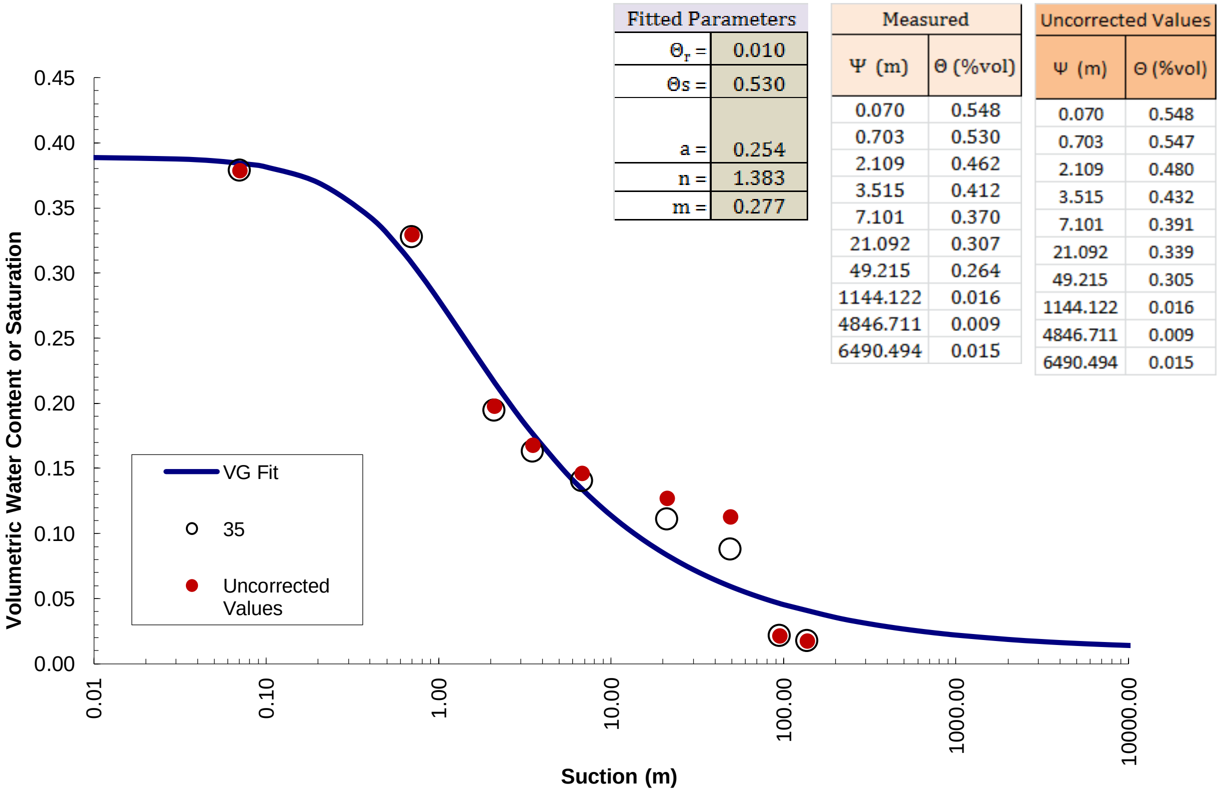

Fitted Parameters	
Θ_r =	0.010
Θs =	0.530
a =	0.254
n =	1.383
m =	0.277

Measured	
Ψ (m)	Θ (%vol)
0.070	0.548
0.703	0.530
2.109	0.462
3.515	0.412
7.101	0.370
21.092	0.307
49.215	0.264
1144.122	0.016
4846.711	0.009
6490.494	0.015

Uncorrected Values	
Ψ (m)	Θ (%vol)
0.070	0.548
0.703	0.547
2.109	0.480
3.515	0.432
7.101	0.391
21.092	0.339
49.215	0.305
1144.122	0.016
4846.711	0.009
6490.494	0.015

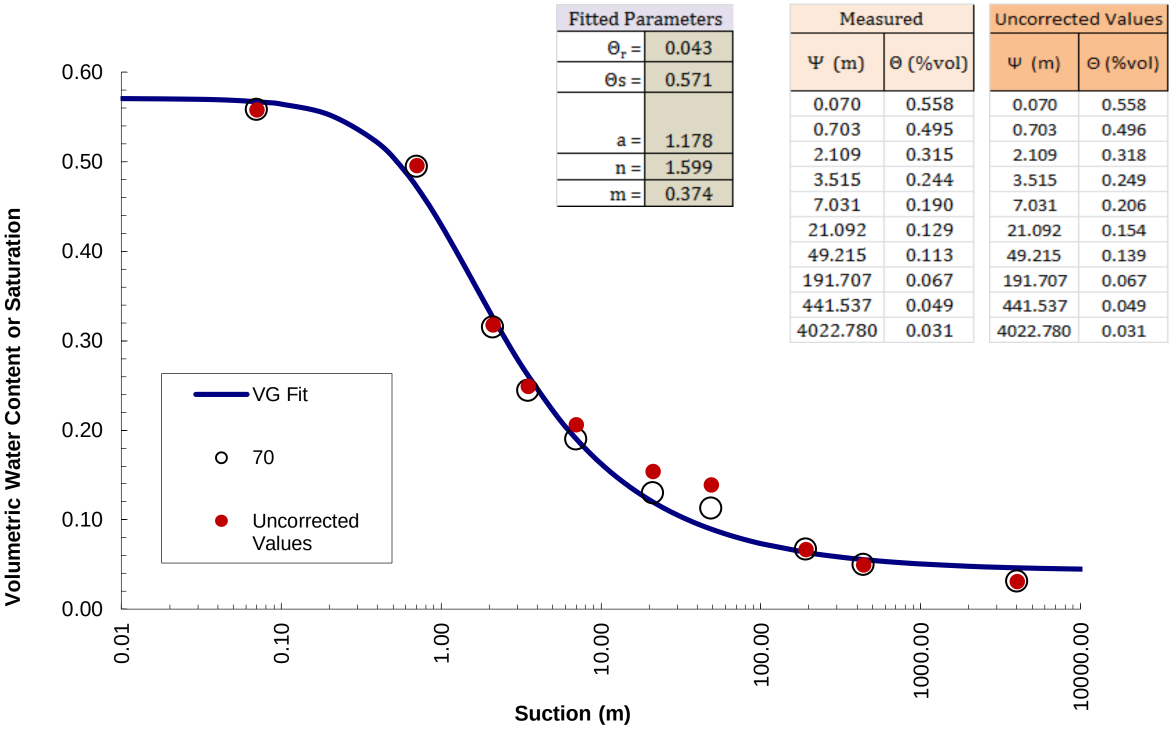

Fitted Parameters	
Θ_r =	0.043
Θs =	0.571
a =	1.178
n =	1.599
m =	0.374

Measured		Uncorrected Values	
Ψ (m)	Θ (%vol)	Ψ (m)	Θ (%vol)
0.070	0.558	0.070	0.558
0.703	0.495	0.703	0.496
2.109	0.315	2.109	0.318
3.515	0.244	3.515	0.249
7.031	0.190	7.031	0.206
21.092	0.129	21.092	0.154
49.215	0.113	49.215	0.139
191.707	0.067	191.707	0.067
441.537	0.049	441.537	0.049
4022.780	0.031	4022.780	0.031

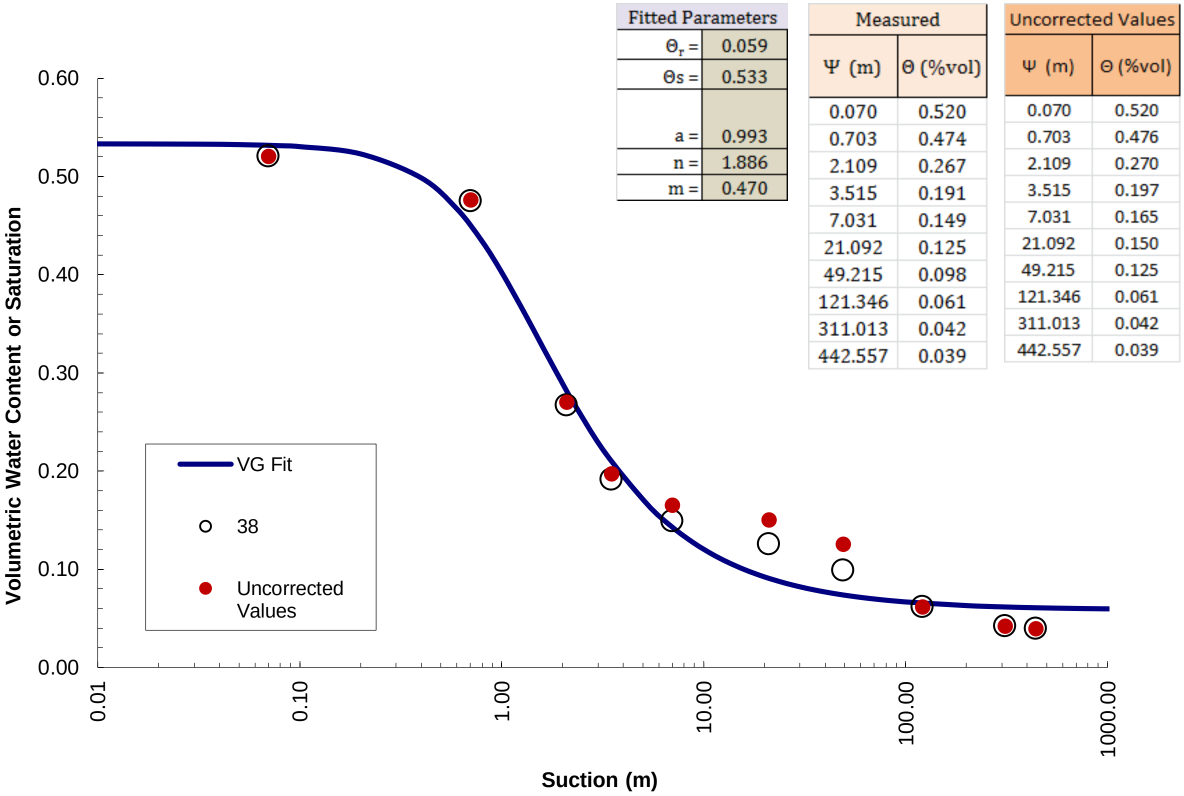

Fitted Parameters	
Θ_r =	0.059
Θs =	0.533
a =	0.993
n =	1.886
m =	0.470

Measured		Uncorrected Values	
Ψ (m)	Θ (%vol)	Ψ (m)	Θ (%vol)
0.070	0.520	0.070	0.520
0.703	0.474	0.703	0.476
2.109	0.267	2.109	0.270
3.515	0.191	3.515	0.197
7.031	0.149	7.031	0.165
21.092	0.125	21.092	0.150
49.215	0.098	49.215	0.125
121.346	0.061	121.346	0.061
311.013	0.042	311.013	0.042
442.557	0.039	442.557	0.039

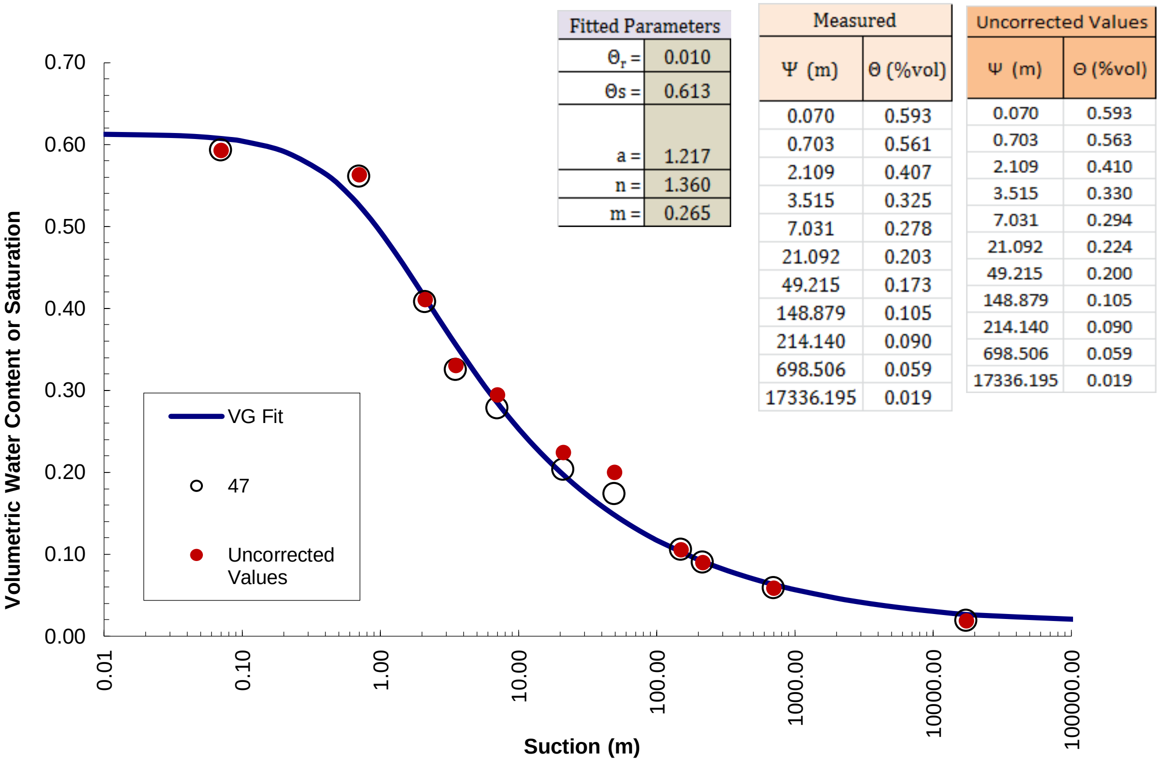

Fitted Parameters	
θ_r =	0.010
θs =	0.613
a =	1.217
n =	1.360
m =	0.265

Measured	
Ψ (m)	Θ (%vol)
0.070	0.593
0.703	0.561
2.109	0.407
3.515	0.325
7.031	0.278
21.092	0.203
49.215	0.173
148.879	0.105
214.140	0.090
698.506	0.059
17336.195	0.019

Uncorrected Values	
Ψ (m)	Θ (%vol)
0.070	0.593
0.703	0.563
2.109	0.410
3.515	0.330
7.031	0.294
21.092	0.224
49.215	0.200
148.879	0.105
214.140	0.090
698.506	0.059
17336.195	0.019

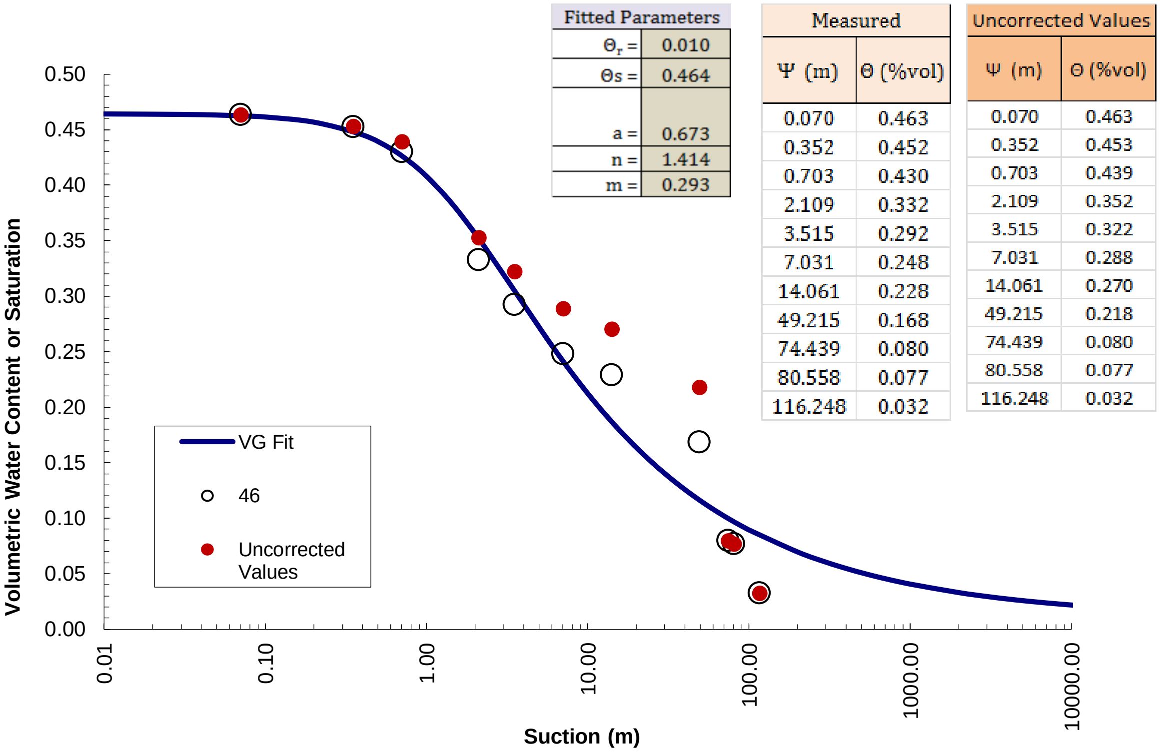

Fitted Parameters	
θ_r =	0.010
θs =	0.464
a =	0.673
n =	1.414
m =	0.293

Measured	
Ψ (m)	Θ (%vol)
0.070	0.463
0.352	0.452
0.703	0.430
2.109	0.332
3.515	0.292
7.031	0.248
14.061	0.228
49.215	0.168
74.439	0.080
80.558	0.077
116.248	0.032

Uncorrected Values	
Ψ (m)	Θ (%vol)
0.070	0.463
0.352	0.453
0.703	0.439
2.109	0.352
3.515	0.322
7.031	0.288
14.061	0.270
49.215	0.218
74.439	0.080
80.558	0.077
116.248	0.032

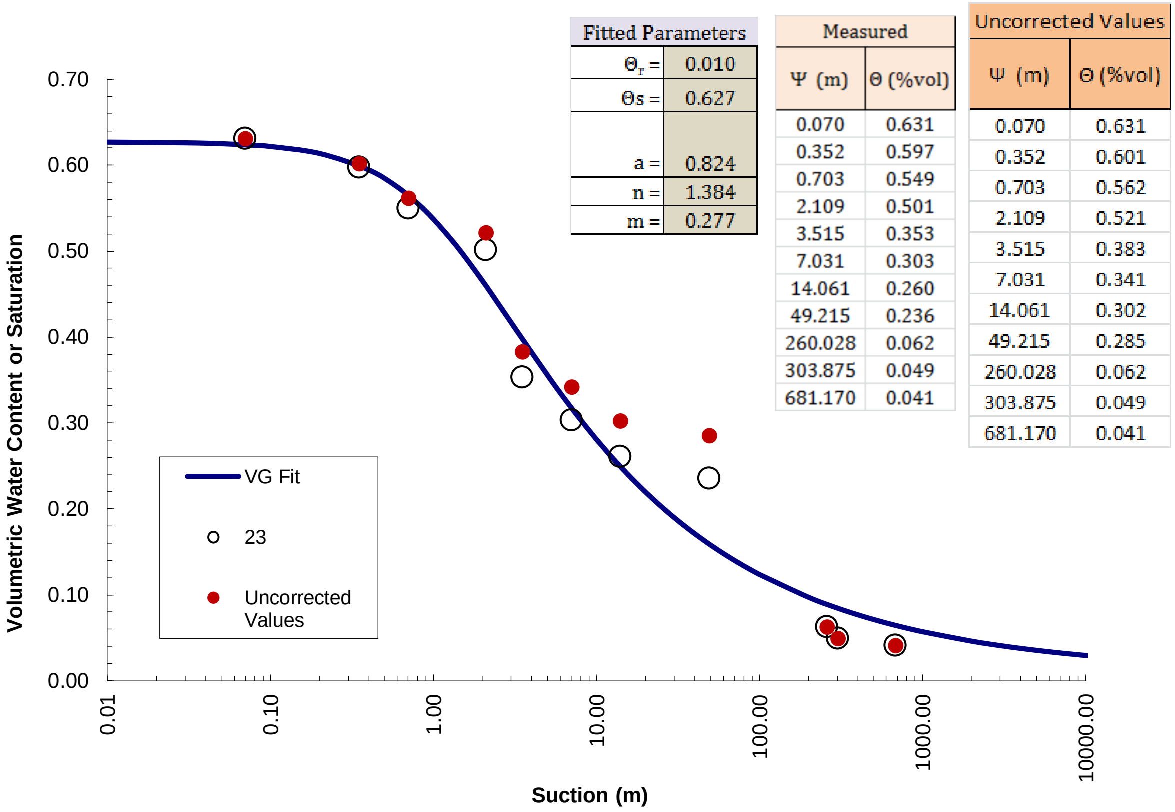

Fitted Parameters	
Θ_r =	0.010
Θs =	0.627
a =	0.824
n =	1.384
m =	0.277

Measured	
Ψ (m)	Θ (%vol)
0.070	0.631
0.352	0.597
0.703	0.549
2.109	0.501
3.515	0.353
7.031	0.303
14.061	0.260
49.215	0.236
260.028	0.062
303.875	0.049
681.170	0.041

Uncorrected Values	
Ψ (m)	Θ (%vol)
0.070	0.631
0.352	0.601
0.703	0.562
2.109	0.521
3.515	0.383
7.031	0.341
14.061	0.302
49.215	0.285
260.028	0.062
303.875	0.049
681.170	0.041

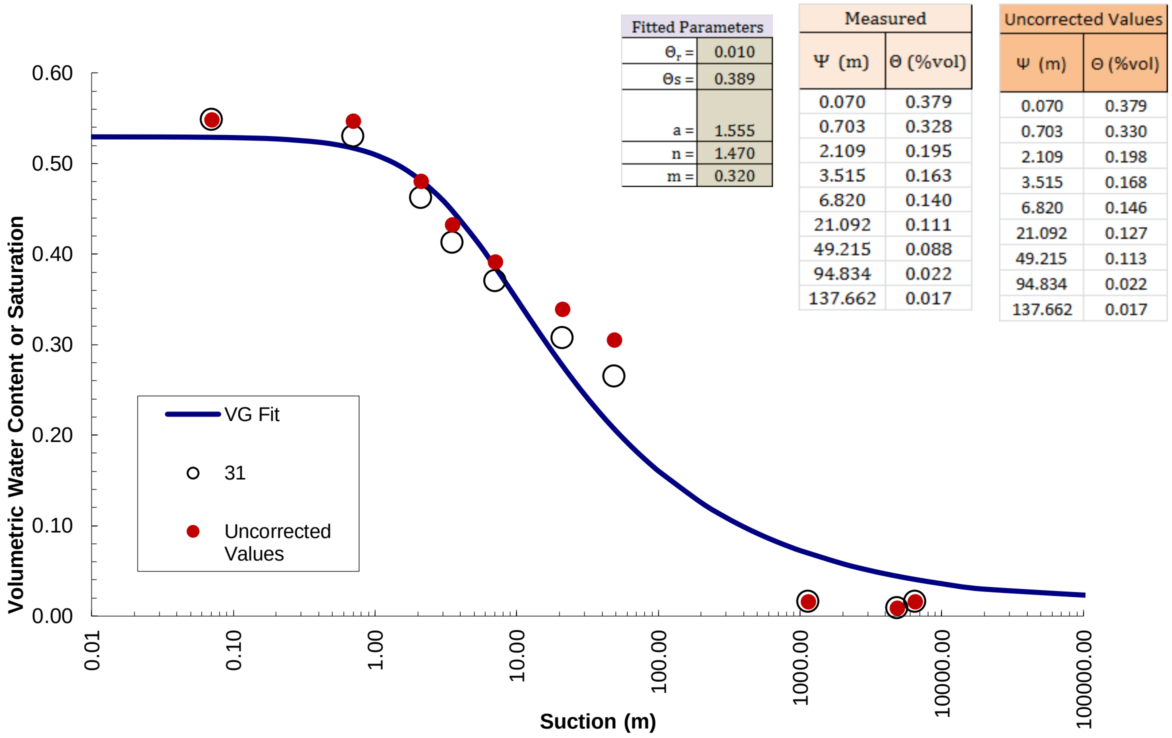

Fitted Parameters	
Θ_r =	0.010
Θs =	0.389
a =	1.555
n =	1.470
m =	0.320

Measured	
Ψ (m)	Θ (%vol)
0.070	0.379
0.703	0.328
2.109	0.195
3.515	0.163
6.820	0.140
21.092	0.111
49.215	0.088
94.834	0.022
137.662	0.017

Uncorrected Values	
Ψ (m)	Θ (%vol)
0.070	0.379
0.703	0.330
2.109	0.198
3.515	0.168
6.820	0.146
21.092	0.127
49.215	0.113
94.834	0.022
137.662	0.017

Appendix C

Particle Size Distribution Curves

The particle size distribution curves were measured for each of the 19 samples used in this study. We used the ASTM Standard D 7348-08 to measure the distributions. The mechanical sieving portion of the procedure is plotted in blue, and the hydrometer portion of the procedure is plotted in red.

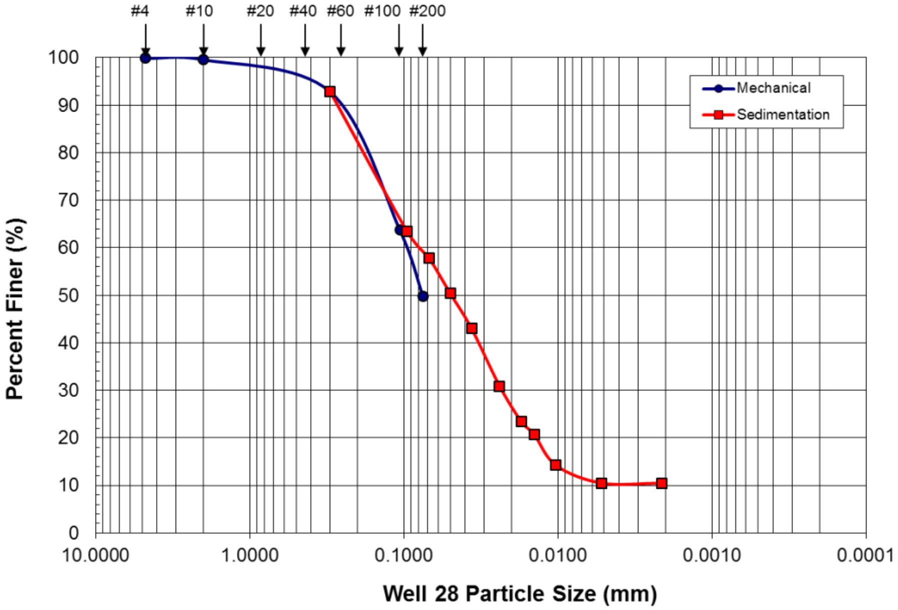

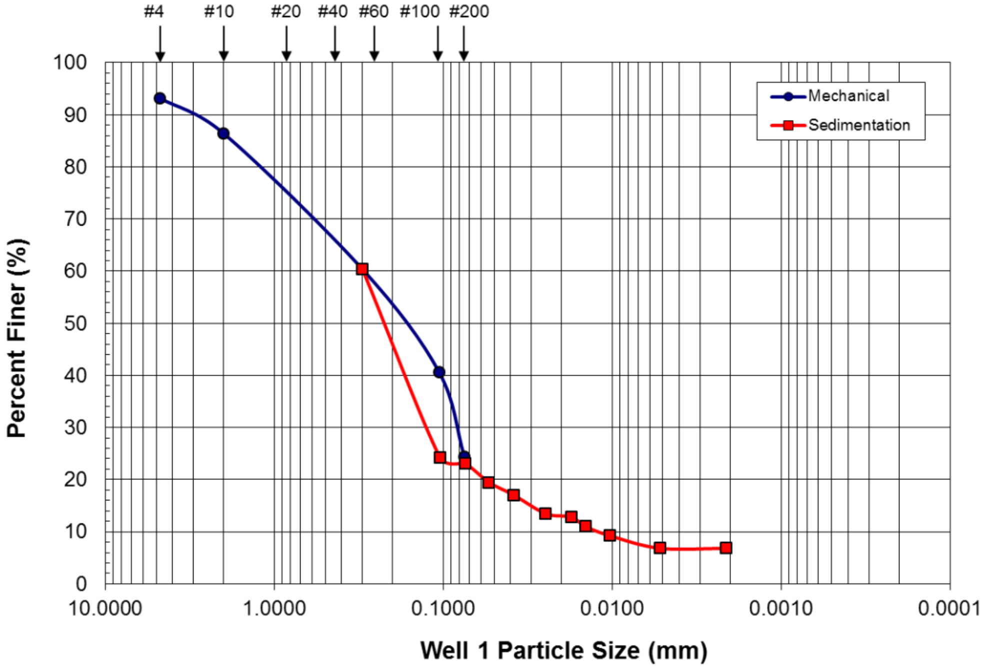
#4
#10
#20
#40
#60
#100
#200
100
90
80
70
60
50
40
30
20
10
0
Percent Finer (%)
10.0000
1.0000
0.1000
0.0100
0.0010
0.0001
Well 1 Particle Size (mm)
Mechanical
Sedimentation

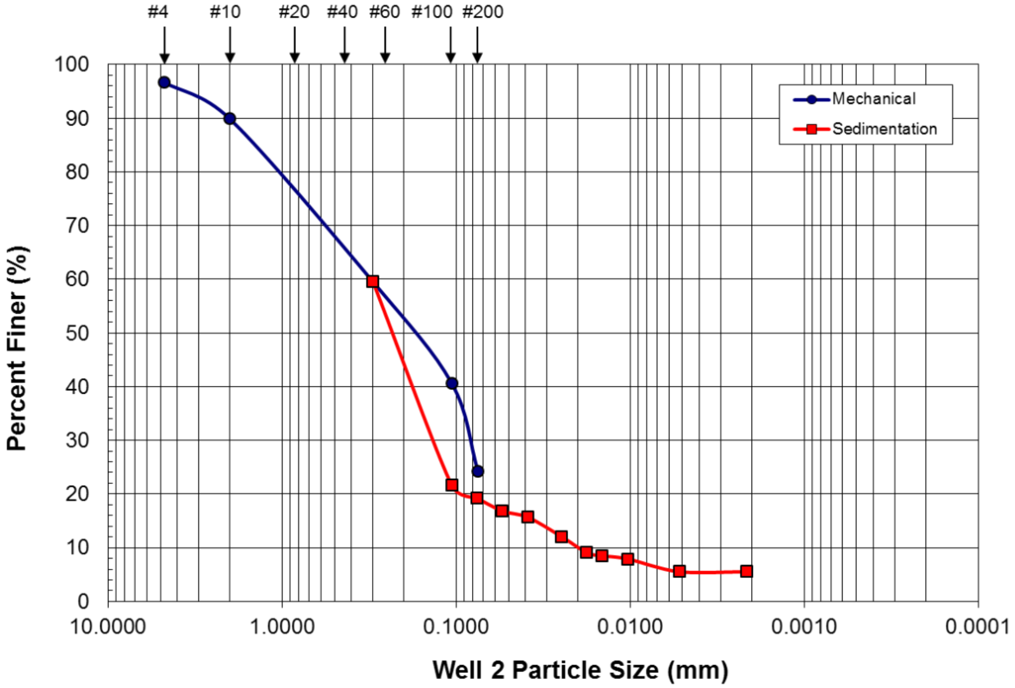
#4
#10
#20
#40
#60
#100
#200
100
90
80
70
60
50
40
30
20
10
0
Percent Finer (%)
10.0000
1.0000
0.1000
0.0100
0.0010
0.0001
Well 2 Particle Size (mm)
Mechanical
Sedimentation

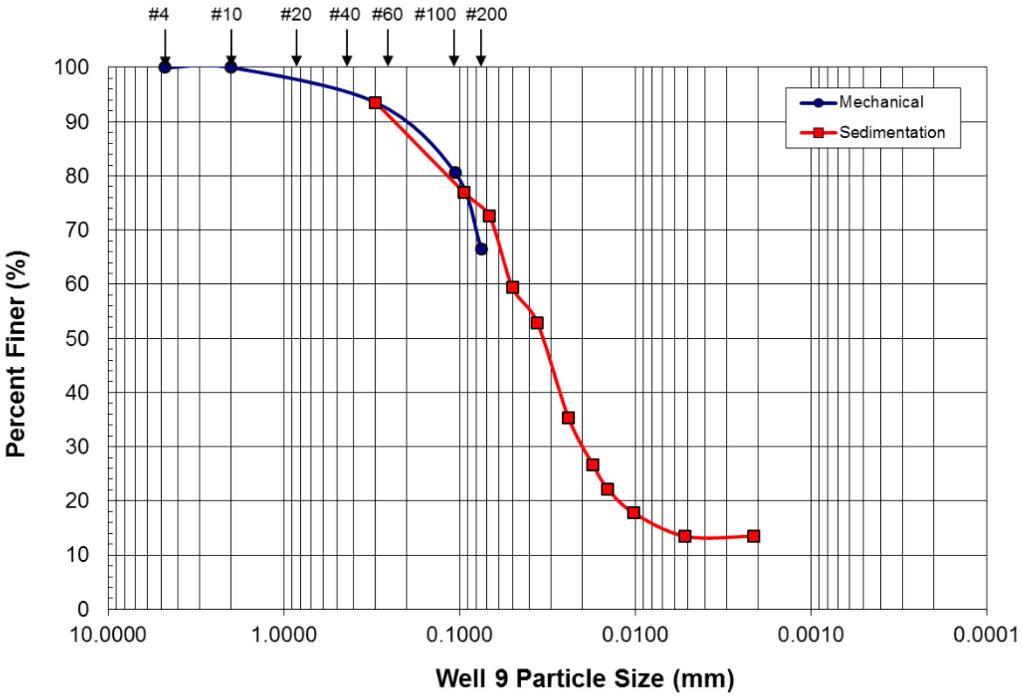
#4
#10
#20
#40
#60
#100
#200
100
90
80
70
60
50
40
30
20
10
0
Percent Finer (%)
10.0000
1.0000
0.1000
0.0100
0.0010
0.0001
Well 9 Particle Size (mm)
Mechanical
Sedimentation

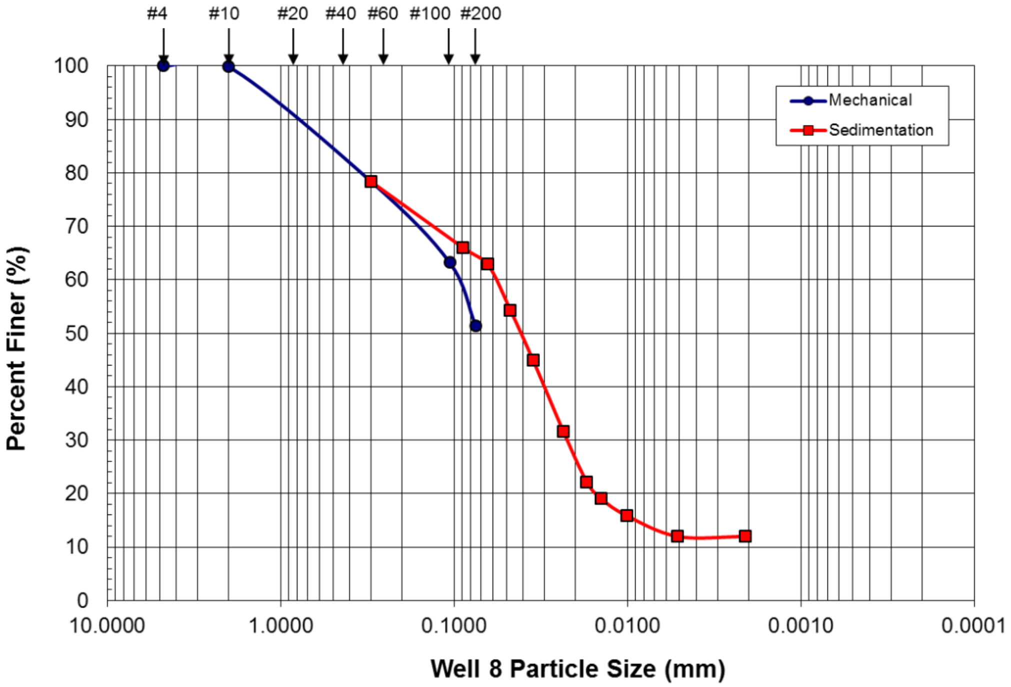
#4
#10
#20
#40
#60
#100
#200
100
90
80
70
60
50
40
30
20
10
0
Percent Finer (%)
10.0000
1.0000
0.1000
0.0100
0.0010
0.0001
Well 8 Particle Size (mm)
Mechanical
Sedimentation

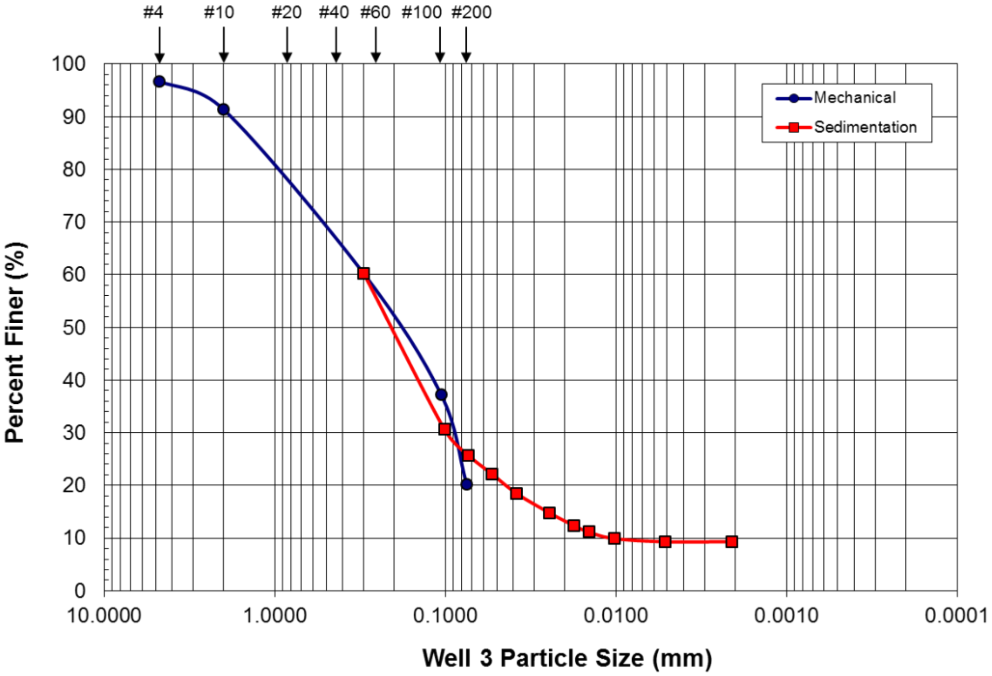
#4
#10
#20
#40
#60
#100
#200
100
90
80
70
60
50
40
30
20
10
0
Percent Finer (%)
10.0000
1.0000
0.1000
0.0100
0.0010
0.0001
Well 3 Particle Size (mm)
Mechanical
Sedimentation

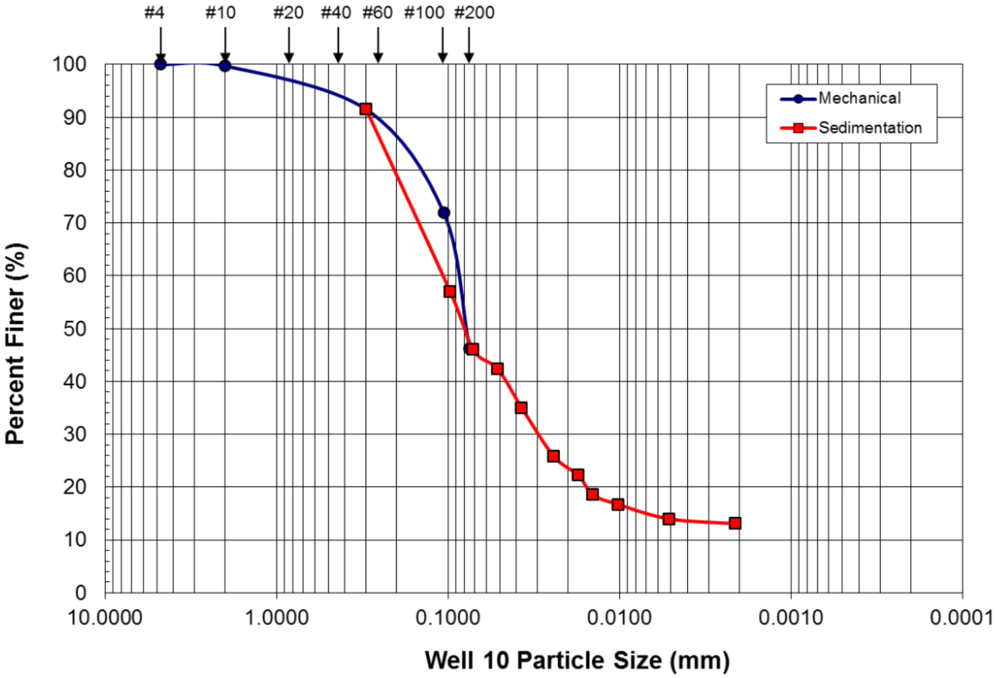
#4
#10
#20
#40
#60
#100
#200
100
90
80
70
60
50
40
30
20
10
0
Percent Finer (%)
10.0000
1.0000
0.1000
0.0100
0.0010
0.0001
Well 10 Particle Size (mm)
Mechanical
Sedimentation

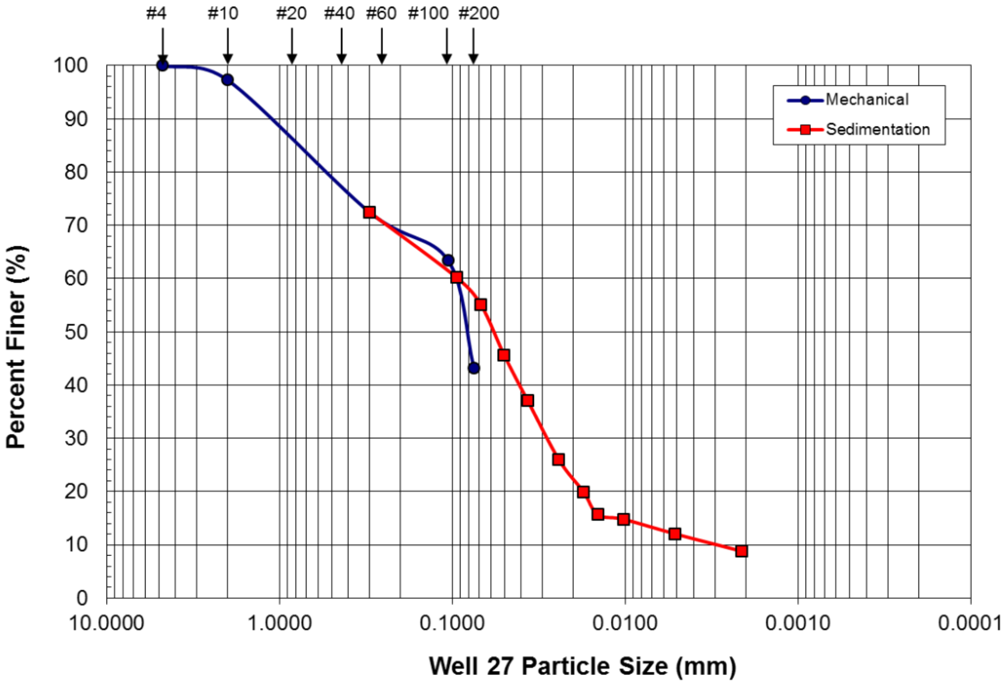
#4
#10
#20
#40
#60
#100
#200
100
90
80
70
60
50
40
30
20
10
0
Percent Finer (%)
10.0000
1.0000
0.1000
0.0100
0.0010
0.0001
Well 27 Particle Size (mm)
Mechanical
Sedimentation

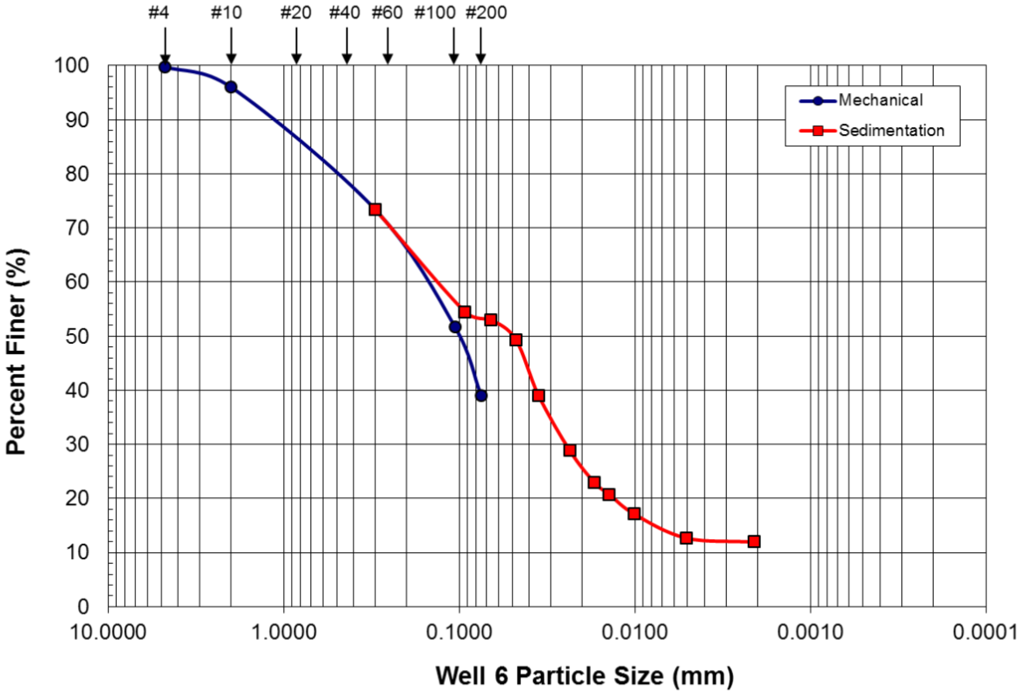
#4
#10
#20
#40
#60
#100
#200
100
90
80
70
60
50
40
30
20
10
0
Percent Finer (%)
10.0000
1.0000
0.1000
0.0100
0.0010
0.0001
Well 6 Particle Size (mm)
Mechanical
Sedimentation

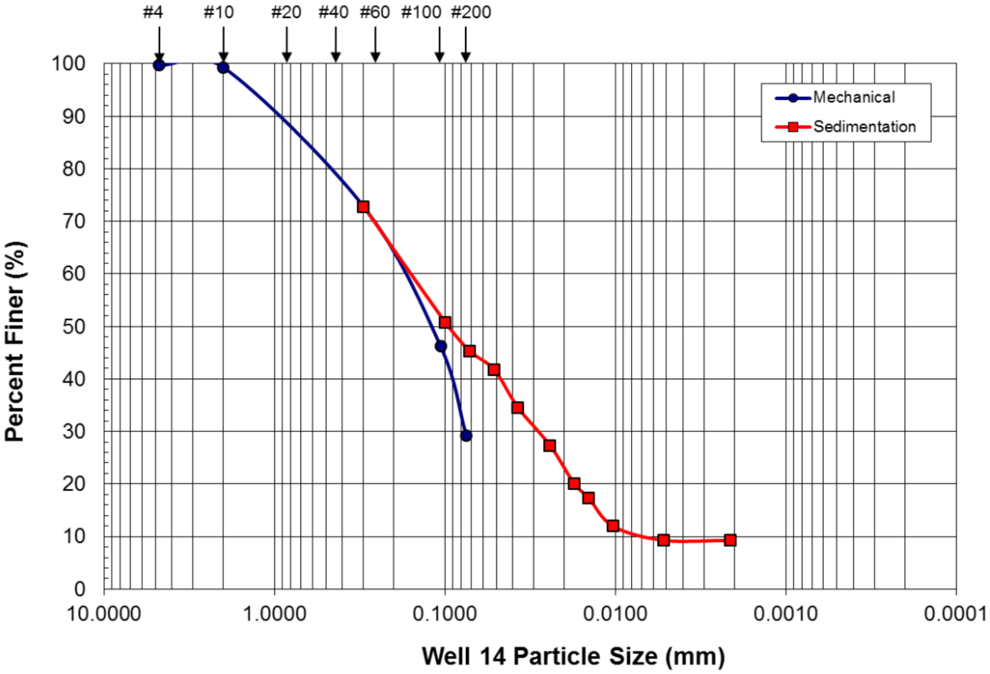
#4
#10
#20
#40
#60
#100
#200
100
90
80
70
60
50
40
30
20
10
0
Percent Finer (%)
10.0000
1.0000
0.1000
0.0100
0.0010
0.0001
Well 14 Particle Size (mm)
Mechanical
Sedimentation

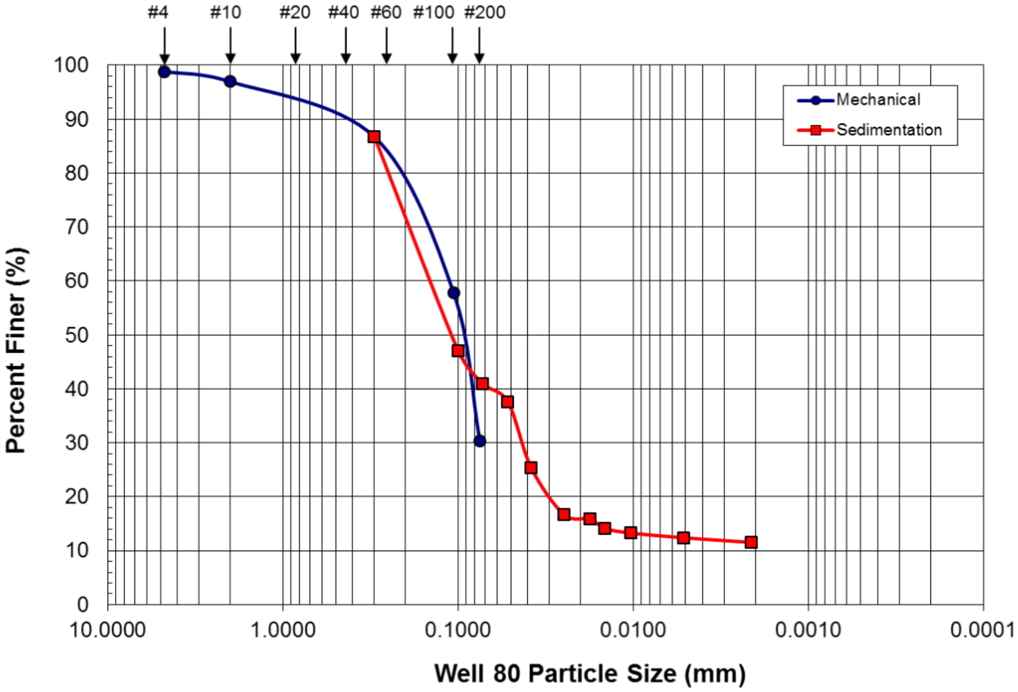
#4
#10
#20
#40
#60
#100
#200
100
90
80
70
60
50
40
30
20
10
0
Percent Finer (%)
10.0000
1.0000
0.1000
0.0100
0.0010
0.0001
Well 80 Particle Size (mm)
Mechanical
Sedimentation

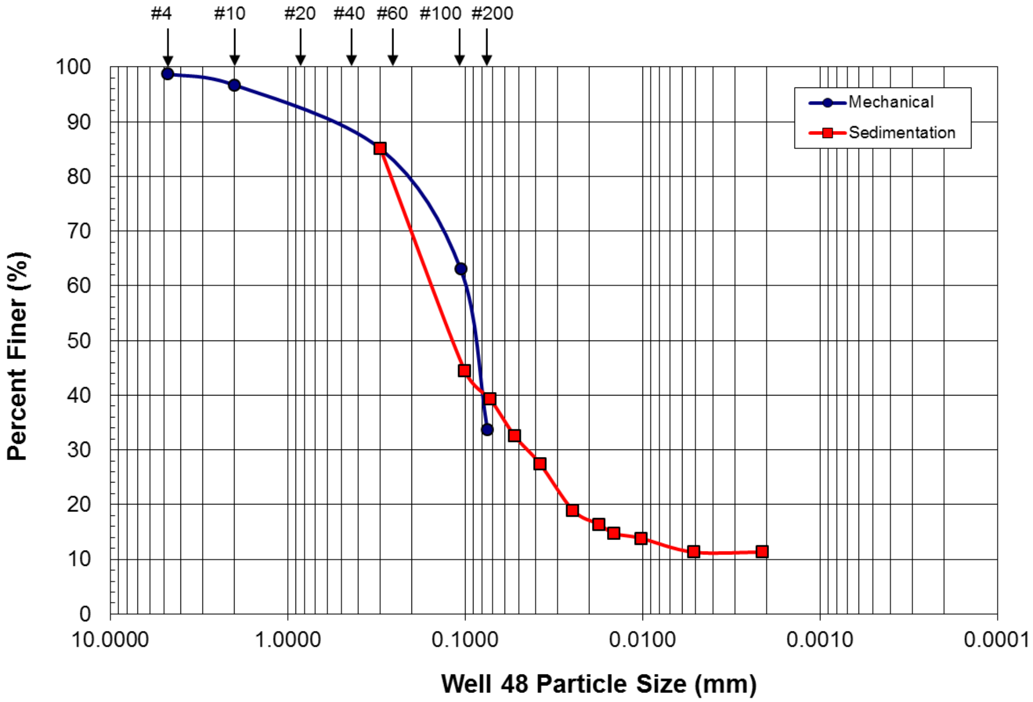
#4
#10
#20
#40
#60
#100
#200
100
90
80
70
60
50
40
30
20
10
0
Percent Finer (%)
10.0000
1.0000
0.1000
0.0100
0.0010
0.0001
Well 48 Particle Size (mm)
Mechanical
Sedimentation

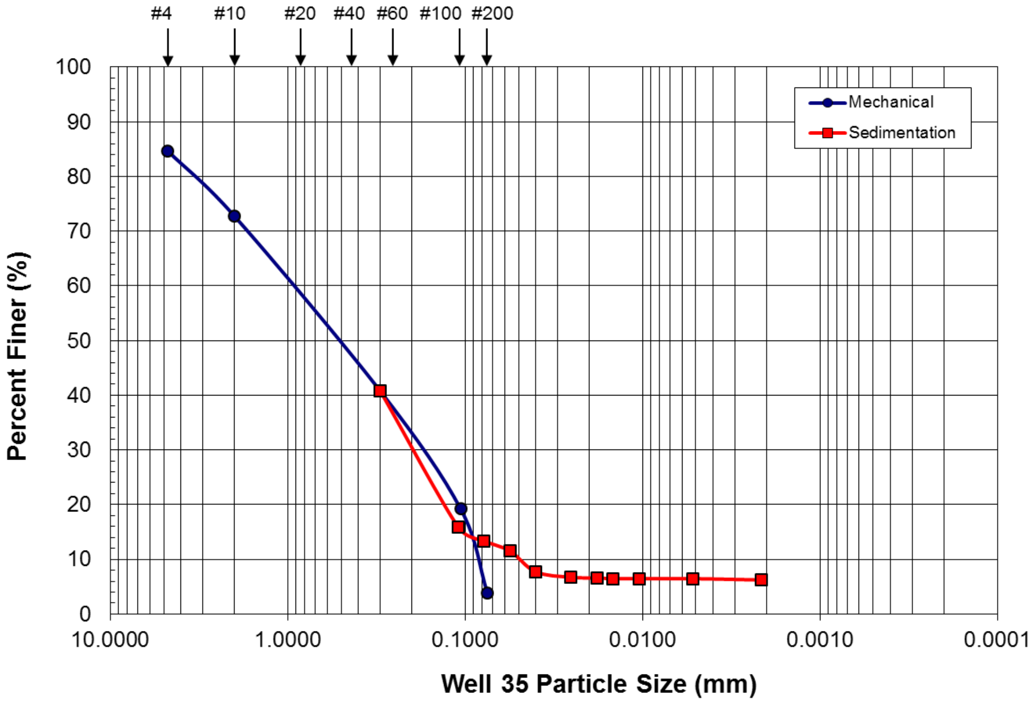
#4
#10
#20
#40
#60
#100
#200
100
90
80
70
60
50
40
30
20
10
0
Percent Finer (%)
10.0000
1.0000
0.1000
0.0100
0.0010
0.0001
Well 35 Particle Size (mm)
Mechanical
Sedimentation

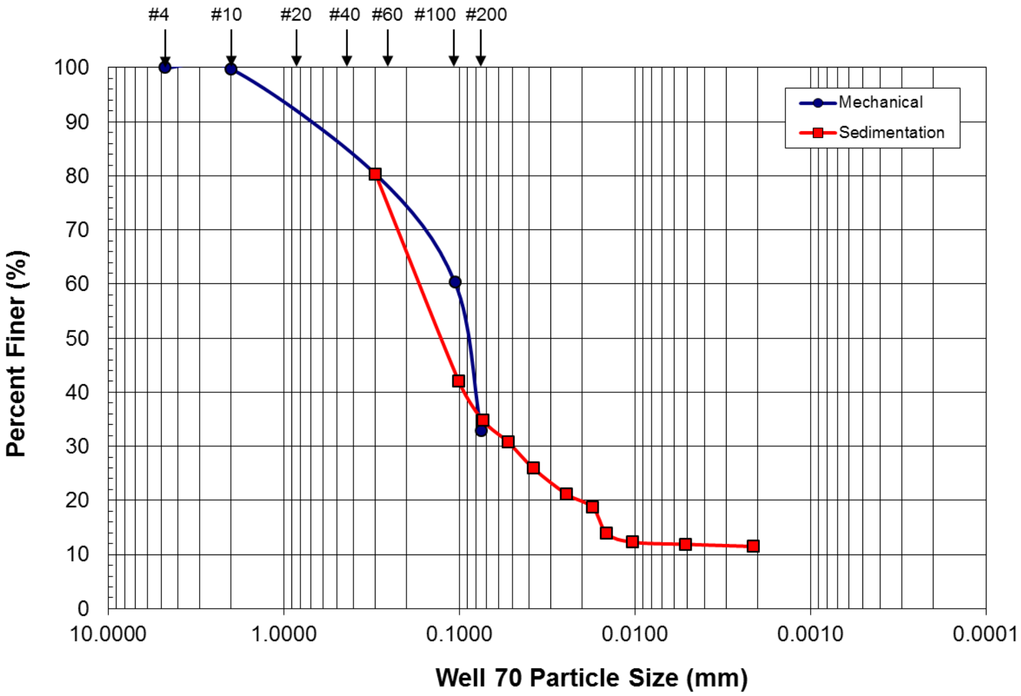
#4
#10
#20
#40
#60
#100
#200
100
90
80
70
60
50
40
30
20
10
0
Percent Finer (%)
10.0000
1.0000
0.1000
0.0100
0.0010
0.0001
Well 70 Particle Size (mm)
Mechanical
Sedimentation

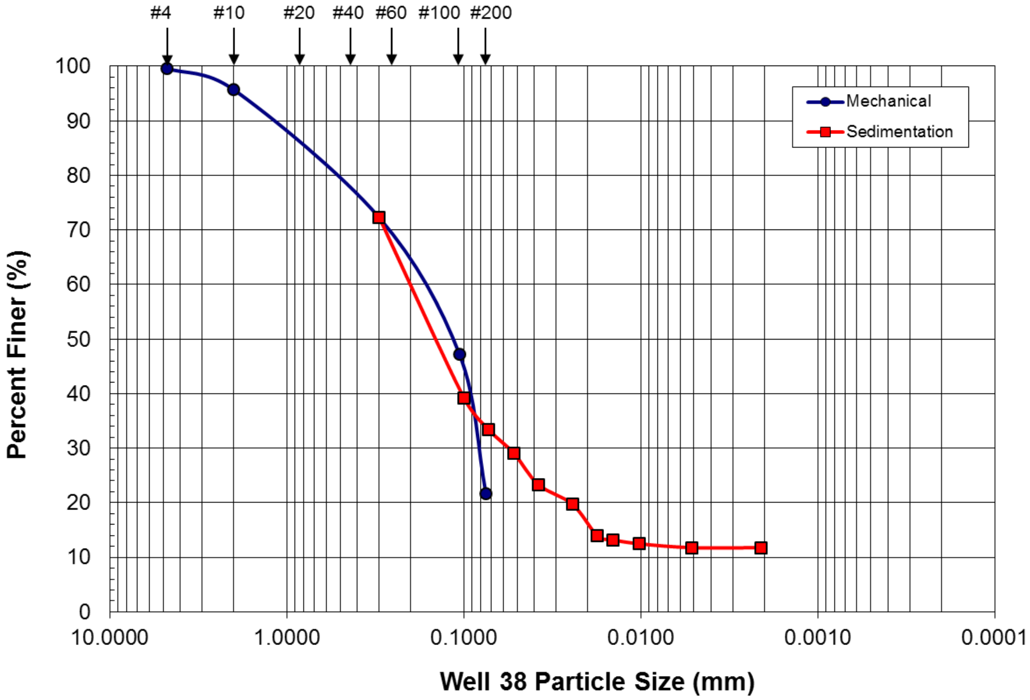
#4
#10
#20
#40
#60
#100
#200
100
90
80
70
60
50
40
30
20
10
0
Percent Finer (%)
10.0000
1.0000
0.1000
0.0100
0.0010
0.0001
Well 38 Particle Size (mm)
Mechanical
Sedimentation

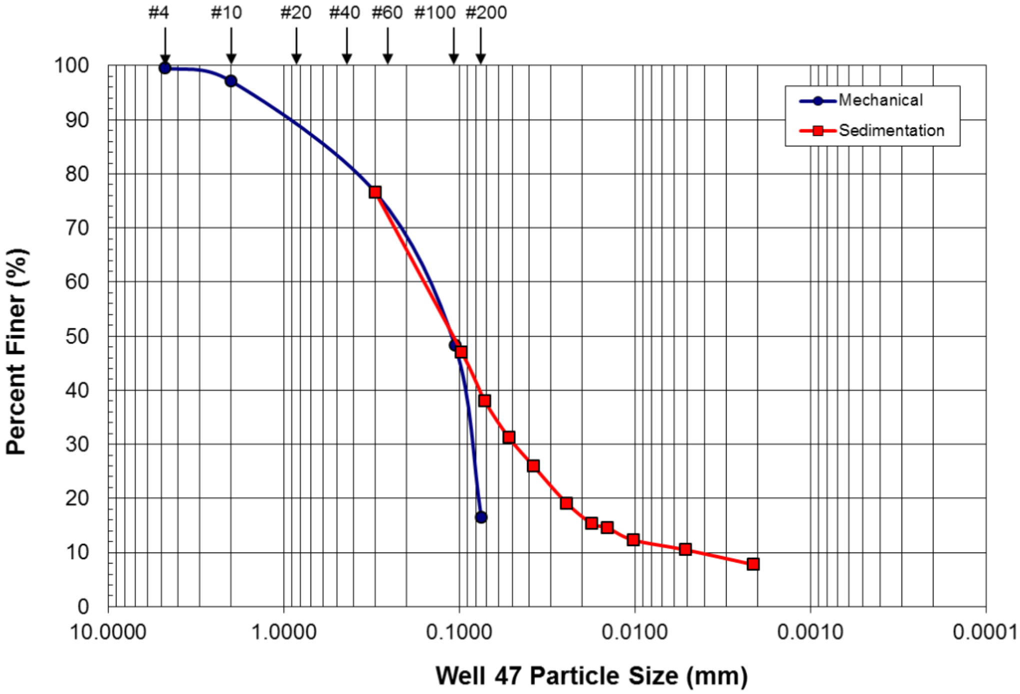
#4
#10
#20
#40
#60
#100
#200
Percent Finer (%)
100
90
80
70
60
50
40
30
20
10
0
10.0000
1.0000
0.1000
0.0100
0.0010
0.0001
Well 47 Particle Size (mm)
Mechanical
Sedimentation

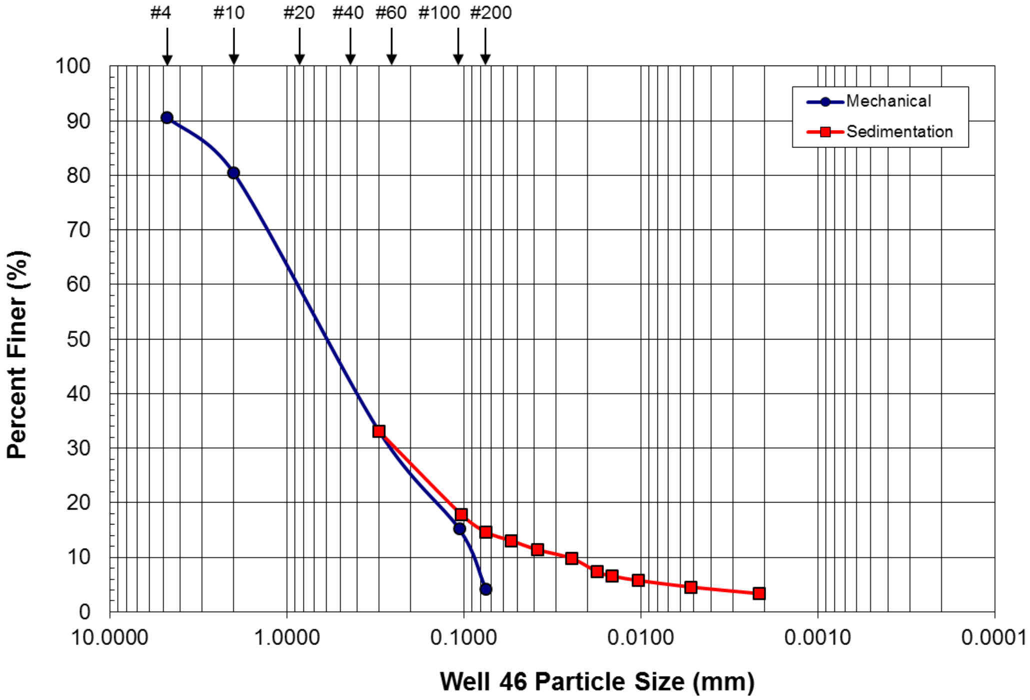
#4
#10
#20
#40
#60
#100
#200
Percent Finer (%)
100
90
80
70
60
50
40
30
20
10
0
10.0000
1.0000
0.1000
0.0100
0.0010
0.0001
Well 46 Particle Size (mm)
Mechanical
Sedimentation

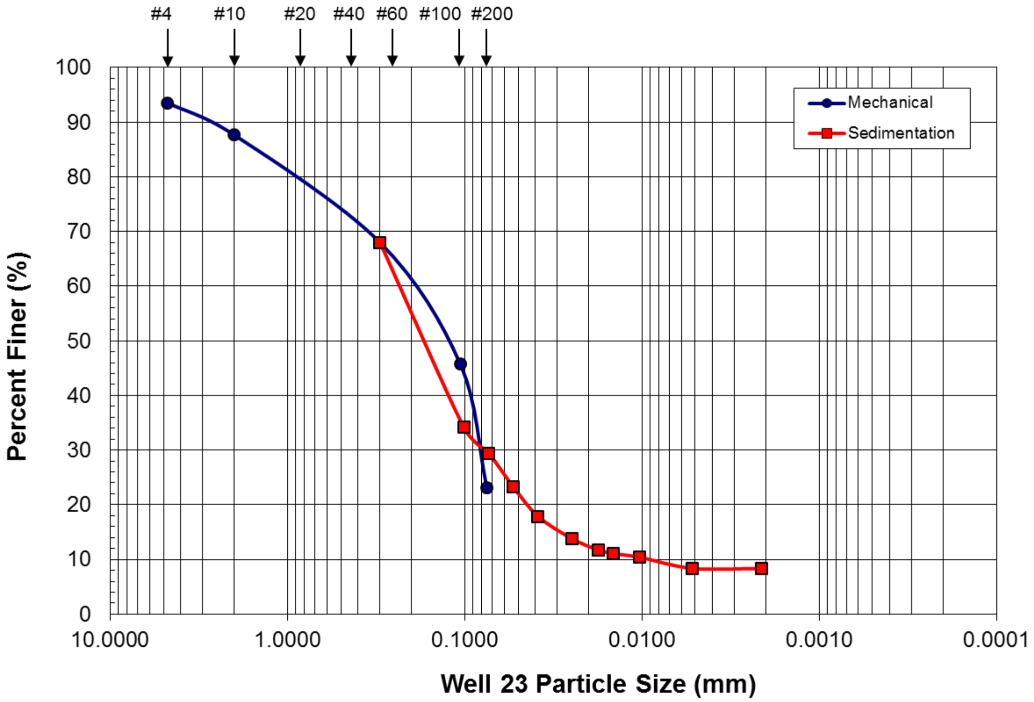
#4
#10
#20
#40
#60
#100
#200
Mechanical
Sedimentation
Percent Finer (%)
100
90
80
70
60
50
40
30
20
10
0
10.0000
1.0000
0.1000
0.0100
0.0010
0.0001
Well 23 Particle Size (mm)

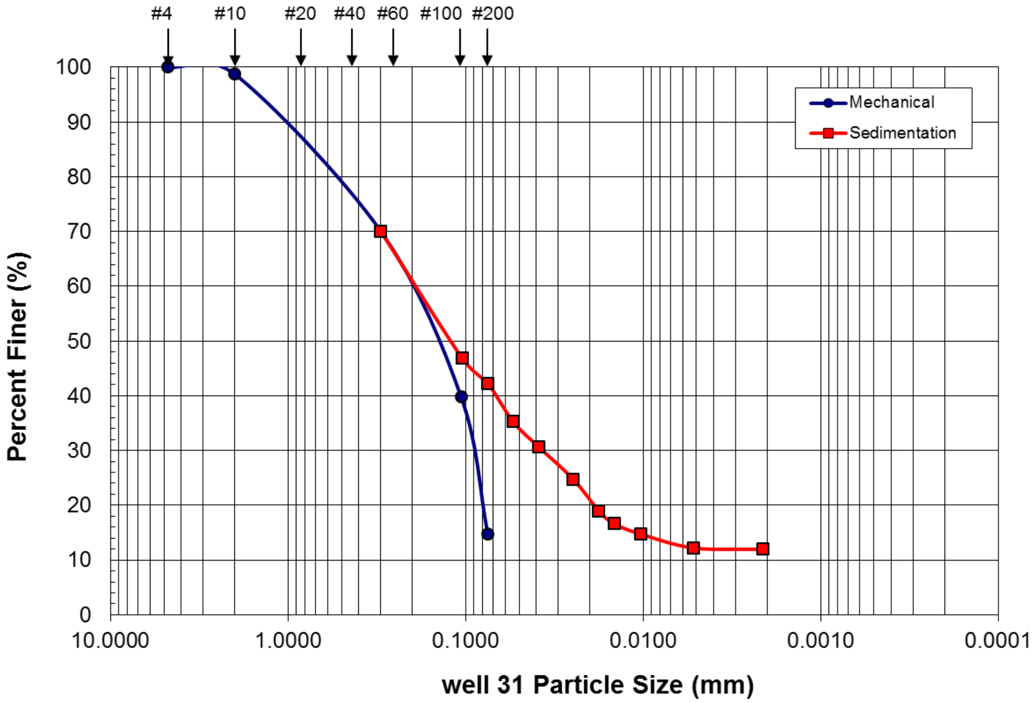
#4
#10
#20
#40
#60
#100
#200
Mechanical
Sedimentation
Percent Finer (%)
100
90
80
70
60
50
40
30
20
10
0
10.0000
1.0000
0.1000
0.0100
0.0010
0.0001
well 31 Particle Size (mm)

Appendix D

Soil Sample Parameters and a Map of Tuolumne Meadows

In this appendix we provide a concise summary of the 19 soil samples used in this study, and indicate the location and organic content of each sample with a map. The table below summarizes the Van Genuchten retention parameters, organic content (OM) and the well identification number where the sample was taken.

Well #	Θr	Θs	α [1/m]	n	OM [g/g]
35	0.010683	0.39	1.32	1.41	0.027
46	0.01	0.47	0.59	1.21	0.041
1	0.016133	0.45	1.11	1.93	0.048
80	0.050995	0.52	1.04	1.83	0.049
70	0.045539	0.57	1.17	1.73	0.051
38	0.057833	0.53	1.13	2.33	0.055
31	0.01	0.54	0.22	1.11	0.068
2	0.018087	0.50	0.77	1.47	0.075
48	0.048486	0.56	0.85	1.81	0.078
3	0.021579	0.52	0.69	1.51	0.091
8	0.01	0.56	0.55	1.14	0.091
10	0.01	0.62	0.81	1.04	0.093
6	0.051637	0.58	0.92	1.00	0.095
47	0.022571	0.62	0.96	1.15	0.126
9	0.01	0.58	0.41	1.46	0.132
14	0.01	0.70	0.56	1.00	0.150
23	0.01	0.64	0.71	1.13	0.159
28	0.017123	0.59	0.43	1.11	0.164
27	0.01	0.62	0.12	1.44	0.174

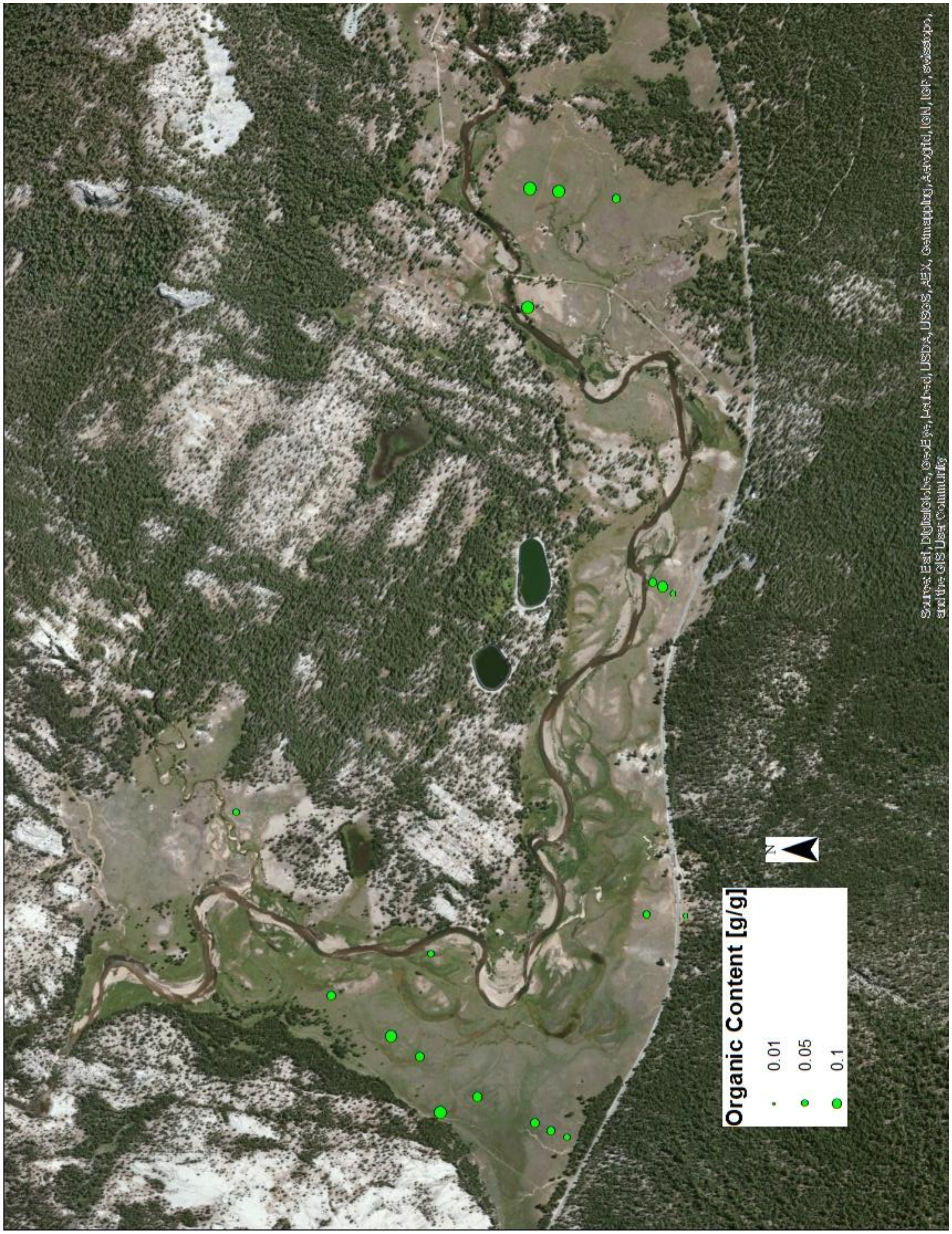
Organic Content [g/g]
0.01
0.05
0.1
N
Source: Esri, DigitalGlobe, GeoEye, i-cubed, USDA, USGS, AEX, Getmapping, Aerogrid, IGN, IGP, swisstopo, and the GIS User Community